

SYNTHESIS AND CHARACTERIZATION OF
RHENIUM (VII) AND RHUTHENIUM (II) DENDRITIC
CATALYSTS: OXIDATIVE CLEAVAGE AND
EPOXIDATION OF ALKENES

Asanda V. Busa

*A dissertation in partial fulfilment of the requirements for the degree
of Master of Science in the Department of Chemistry, University of
the Western Cape, South Africa*

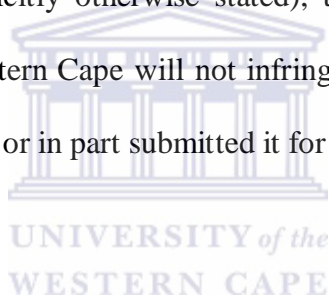
UNIVERSITY of the
WESTERN CAPE

Supervisor: Dr. Martin O. Onani

Co-supervisor: Prof. Selwyn F. Mapolie

DECLARATION

I, Asanda Vincent Busa, declare that “SYNTHESIS AND CHARACTERISATION OF RHENIUM(VII) AND RUTHENIUM (II) DENDRITIC CATALYST: OXIDATIVE CLEAVAGE AND EPOXIDATION OF ALKENES.” is my own work and that all sources I have used or quoted have been acknowledged by means of complete referencing at the end of each chapter. By submitting this thesis/dissertation, I declare that the entirety of the work contained therein is my own, original work, that I am the sole author thereof (save to the extent explicitly otherwise stated), that reproduction and publication thereof by University of the Western Cape will not infringe any third party rights and that I have not previously in its entirety or in part submitted it for obtaining any qualification.



.....

Asanda Vincent Busa

.....

Date

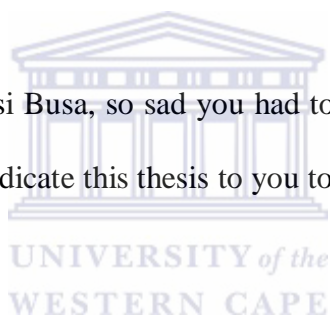
DEDICATION

This dissertation is dedicated to the love and memory of the late grandparents: Zolile Ntlantsana and Josephine Ntlantsana. Your guidance and love yielded this. Thank you.

And to my late sister, you are forever engraved in my heart. This is for YOU LOVEY!

And to Luniko Mketsu, the short time we spent with you was a total bliss. Life will never be the same boy, but do know that your Godfather will always keep you at heart

To Mzoxolo “Lolly” and Mlungisi Busa, so sad you had to depart inches before you see this one as well. In your memory, I dedicate this thesis to you too.



ACKNOWLEDGEMENTS

al-ḥamdu lillahi al-raḥmāni, l-raḥīmi! You are worthy to be praised!

To my supervisor Dr. Marin O. Onani, your tutelage carried me through the dark and I hope this will serve as a “little” light from me. Thank you for allowing me to explore. Your enthusiasm fuelled me to finish this strong. I’m looking forward to any future endeavours.

I would also like to thank Prof. Selwyn F. Mapolie for being part of this work. Your feedback and advice helped greatly in finishing this work.

To Professor Ebbe Nordlander, Thank You for wise-consult. Your contribution during my visit in your lab had an immense impact on the understanding and execution of the work. Looking forward working with you in the future, Tack så mycket!

For financial support I would like to thank NRF, CSIR and EUROS

To my family, you have been extremely patient with me. You have all been a backbone throughout the trialling times. At the time when we lost everything, your love strengthened. I cannot ask more from this life, you (all) are an epitome of strength! Your love is evidence that together we can conquer all.

To my cousin, Sinethemba “Sketch” Busa, once again “sasitshilo baba”! I’ve brought it home. This is for US! Let’s raise our “champagne flutes” as we toast to what we didn’t have, “hustle” plus muscle equals success I did the maths.

To the Organic and Organometallic research group: Paul Mushonga, William Motswainyana, Linda Ouma, Mududuzi Radebe, Henry Mwangi, Ndikho Nako, thanks for the extremely intense sessions and crazy times we had in the lab. Hope to work with you again in the future.

ACKNOWLEDGEMENTS

To my friends, WOW! I don't know where to begin, all I can say is "SPONKY PONKY LOVE, the LOVE THAT YOU CAN'T RESIST" BOSS!

A special thanks to a crazy colleague/friend, Mduduzi Radebe, it has been wild and I don't know what's next. From Sweden to Denmark to here and there, this is to US as well hommy!

And to you...THANK YOU, for being "there"...I just know you know.

To the love of my life...my MOM: Lulama Busa, enkosi s'thandwa sam! Ndiyabulela kakhulu ngento yonke. Uyintsika apha ebomini bam. Ngaphandle kwakho nguMdali yedwa owaziyo ngediphi. Maz'enethole!



CONFERENCE CONTRIBUTIONS

Asanda Busa, Martin Onani and Selwyn Mapolie

*Synthesis and Characterization of Ruthenium and Rhenium dendritic catalysts:
Application in the Epoxidation and Oxidative Cleavage of Selected Alkenes.* Cape
Organometallic Symposium, University of Cape Town, Cape Town, South Africa ,26-10-
2012.

Asanda Busa, Martin Onani and Selwyn Mapolie

*Synthesis and Characterization of Ruthenium and Rhenium dendritic catalysts:
Application in the Epoxidation and Oxidative Cleavage of Selected Alkenes.* CATSA
annual conference, Club Mykonos, Langebaan, South Africa, 11-11-2012.

Research Visit:

Synthesis and Characterization of Rhenium dendritic catalysts.

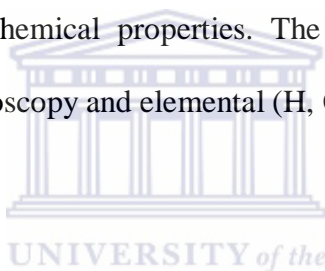
August 2011 – February 2012

Lund University, Sweden

Prof. Ebbe Nordlander

ABSTRACT

Herein we report the successful synthesis of a class of stable and flexible Schiff-base chelators capable of coordinating both ruthenium (II) and rhenium (VII) and which would be catalytically active for oxo-transfer reactions. The synthesis of bidentate (**L1**), tetradentate (**L2-L3**), and multidentate ligands (**DL1-DL4**) of nitrogen was a result of a reaction of primary amine with 2-pyridinecarboxaldehyde. Ligand (**L3**) is reported herein for the first time. The amines (n-propylamine, ethylenediamine, butanediamine, diaminobutane, propylene iminopyridyl (DAB-PPI) dendrimer) were varied as to afford metal complexes that exhibit different physical and chemical properties. The ligands were isolated and fully characterized by IR, NMR spectroscopy and elemental (H, C, N) analysis.

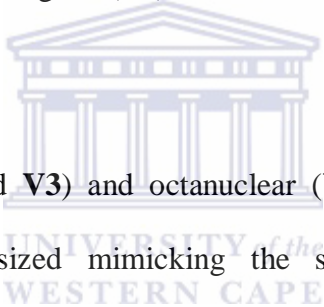


The Schiff-base complexes of methyltrioxorhenium (MTO): Methyl(n-pyridin-2-yl)methylene)propan-1-amine)trioxorhenium (**C1**), Methyl([bis(pyridin-2-yl)formylidene]butane-1,4-diamine)trioxorhenium (**C2**), Methyl(diaminobutane propylene imonopyridyl)trioxorhenium G^1 (**DC1**) and G^2 (**DC2**) have exhibited sensitivity to water than MTO itself. Rapid ligand-exchange reactions in solution are observed at elevated temperatures. The MTO Schiff-base complexes are also slightly sensitive to light and slowly decompose as they are exposed to air. These complexes were isolated and fully characterized by IR, NMR, UV-Vis, EA and MS. In the ESI mass spectra of compound **C1-C2** and **DC1-DC2** show the peaks of the Schiff-base ligand and the MTO moiety separately, without a traceable fragmentation pattern. The isotopic cluster and the molecular ion peak were observed.

ABSTRACT

The mononuclear ruthenium compounds (**B1** and **B3**) were prepared from dichlorotetrakis(dimethyl sulfoxide)ruthenium (II) metal precursor by reacting the synthesized ligands (**L2** and **L3**) with the metal precursor. Compounds (**B2** and **B4**) were obtained by subsequently stabilizing the neutral compounds (**B1** and **B2**) as hexafluorophosphate salts via metathesis employing thallium (I) hexafluorophosphate (**V**).

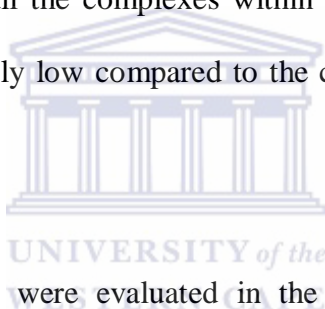
The homobimetallic cationic compound (**B5**) was synthesized by reacting the dinuclear complex $[(p\text{-cymene})_2\text{RuCl}_2]_2$ with ligand (**L4**).



The neutral tetranuclear (**V1** and **V3**) and octanuclear (**V2** and **V4**) (*N,N*) ruthenium(II) metallodendrimers were synthesized mimicking the same route as for the neutral mononuclear compounds (**B1** and **B3**). The compounds (**V1-V4**) were prepared from the dichlorotetrakis(dimethyl sulfoxide)ruthenium(II) based on the synthesized dendritic scaffolds (**DL1-DL4**). Compounds (**V5** and **V6**) were fashioned in a similar manner to compound (**B5**), by reacting the iminopyridyl dendritic scaffolds (**DL1** and **DL3**) with the dinuclear precursor $[(p\text{-cymene})_2\text{RuCl}_2]_2$ to afford two complexes of the type $[(p\text{-cymene})\text{RuCl}_2]_4\text{G}^1$, **V5** and $[(p\text{-cymene})\text{RuCl}_2]_8\text{G}^2$, **V6**. Electronic spectra of the prepared complexes were obtained (in a Sharpless Biphasic solvent system: $\text{CCl}_4:\text{MeCN}:\text{H}_2\text{O}$) in order to understand the nature of the active species in the catalytic cycle and to propose a mechanism for the catalytic cycle. Confirmation of the prepared complexes (**B1-V6**) was done using several spectroscopic techniques (IR, NMR, UV-Vis, ESI-MS) in conjunction with elemental analysis.

ABSTRACT

The compounds **C1-DC2** were then tested towards the epoxidation of selected cyclic alkenes i.e cyclohexene and cis-cyclooctene, respectively and straight chain alkenes. The catalyzed epoxidation reactions were carried out at room temperature employing using Urea hydrogen peroxide adduct (UHP) as the oxidant and dichloromethane (DCM) as the solvent. The complexes displayed high catalytic activity and selectivity when applied to the epoxidation of cyclohexene and cis-cyclooctene with urea hydrogen peroxide adduct (UHP) as oxidant in dichloromethane. The epoxidation reaction was quantified using gas chromatography. Conversions reached 100% for all the complexes within 6 hours. The catalytic activity of complex **C1** and **C2** was relatively low compared to the catalytic activity of complex **DC1** and **DC2**.



Ruthenium compounds (**B1-V6**) were evaluated in the catalyzed oxidative cleavage of straight chain alkene. The substrate chosen was 1-octene. The oxidative cleavage reactions were carried out at room temperature in a Sharpless biphasic solvent system (CCl₄:MeCN:H₂O) using sodium periodate (NaIO₄) as the cooxidant. The catalysts were found to be active in the oxidative cleavage of 1-octene with the metallodendrimers exhibiting superior catalytic efficiency.

TABLE OF CONTENTS

DECLARATION	i
DEDICATION	ii
ACKNOWLEDGEMENTS	iii
CONFERENCE CONTRIBUTIONS	v
ABSTRACT	vi
Table of Contents	ix
List of Figures	xvi
List of Schemes	xix
List of Tables	xxi
List of Abbreviations	xxiii



1 Chapter 1: Introduction to Ruthenium and Rhenium complexes in catalyzed oxidation

of alkenes.

<i>1.1 Ruthenium in the catalyzed transformation of alkenes.</i>	1
1.1.1 Introduction.	1
1.1.2 One-step oxidative cleavage of applying ruthenium and percarboxylic acids as oxidants.....	2
1.1.3 Some of the ruthenium catalysts documented in the literature for oxidation reactions.....	7

1.1.3.1 Synthesis and study of mononuclear ruthenium(II) complexes of sterically hindered diimine chelates.....	7
1.1.3.2 Synthesis of ruthenium (II) perchlorate complexes.....	7
1.1.3.3 Synthesis of ruthenium (II) bipyridine complex, [RuCl ₂ (bpy) ₂].....	8
1.2 Optimized catalyst system and reaction conditions.....	8
1.3 Why ruthenium?.....	11
1.4 <i>Introduction to Epoxidation</i>	12
1.4.1 Discovery of methyltrioxorhenium (MTO).....	12
1.4.2 Methyltrioxorhenium (MTO) in the epoxidation reactions of olefins.....	12
1.4.2 Mechanism of the catalytic cycle of methyltrioxorhenium (MTO).....	13
1.5 Aims and Objectives of the study.....	17

Chapter 2: Synthesis and Characterization of mono-, bi- and multinuclear Ru(II) and

<i>Re(VII) complexes directed towards catalytic studies</i>	24
2.1 Introduction.....	24
2.1.1 Diimine ligands.....	24
2.1.2 Schiff-base/diimine complexes of methyltrioxorhenium (MTO).....	26
2.2 Results and Discussions.....	27
2.2.1 Mono- and bifunctional Schiff-base/diimine ligand synthesis, L1-L4	27

2.2.2 Schiff-base complexes of Methyltrioxorhenium (MTO), C1 and C2	36
2.2.3 Neutral mononuclear ruthenium(II) complexes, B1 and B2	40
2.2.4 Cationic mononuclear ruthenium(II) complexes, B3 and B4	43
2.2.5. Cationic homobimetallic ruthenium complex, B5	44
2.3.1 Dendrimers as ligands.....	46
2.3.2 Approaches devised for the synthesis of dendrimers.....	47
2.3.2.1 Divergent Approach.....	47
2.3.2.2 Convergent Approach.....	48
2.4.1 Synthesis of peripherally modified PPI dendrimers.....	50
2.4.1.1 Synthesis and Characterization of dendritic ligands, DL1-DL4	50
2.5.1 Synthesis and characterization of dendritic complexes, DC1-DC2 and V1-V6	56
2.5.1.1 Dendritic Schiff-base complexes of MTO, DC1 and DC2	56
2.5.1.2 Neutral dendritic ruthenium(II) complexes, V1-V4	57
2.5.1.3 Cationic dendritic ruthenium complexes, V5-V6	58
2.6 Conclusions.....	64
2.7 Materials and Methods.....	64
2.7.1 Synthesis of mono- and bifunctional diimine ligands.....	65
2.7.1.1 (E)-N-((pyridine-2-yl)methylene)propan-1-amine, L1	65
2.7.1.2 (7E, 10E)-N1,N2-bis((pyridine-2-yl)methylene)ethane-1,2-diamine, L2	65

2.7.1.3 (7E, 10E)-N1,N2-bis((quinolin-2-yl)methylene)ethane-1,2-diamine, L3	65
2.7.1.4 (7E, 8E)-N1,N2-bis((pyridine-2-yl)methylene)butane-1,4-diamine, L4	66
2.7.2 Synthesis of mono and bifunctional Ru(II) and Re(VII) complexes, C1-C2 and B1-B5	66
2.7.2.1 Synthesis of Schiff-base MTO complex, C1	67
2.7.2.2 Synthesis of homobimetallic Schiff-base MTO complex, C2	67
2.7.2.3 Synthesis of mononuclear Ru(II) complex, B1	70
2.7.2.4 Synthesis of mononuclear Ru(II) complex, B2	68
2.7.2.5 Synthesis of cationic mononuclear Ru(II) derivative, B3	69
2.7.2.6 Synthesis of cationic mononuclear Ru(II) derivative, B4	69
2.7.2.7 Synthesis of cationic homobimetallic Ru(II) complex, B5	70
2.7.3 Synthesis of dendritic ligands, DL1-DL4	70
2.7.3.1 G1 DAB-[N=CH-(2-pyr) ₄], DL1	71
2.7.3.2 G2 DAB-[N=CH-(2-pyr) ₈], DL2	71
2.7.3.3 G1 DAB-[N=CH-(2-quinol) ₄], DL3	72
2.7.3.4 G2 DAB-[N=CH-(2-quinol) ₈], DL4	72
2.7.4 Synthesis of Schiff-base multinuclear dendritic MTO complexes, DC1 and DC2	73
2.7.4.1 G1 DAB-MTO complex, DC1	73

2.7.4.2 G2 DAB-MTO complex, DC2	73
2.7.5 Synthesis of G1 and G2 pyridyl/quinolyimine Ru(II) complexes, V1-V6	74
2.7.5.1 G1 DAB pyridylimine Ru(II) complex, V1	74
2.7.5.2 G2 DAB pyridylimine Ru(II) complex, V2	75
2.7.5.3 G1 DAB quinolyimine Ru(II) complex, V3	75
2.7.5.4 G2 DAB quinolyimine Ru(II) complex, V4	76
2.7.5.5 G1 DAB cationic pyridylimine Ru(II) complex, V5	76
2.7.5.6 G2 DAB cationic pyridylimine Ru(II) complex, V6	77



Chapter 3: Catalytic Application of mono-, bi-, and multinuclear Schiff-base complexes of Methyltrioxorhenium.

UNIVERSITY of the
WESTERN CAPE

3.1 Introduction.....	81
3.2 Methyltrioxorhenium (MTO) complexes in the catalysed epoxidation of olefins.	81
3.2.1 Mechanism of MTO in the epoxidation reactions of olefins.....	83
3.3 Results and Discussions: Epoxidation of cyclohexene and <i>cis</i> -cyclooctene.....	87
3.3.1 Epoxidation catalysed by mono-(C1), and binuclear(C2) Schiff-base MTO complexes.....	87
3.3.2 Epoxidation catalysed multinuclear Schiff-base complexes of MTO metallodendrimers, DC1 and DC2	93

3.4 Conclusions.....	99
3.5 Materials and Methods.....	99
3.5.1 General procedure for the epoxidation of cyclohexene and <i>cis</i> -cyclooctene....	100

Chapter 4: Application of mono-, bi-, and multinuclear neutral and cationic

Ru(II) catalysts in the oxidative cleavage of 1-octene.

4.1 Introduction.....	104
4.2 Catalytic oxidative cleavage of alkenes by ruthenium compounds.....	104
4.2.1 In situ generated ruthenium tetroxide promoted oxidations.....	105
4.2.2.1 Oxidative cleavage of alkenes.....	106
4.3 Mechanism of catalysed oxidative cleavage of alkenes by ruthenium.....	107
4.4 Results and Discussions: Oxidative Cleavage of 1-octene by ruthenium catalysts.....	109
4.4.1 Oxidative cleavage of 1-octene by neutral and cationic mono, bi-, and multinuclear ruthenium catalysts.....	109
4.5 Conclusions.....	116
4.6 Materials and Methods.....	116
4.6.1 General procedure for oxidative cleavage of 2-octene.....	117

Chapter 5: General conclusions and Recommendations.

5.1 General conclusions.....	120
------------------------------	-----

5.2 Recommendations.....121

Annexure:.....123



List of Figure

Chapter 1:

- Figure 1.1: Addictives in the methyltrioxorhenium (MTO) mediated epoxidation with 30% H₂O₂ [31].....15
- Figure 1.2 Binuclear first generation pyridinal imine Ru(II) complex.....17
- Figure 1.3: Tetranuclear second generation quinoline-imine Ru(II) complex.....18

Chapter 2: Synthesis and Characterization of mono-, bi- and multinuclear Ru(II) and Re(VII) complexes directed towards catalytic studies.

- Figure 2.1 General structures of three types of diimine ligands.....25
- Figure 2.2: Some of Schiff-base MTO complexes documented in the literature.....26
- Figure 2.3: A Schematic representation of the synthesized ligands, **L1-L4**, with numbering for NMR analysis.30
- Figure 2.4: ¹H NMR spectrum of **L2**.....34
- Figure 2.5: Plausible fragmentation pathway for bifunctional diimine ligand **L3**.....35
- Figure 2.6: FT-IR spectrum of the complex **C2** recorded using KBr pellets.....38
- Figure 2.7: Schematic representation of a 4th Generation Dendrimer.....47

Figure 2.8: A schematic representation of divergent(left) and convergent (right) approaches to dendrimer synthesis.....	49
Figure 2.9: A schematic representation of the synthesized ligands with numbering for NMR analysis.....	54
Figure 2.10(a): General abbreviation of the diaminobutane skeleton in the dendritic complexes DC1-DC2 and V1-V6.....	56
Figure 2.10(b): General representation the synthesis of MTO dendritic complexes.....	57
Figure 2.11: General representation of the synthesis of neutral Ru(II) dendritic complexes.....	57
Figure 2.12: General representation of the synthesis of cationic dendritic Ru(II) complexes.....	58
Figure 2.13: Electronic spectrum of the catalyst system (V5) system.....	61
Figure 2.14: ¹ H NMR spectrum of dendritic complex, V3 , with inset displaying the aromatic region.....	62

Chapter 3: Catalytic Application of mono-, bi-, and multinuclear Schiff-base complexes of Methyltrioxorhenium

Figure 3.1: Suggested mechanism of methyltrioxorhenium (MTO, C) catalysed epoxidation of alkenes [21,22].....	85
Figure 3.2: A general epoxidation reaction of the alkene substrates.....	87

Figure 3.3: A schematic representation of the Schiff-base MTO complexes.....	88
Figure 3.4: Plot of the consumption of cyclohexene as a function of time.....	91
Figure 3.5: A representation of the novel 1 st and 2 nd generation Re(VII) metallodendrimer tested in the epoxidation of cyclohexene/cis-cyclooctene.....	95
Figure 3.6: Plot of consumption of <i>cis</i> -cyclooctene as a function of time.....	97

Chapter 4: Application of mono-, bi-, and multinuclear neutral and cationic

Ru(II) catalysts in the oxidative cleavage of 1-octene.

Figure 4.1: A general scheme showing the usage of catalytic amounts of RuCl ₃ [10]	105
Figure 4.2: A general scheme pertaining to the synthesis of carboxylic acids [12].....	106
Figure 4.3: A general selective scheme for the synthesis of cis-dihydroxyles [11].....	107
Figure 4.4: A general ruthenium scheme for the epoxidation of alkenes [13].....	107
Figure 4.5: A catalytic cycle for ruthenium-catalyzed oxidative cleavage of olefins [7].....	108
Figure 4.6: A general oxidative cleavage of 1-octene in a biphasic solvent.....	109
Figure 4.7(a): Scheme representing mono- and binuclear neutral and cationic (<i>N,N</i>) Ru(II) catalysts.....	111
Figure 4.7(b): Scheme representing tetra- and octanuclear neutral and cationic (<i>N,N</i>) Ru(II) catalysts.....	112

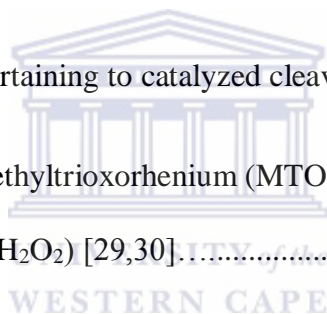
Figure 4.8: ^1H NMR spectra of the crude product (IV) obtained after the ruthenium-catalyzed oxidation of 1-octene (III).....115



Chapter 1: Introduction to Ruthenium and Rhenium complexes in catalyzed oxidation

alkenes.

Scheme 1.1: A general depiction of the catalytic cycle of RuO ₄ [5].....	3
Scheme 1.2: Catalytic cycle of oxidative cleavage of alkenes to acids by cis- [RuCl ₂ (bpy) ₂].2H ₂ O/IO(OH) ₅ [14].....	5
Scheme 1.3: Synthesis of RuCl ₂ (bpy) ₂ compound.....	8
Scheme 1.4: A general scheme pertaining to catalyzed cleavage of 1-octene [15].....	10
Scheme 1.5: Catalytic cycle of methyltrioxorhenium (MTO) mediated epoxidation with hydrogen peroxide (H ₂ O ₂) [29,30].....	13



Chapter 2: Synthesis and Characterization of mono-, bi- and multinuclear Ru(II) and Re(VII) complexes directed towards catalytic studies.

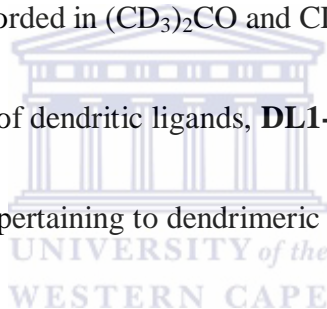
Scheme 2.1: General representation of a Schiff-base condensation reaction.....	24
Scheme 2.2: A Schematic representation of the synthesis of mono- and bi-functional diimine ligands, L1-L4.....	28
Scheme 2.3: General representation of the Schiff-base complexes of MTO.....	36

Scheme 2.4: General representation of the synthesis of neutral mononuclear ruthenium (II) complexes.....	40
Scheme 2.5: General representation of the synthesis of cationic mononuclear cationic ruthenium(II) complexes.....	43
Scheme 2.6: Representation of the synthesis of cationic homobimetallic ruthenium(II) complex B5	44
Scheme 2.7: General representation of the synthesis of dendritic scaffolds, DL1-DL4	51



Chapter 2: Synthesis and Characterization of mono-, bi- and multinuclear Ru(II) and Re(VII) complexes directed towards catalytic studies.

Table 2.1: Analytical data pertaining to ligand synthesis.....	31
Table 2.2: ¹ H NMR spectroscopic data of Schiff-base ligands, L1-L4 , recorded in CDCl ₃ at 25°C.....	33
Table 2.3: ¹ H NMR spectroscopic data of neutral and cationic mononuclear Ru(II) complexes, B1-B5 , recorded in (CD ₃) ₂ CO and CDCl ₃ at 25°C	45
Table 2.4: ¹ H NMR spectral data of dendritic ligands, DL1-DL4	55
Table 2.5: ¹ H NMR spectral data pertaining to dendrimeric Ru(II) complexes, V1-V6	63



Chapter 3: Catalytic Application of mono-, bi-, and multinuclear Schiff-base complexes of Methyltrioxorhenium.

Table 3.1: Catalytic data of the epoxidation of cyclohexene with MTO (C) and catalysts C1 and C2	90
Table 3.2: Catalytic data of the epoxidation of cis-cyclooctene with MTO (C) and catalysts C1 and C2	93
Table 3.3: Catalytic data of the epoxidation of cis-cyclooctene with MTO and DC1 and DC2	96

Table 3.4: Catalytic data of the epoxidation of cyclohexene with MTO (**C**) and catalysts **DC1** and **DC2**.....98

Chapter 4: Catalytic Application of mono-, bi-, and multinuclear Schiff-base complexes of Methyltrioxorhenium.

Table 4.1: Oxidative cleavage of 1-octene to heptanoic acid by **B1-B5** and **V1-V6/NaIO₄**..... 114



List of Abbreviations

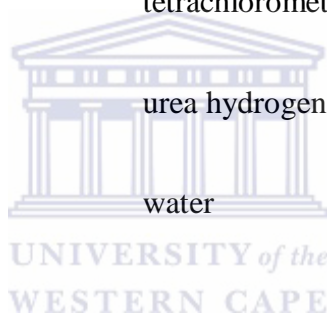
Å	Angstrom
MeCN	Acetonitrile
OAc	Acetate
br	broad
δ	chemical shift
<i>J</i>	coupling constant
COD	1,5-cyclooctadiene
dmp	2,9-dimethyl-1,10-phenanthroline
d	doublet
dd	doublet of doublets
dt	doublet of triplets
DAB	diaminobutane
DMSO	dimethylsulfoxide
DCM	dichloromethane
DMSO- <i>d</i> ₆	deuterated dimethylsulfoxide
ESI-MS	Electron Spray Ionisation Mass Spectrometry
FT-IR	Fourier Transform Infra Red

List of Abbreviations

GC-FID	Gas Chromatography Flame Ionisation Detector
hr(s)	hour(s)
Hz	hertz
m	multiplet
M.p.	melting point
min	minutes
m/z	mass to charge ratio
ml	millilitres
mmol	millimole
Me	methyl
MHz	megahertz
MTO	Methyltrioxorhenium
NMR	Nuclear Magnetic Resonance
PPI	polypropyleneimine
ppm	parts per million
pyr	pyridine
quin	quinoline

List of Abbreviations

r.t	room temperature
r.b.f	round bottom flask
NaIO ₄	Sodium periodate
TBHP	tert-butyl hydrogen peroxide
TO	turn over
CCl ₄	tetrachloromethane
UHP	urea hydrogen peroxide
H ₂ O	water



1.1 *Ruthenium in the catalyzed transformation of alkenes.*

1.1.1 *Introduction.*

Alkenes (synonymously olefins) are a family of hydrocarbons that represent convenient starting material in the synthesis of organic chemicals due to their availability in fairly high purity and at relatively low cost. Much of their reactivity involves the introduction of additional or alternate functional groups to the material, and this is often conveniently achieved by reaction at the carbon-carbon double bond(s).

Alkene oxidation is a subject of fundamental interest, which profoundly impacts the development of synthetic organic chemistry [1]. Oxidation reactions constitute core technologies for the synthesis of chemical intermediates in the production of both high-tonnage commodities [2] and high-value fine chemicals, such as agrochemical and pharmaceutical precursors.

One of the fundamental oxidation reactions is the oxidative cleavage of alkenes. This has been previously done using stoichiometric reagents such as KMnO_4 . For the past few decades catalyzed oxidative cleavage has gained intense focus.

Literature documents two main pathways for the oxidative cleavage, namely:

- Transformation of olefins into 1,2-diols followed by oxidative cleavage [3a]
- Direct cleavage into a variety of functionalized products dependent on the conditions applied [3b]

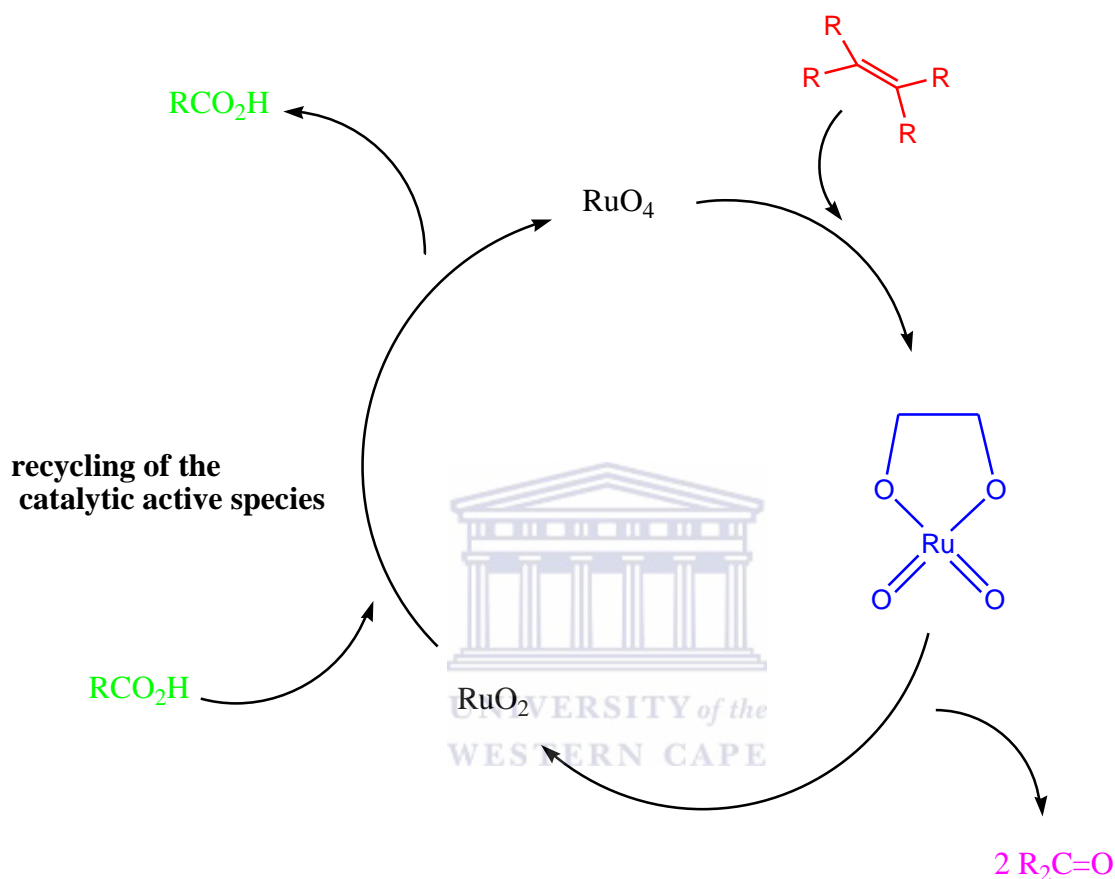
Within the scope of catalyzed reactions, ruthenium compounds constitute a versatile class of catalysts for important synthetic transformations in organic chemistry [4].

1.1.2 *One-step oxidative cleavage applying ruthenium catalysts and percarboxylic acids as oxidants.*

The short-comings that are associated with the two-step synthesis are: low overall selectivity and poor yields for a variety of long chain substrates. These drawbacks that are imposed by the previous invention are well addressed by the catalyst systems with only one metal species. For the fragmentation of the olefinic bonds, only one metal proves superior in the one-step cleavages i.e. ruthenium.

Ruthenium tetroxide (RuO_4) was introduced by Djerassi and Engle in 1953 as an organic oxidant [5]. Dating from then, its utility for a variety of oxidative transformations has been recognized immensely [6]. The expense of ruthenium metal provided incentive for the development of catalytic procedures, the most popular of which involve use of periodate or hypochlorite as the stoichiometric oxidant [6]. Since it is toxic and volatile it is usually made *in situ* from $\text{RuCl}_3 \cdot n\text{H}_2\text{O}$ or $\text{RuO}_2 \cdot n\text{H}_2\text{O}$ with co-oxidant, normally sodium periodate, NaIO_4 .

Parallel to osmium-catalysed fragmentations, ruthenium tetroxide, RuO_4 , when reacting with the olefinic carbons confers the ruthenate (VI) ester intermediate. In a study disclosed by Muharashi *et al.*, the nature of the active species was investigated [5] due to suggestions of the formation of metal-oxo intermediate by low-valent ruthenium complexes.



Scheme 1.1: A general depiction of the catalytic cycle of RuO₄ [5].

The availability of alkenes as convenient starting materials for functionalization so as to obtain desired functionality steered scientists in exploring ways to take advantage of the oxo-transfer reactions. Oxidative cleavage of alkenes is one way of converting unsaturated hydrocarbons to more valuable oxygenates. In the previous invention this was done in a stoichiometric manner using ozone or permanganate solutions and the more recent adjustments indicated that it can also be performed catalytically using a transition metal and

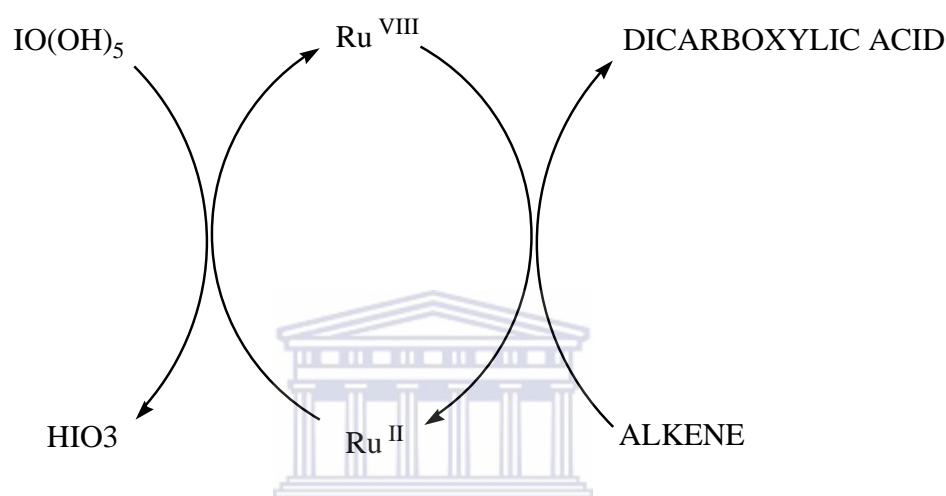
an oxidant such as IO_4^- or H_2O_2 . Typically group 7 and 8 metals have been found to be effective as catalysts for this process [7-9].

Transition metal complexes with their tunable coordination environments and versatile redox and spectral properties have been used for oxidative cleavage of DNA and as a model for chemotherapeutic agents. Typical examples of these DNA cleavers are iron-bleomycin, Fe(II)-EDTA, Mn(II)-porphyrin, nickel complexes, Co, Rh, and Ru complexes of phenanthroline or bipyridine and $[\text{Cu}(\text{Phen})_2]^{2+}$ [10].

$\text{RuCl}_3 \cdot n\text{H}_2\text{O}$ is no stranger to oxidative cleavage of alkenes to acids, it has been used in a number of systems. Wolfe *et al.* [11] reported the oxidation of cyclohexene to adipic acid by stirring a solution of cyclohexene in CH_2Cl_2 with an aqueous solution of $\text{RuCl}_3 \cdot n\text{H}_2\text{O}$ and NaOCl . The most widely used procedure is reported by Carlesen *et al.*, in which cyclopentene was converted into glutaric acid by employing $\text{RuCl}_3 \cdot n\text{H}_2\text{O}$ as a catalyst with NaIO_4 as a cooxidant in a biphasic $\text{CH}_3\text{CN}-\text{CCl}_4-\text{H}_2\text{O}$ solution [17]. Haloalkenes were oxidized to their acids using $\text{RuO}_2 \cdot n\text{H}_2\text{O}$ with either NaIO_4 or NaOCl as cooxidants. However, the observable hindrance of these prepared catalyst systems is the formation of the sparingly soluble NaIO_3 and/or NaCl throughout the oxidation process in water with a specified solvent quantity. These solids impact on the workup of the reaction by remaining at the end of the reaction. Shoair *et al.* reported on the proposed mechanism for the oxidative cleavage of alkenes with the catalyst system $\text{cis}-[\text{RuCl}_2(\text{bpy})_2] \cdot 2\text{H}_2\text{O}/\text{IO}(\text{OH})_5$ [14]. The oxidative cleavage of alkenes to acids by the catalyst system is likely to proceed through a similar mechanism as that suggested for RuO_4 . In this mechanism, the produced RuO_4

cleaves the alkene to acid and itself converts into RuO_2 , which in turn will be further oxidized to RuO_4 by excess $\text{IO}(\text{OH})_5$ according to the following scheme 1.2.

:



Scheme 1.2: Catalytic cycle for oxidative cleavage of alkenes to acids by *cis*- $[\text{RuCl}_2(\text{bpy})_2] \cdot 2\text{H}_2\text{O}/\text{IO}(\text{OH})_5$ [14].

Ruthenium tetraoxide, RuO_4 , has long been known for being a much more vigorous oxidant than its osmium analogue, capable of readily cleaving $\text{C}=\text{C}$ double bonds. The reaction can be carried out with catalytic amounts of RuO_4 , which is neither explosive nor poisonous and therefore has advantage over ozonolysis reactions and the $\text{C}=\text{C}$ bond cleavage with chromium oxide [16]. Alkenes that have been functionalized into corresponding acids with additional or alternate functional groups carry more benefits. One commonly used method of introducing functionality is to employ an oxidative cleavage reaction of the $\text{C}=\text{C}$ double bond to produce one or more hydroxyl and/or carbonyl groups. Several methods are available for achieving this, including the use of reagents such as potassium permanganate, osmium and ruthenium tetraoxide, often known as stoichiometric reagents. Despite the reported high yields ranging

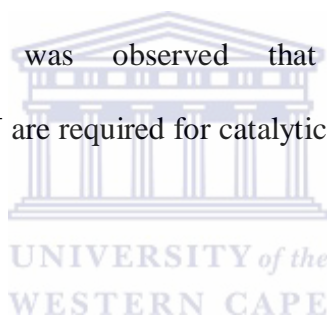
from 80 to 97% of osmium tetroxide catalysed-oxidative cleavage of olefins with acids, the osmium derivatives bear a negative aspect such as high-priced oxidant, ozone, in stoichiometric amounts with the handling complexity that it encompasses. A recent report on four different “easy-to-handle” osmium sources, that are an alternative to the previously employed osmium tetroxide (OsO_4), exhibited enhanced catalytic activity than the osmium tetroxide., OsO_4 [9].

As a result of the problems encountered with the previous mentioned inventions, a catalyst system, RuCl_3 , reported by Barak and Sasson *et al.* [12] identified a new route being undertaken for the catalytic oxidation of styrene to benzaldehyde or acetophenone with hydrogen peroxide, H_2O_2 , as an oxidant. The report of Shoair and Mohamed *et al.* on the oxidative cleavage of alkenes to carboxylic acids by $\text{cis-}[\text{RuCl}_2(\text{bpy})_2]\cdot 2\text{H}_2\text{O}$ in the presence of $\text{IO}(\text{OH})_5$ was reported to lack ability to oxidatively cleave some of the commercially prominent substrates such as oct-1-ene and non-2-ene. A system that employs peracetic acid reported by Warwel *et al.* in their publication covered the failure of their system when hydrogen peroxide was used as an oxidant.

1.1.3 *Some of the ruthenium catalysts documented in the literature for oxidation reactions:*

1.1.3.1 *Synthesis and Study of Mononuclear Ruthenium(II) Complexes of Sterically hindered diimine Chelates.*

Colins and Sauvage reported on the synthesis and study of mononuclear ruthenium(II) complexes with sterically hindered diimine chelates. They used 6,6'-dimethyl-12,2'-bipyridine (6,6'-dmbp) or 2,9-dimethyl-1,10-phenanthroline (2,9-dmp) in their study. The electrochemical behaviour of the complexes was investigated in relation to the oxidation of water to form molecular oxygen. The study concluded that the complexes were not active for the catalyzed oxidation of water as it was observed that dinuclear species such as $(\text{bpy})_2(\text{H}_2\text{O})\text{RuORu}(\text{H}_2\text{O})(\text{bpy})_2^{4+}$ are required for catalytic regeneration of molecular oxygen from water [16(a)].

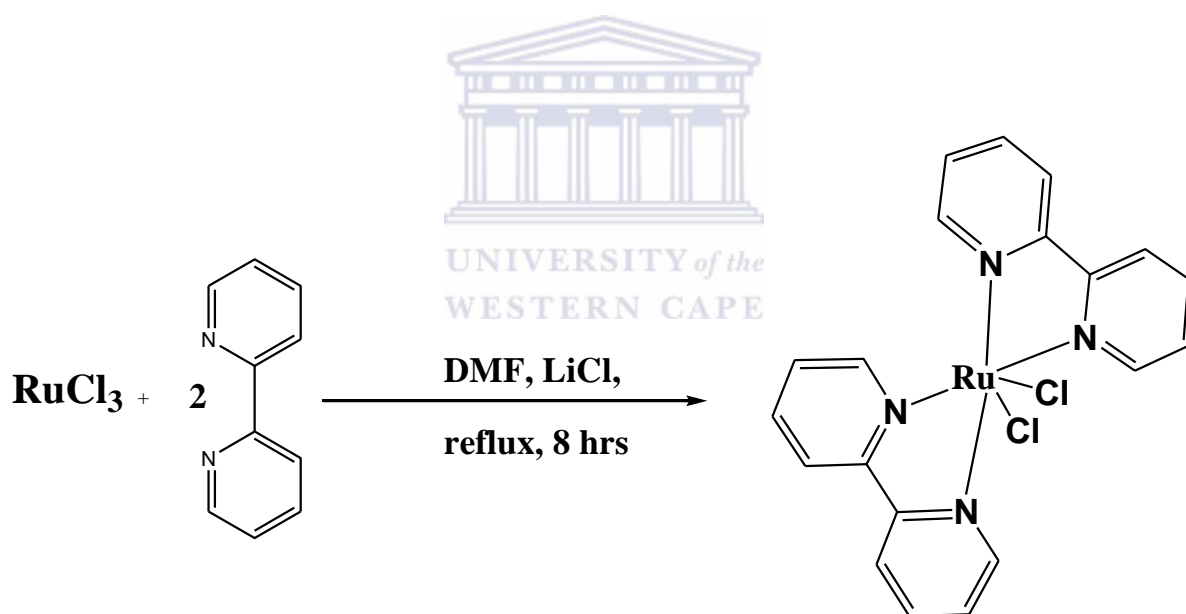


1.1.3.2 *Synthesis of ruthenium (II) perchlorate complexes.*

Vancheesa *et al.* [16(b)] reported the catalytic oxidation of alkenes with ruthenium (II) perchlorate complexes $([\text{Ru}(\text{dppm})_3(\text{ClO}_4)]\text{ClO}_4$, $[\text{Ru}(\text{dppe})_3(\text{ClO}_4)]\text{ClO}_4$, $[\text{Ru}(\text{dpae})_3(\text{ClO}_4)]\text{ClO}_4$) under mild and homogeneous conditions in the liquid phase with TBHP and H_2O_2 as oxidizing agents. The ruthenium complexes that were employed were prepared as reported in literature [5]. The complexes were prepared by the general method of treating ruthenium (III) perchlorate with excess of the ligand (L-L) in absolute alcohol under reflux. Complexes $[\text{Ru}(\text{dppe})_3(\text{ClO}_4)]\text{ClO}_4$ and $[\text{Ru}(\text{dpae})_3(\text{ClO}_4)]\text{ClO}_4$ were obtained by an alternative route through the interaction of $[\text{RuCl}_3(\text{AsPh}_3)(\text{MeOH})]$ with a 10-mol excess of sodium perchlorate followed by the addition of the ligands 1,2-bis(diphenylphosphino)ethane (dppe) and 1,2-bis(diphenylarsino)ethane (dpae), respectively.

1.1.3.3 *Synthesis of ruthenium (II) bipyridine complex, RuCl₂(bpy)₂.*

The modification, as depicted below, for the preparation of the complex *cis*-(bpy)₂RuCl₂·2H₂O was developed by weaver *et al.* and was utilized to give good yields of the complex. The complex was used in chemoselective degradation of a range of phenyl and fused hydroaromatic substrates with NaIO, in CH₂Cl₂-H₂O solution at room temperature to their corresponding monocarboxylic and dicarboxylic acids and it was found to be highly effective catalytic system with RuO₄ generated *in situ* [16c,16d].



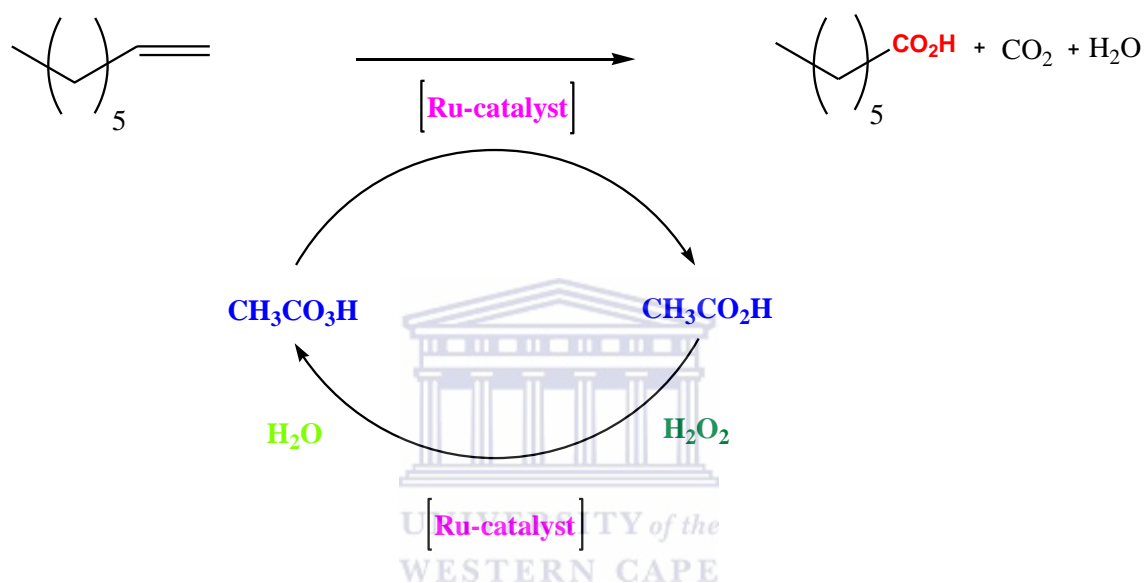
Scheme 1.3: Synthesis of RuCl₂(bpy)₂ compound.

Yang *et al.* [13] reported the use of RuCl₃ as the catalyst system for the oxidative cleavage of olefins to aldehydes instead of carboxylic acids from olefins that were not fully substituted.

1.1 *Optimized catalyst systems and reaction conditions.*

The system “RuO₄”/peracetic acid (on-site-formed peroxyacetic acid from H₂O₂, acetic acid, and H₂SO₄ as catalyst) upon reacting with an olefin i.e., 1-octene, yields two different primary products, i.e. 1-heptanal and formic acid, mediated by the ruthenium catalyst, and 1-octenoxide, formed by direct epoxidation of the olefin by peracetic acid. The octene oxide can further be oxidized to the corresponding acid by the peracid, this is achieved by solvolysis into the glycol. The theoretical value of ¼ for the molar ratio of olefins to peroxyacid generally needed is great i.e. 1/5 to 1/6, an excess of peroxyacetic acid increases the yield of the desired carboxylic acid at an optimized pH of ca. 2 (Na₂CO₃/H₂SO₄ buffer). The ratio that is normally used for the catalyst to substrates totals to 1/1000, conceding the best selectivities. However, the extraordinary activity of the ruthenium-containing catalyst can be followed to even higher catalyst/substrate ratio i.e. 1/60000, with a reported 15% yield of heptanoic acid. Thus, the outstanding catalytic activity rendered by the ruthenium catalyst singles out this metal for the oxidative cleavage of C=C double bonds. The best solvents have been reported to be water/n-hexane mixtures (two-phase) system. Strong coordinating solvents such as DMF, acetonitrile, or THF are less suitable. The most prominent drawback of the ruthenium catalysts is their high activity in decomposing hydrogen peroxide. Donor ligand-substituted ruthenium compounds like RuCl₃(PPh)₃ or RuCl₃(dmp)₂ exhibited significantly notable lower decomposition of the environmentally benign oxidant, H₂O₂, than RuO₄ or RuCl₃. Thus, by employing these complexes in acetic acid as a solvent, it is possible to activate H₂O₂ without its quick degradation with an increase in the acid formation

accompanied by increased conversion as well. It has been speculated that *In-situ*-formed peracetic acid is acting as the chief oxidant during the catalytic cycle (scheme 4) [15].



Scheme 1.4: A general scheme pertaining to catalyzed cleavage of 1-Octene [15].

From the previous problems of assembling a catalyst precursor that would produce some of the commercially in demand carboxylic acids from readily available alkenes, it has been discovered that various “novel” low-valent ruthenium-catalyzed reactions can be explored.

It is within the scope of this review to report on the previous inventions as rudimentary tools for the synthesis of even more sterically demanding catalyst systems for selective oxidation/epoxidation of selected olefins. Hence this review seeks to address some of the short-comings of the previous catalytic endeavours for these olefinic fragmentation/oxo-transfer patterns and to introduce a new mode of these fragmentation employing dendrimeric

ruthenium/rhenium skeletons that would be complemented by the electronic and steric factors to accomplish the desired mission: selective oxidative cleavage and epoxidation of alkenes catalytically.

1.3 *Why ruthenium?*

Ruthenium is found in group 8, directly beneath iron, within the d-block of the periodic table. Ruthenium has an extremely extensive coordination chemistry that combines relatively facile ligand substitution reactions with good product stability. Its complexes show well-understood redox and photochemical properties and are of interest for various practical applications, both currently (e.g. in catalysis) and future (e.g., in molecular electronics). Osmium tetroxide is expensive and very poisonous, and it seemed of interest, therefore, to investigate the behaviour of the corresponding ruthenium derivative, since ruthenium appears immediately above osmium in the periodic table. Being isoelectronic with OsO₄, RuO₄ is a powerful oxidant that cleaves the C=C bond upon reaction with alkenes [16].

1.4 *Introduction to Epoxidation.*

The oxidation of organic compounds and the transformation of stoichiometric reactions into catalytic processes have been under active investigation for several decades [19]. Epoxidation is an important transformation of alkenes, because epoxides are versatile intermediates in organic synthesis. The use of transition metal complexes as epoxidation

catalysts is of particular interest [20], due to their ability to activate environmentally benign oxidants such as molecular oxygen [21] and hydrogen peroxide, H_2O_2 [22,23]. Industrial transformations of olefins into epoxides commonly involve the use of catalysts associated with oxygen, hydrogen peroxide or organic peroxides. Stoichiometric oxidants are still commonly used mainly for the oxidation of fine chemicals [24].

1.4.1. Discovery of *Methyltrioxorhenium (MTO)*.

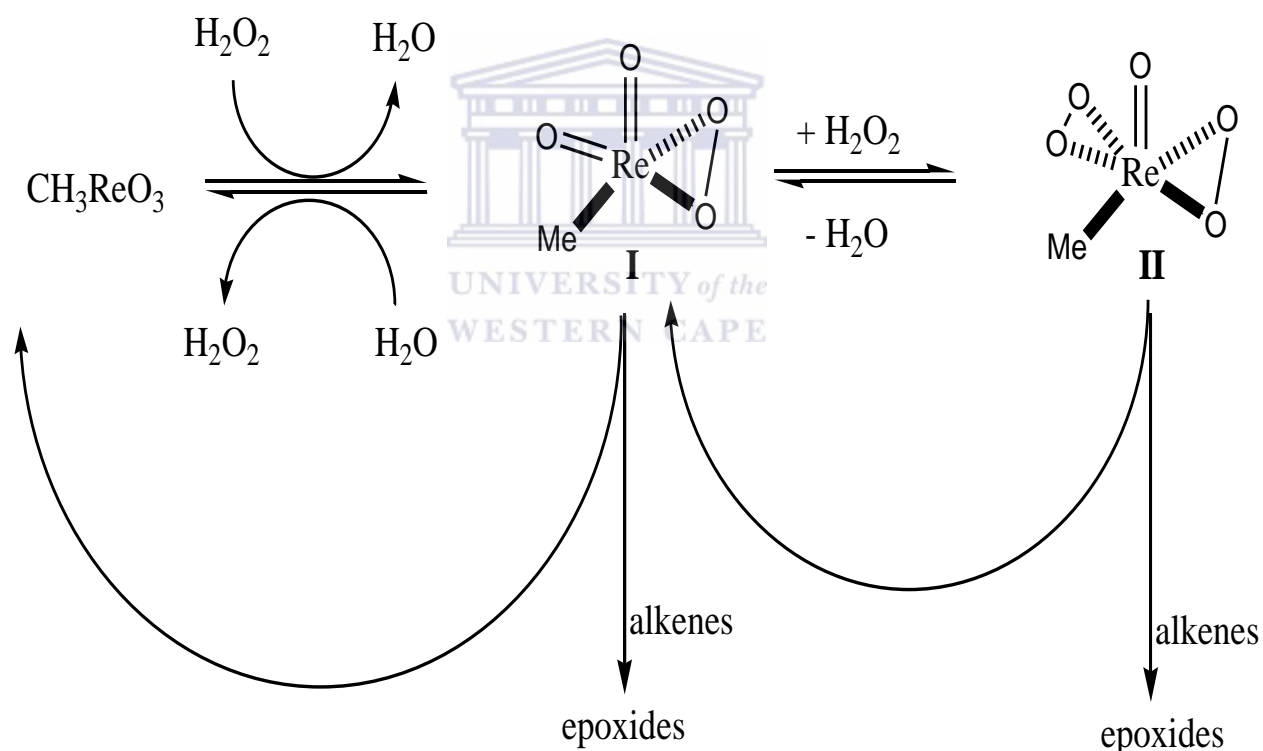
An important improvement in the field of catalytic epoxidation arose with the discovery of the catalytic activity of methyltrioxorhenium (VII) (CH_3ReO_3 , MTO) [24] by Herrmann and co-workers in 1991 [25]. With its exposure, MTO has emerged as one of the most active catalysts for alkene epoxidation in the presence of H_2O_2 as the terminal oxidant.

1.4.2 *Methyltrioxorhenium (MTO) in the epoxidation reactions of olefins.*

MTO-catalyzed epoxidation was initially investigated in a homogeneous medium using tert-BuOH as solvent with anhydrous H_2O_2 [27, 28]. While high yields of certain epoxides may be obtained by this procedure, the main disadvantage, however, was the low selectivity in the cases where acid sensitive epoxides were formed. The Lewis acidity of the rhenium centre caused hydrolysis and the concomitant cleavage of the epoxide ring leading to the formation of 1,2-diols in the presence of water [27]. Several methods have been suggested during recent years to overcome this problem [28].

1.4.3 Mechanism of the catalytic cycle of methyltrioxorhenium (MTO).

MTO does not undergo redox chemistry during catalytic reactions; it remains in the +VII oxidation state. MTO activates H_2O_2 through an equilibrium formation of the η^2 -peroxo species I and II. The structure of II (scheme 1.5) was confirmed crystallographically, and the methyl resonances of I and II were detected by both ^1H and ^{13}C NMR [29, 30].

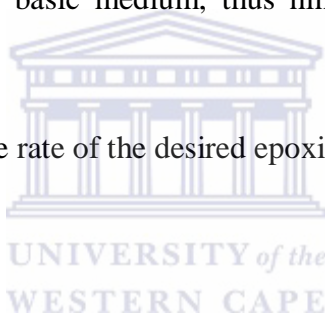


Scheme 1.5: Catalytic cycle of methyltrioxorhenium (MTO) mediated epoxidation with hydrogen peroxide (H_2O_2) [29, 30].

A very interesting approach to limit the deleterious side reactions is the use of Lewis bases as additive to the biphasic (H₂O/organic solvent) catalytic system [27].

None of the procedural-modifications to MTO-mediated epoxidations satisfactorily addressed the issue of acidity until Sharpless and co-workers tested pyridine in the system [32]. This additive confers two important features.

- First, it creates a slightly basic medium, thus hindering ring opening of the acid-sensitive epoxides, and
- Secondly, it accelerates the rate of the desired epoxidation reaction



Herrmann had previously investigated the use of nitrogen bases in MTO-catalyzed epoxidations but did not observe significant ligand-accelerated catalysis [33] because the amines used were oxidized to amine N-oxides under the reaction conditions [34,35]. Additionally, it was found that the use of 3-cyanopyridine and pyrazole as the Lewis bases is more effective and less problematic than the use of pyridine as additive in methyltrioxorhenium-mediated epoxidations as depicted in Figure 1.1. The pyridine oxide forms a highly selective though less active cocatalyst with MTO/H₂O. Conversely, it has been reported that bipyridine N,N-dioxide is an effective species with respect to reducing the acidity of the catalytic system, suppressing the diol formation [19].

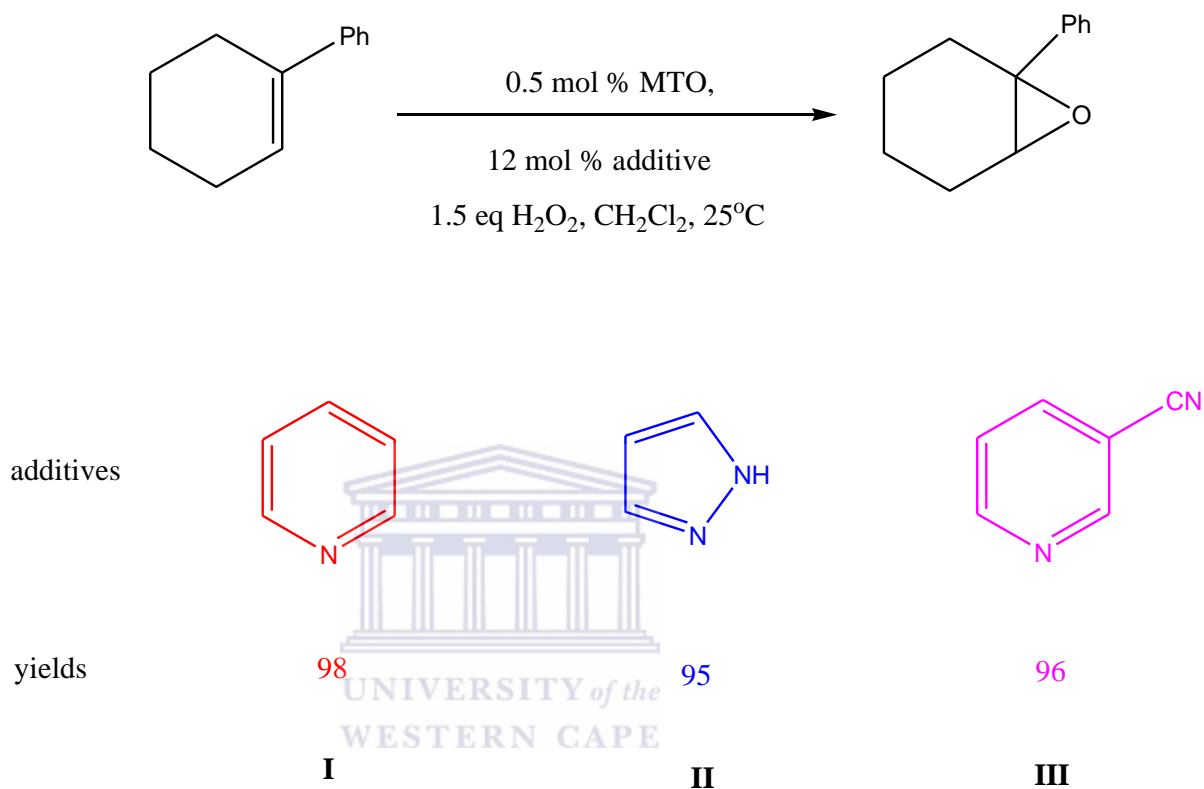


Figure 1.1: Additive in the methyltrioxorhenium (MTO) mediated epoxidation with 30% H₂O₂ [31].

Whilst the conversion of the amines (to amine N-oxides) was observed, amine N-oxides also exhibited weaker donor capacity than the corresponding amines, resulting in less selective but more active complexes.

There are relatively few documented disadvantages of MTO/base systems in epoxidation.

Some of the documented cases include:

- Cases where the separation of the additive from the product was experienced
- Separation of acid-sensitive epoxides from bases having similar boiling points can be experimentally cumbersome since the product may not survive treatment of the crude reaction mixture with acid or exposure to silica.

With few exceptions [36-38], additives only work when used in an aprotic medium like nitromethane or chlorinated solvents, but such solvents pose the risk of explosion and there are toxicity issues for large scale reactions rendering them not suitable. Nevertheless, MTO-catalyzed epoxidations are a very attractive option, particularly for small-scale epoxidation reactions. MTO has been employed in the epoxidation of variety of diverse alkenes with both aliphatic and aromatic substituents.

The scope of this research endeavour is to investigate the epoxidation ability of the prepared dendritic Schiff base-MTO complexes. It is also within the scope of this thesis to investigate the catalytic activity afforded by the synergy of the multinuclear dendrimer compared to the mono- and homobimetallic MTO analogues.

1.5 Aims and Objectives.

The proposed work for this MSc project was to develop dendritic complexes of ruthenium and rhenium which could be employed in the oxidative cleavage/epoxidation reactions of alkenes, respectively. The dendritic complexes are based on dendrimeric diimine ligands of which several types have been reported. An example of a target complex (ruthenium) prepared is shown below. This compound requires a 1:2 molar ratio of a Ruthenium metal complex and the first generation DAB-PPI ligand.



Figure 1.2: Binuclear first generation pyridinal imine Ru(II) complex.

The steric bulk around the complex active site is advantageous in achieving higher yields. In an attempt to increase the steric bulk around the active site we increased the steric bulk of the dendrimer by preparing dendrimeric quinoliny-imine ligands and employing these for the

formation of multinuclear ruthenium complexes. An example of a second generation quinolinyl-imine complex of ruthenium is again shown in Figure 1.3 below.



Figure 1.3: Tetranuclear second generation quinoline-imine Ru(II) complex.

With the aim of evaluating other transition metals as catalysts, our metal precursors were also extended to methyltrioxorhenium (MTO) thus producing novel dendrimeric catalysts. All the dendritic ruthenium complexes were employed as catalyst precursors in the oxidative cleavage of long chain alkenes (C8 and greater) to produce carboxylic acids whilst rhenium dendritic complexes will be exploited for their epoxidation ability. Different oxidants ($\text{IO}(\text{OH})_5$, tetrabutylhydroperoxide, IO_4^- or H_2O_2) were evaluated to ascertain the most

effective catalyst system. The following reaction parameters were thoroughly investigated, including: use of different solvents, reaction time and reaction temperature.

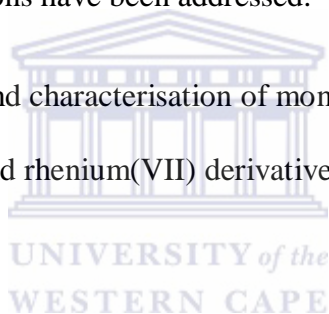
In conclusion the thesis is structured as follows:

Chapter 1 highlights the developments in the literature concerned with the oxidative cleavage and epoxidation, respectively, of alkenes and briefly summarizes how some of the shortcomings of previous inventions have been addressed.

Chapter 2 details the synthesis and characterisation of mono-, bi- and multifunctional ligands and their ruthenium(II) and rhenium(VII) derivatives respectively, in preparation for catalytic studies.

Chapter 3 outlines the use of Schiff-base MTO adducts as catalyst precursors for the epoxidation of selected olefin substrates

In **Chapter 4** extensive comparison of the prepared complexes is discussed pertaining oxidative cleavage of 1-octene.



References:

1. *Modern Oxidation Methods*; Backvall, J.E., Ed.; Wiley-VCH: 2004
2. S-I Murahashi, *Ruthenium in Organic Synthesis*. Wiley-VCH, Weinheim, 2004.
3. (a) K. T. M. Shing, *Comprehensive Organic Synthesis*, (Eds.: Trost, B. M, Flemming, I). 1991, **7**, 703-716, *Pergamon Press, Oxford*, 1991: (b) C. R. Larock, *Comprehensive Organic Transformations*, 2nd edn, Wiley-VCH, 1999, p 1213 – 1215, Wiley-VCH, New York.
4. K. Weissermel, J-J. Arpe, *Industrial Organic Chemistry*, Wiley-VCH, Weinheim, 2003.
5. C. Djerassi, R.R.J. Engle, *J. Am. Chem. Soc.*, 1953, **75**, 3838.
6. D. G. Lee, M. Van den Engh, In "*Oxidation in Organic Chemistry*"; Trahanovsky, W. S., Ed.; Academic Press: **New York**, 1973; Part B, Chapter **4**.
7. A. Haimov, H. Cohen, R. J. Neumann, *J. Am. Chem. Soc.*, 2004, **126**, 11762.
8. J. Sundermeier, C. Dobler, *Modern Oxidation Methods*; Backvall, J. E., Ed.; Wiley-VCH: Weinheim, Germany, 2004; p 1.
9. J. Brinksma, L. Schmeider, G. van Vleit, R. Boaron, R. Hage, D. E. de Vos, D. E.; P. L. Alsters, B. Feringa, *Tetrahedr. Lett.*, 2002, **43**, 2619.
- 10.(a) C. J. Burrows, J. C. Muller, *Chem. Rev.*, 1998, **98**, 1109. (b) C. B. Chen, L. Milner, R. Landgraf, D. M. Perrin, D. S. Sigman, *Chembiochem*, 2001, **2**, 735. (c) H. T. Chifotides, K. R. Dunbar, *Acc. Chem. Res.*, 2005, **38**, 146. (d) A. M. Pizarro, P. J. Sadler, *Biochimie*, 2009, **91**, 1198-1211. (e) W. K. Pogozelski, T. D. Tullius, *Chem. Rev.*, 1998, **98**, 1089.
11. S. Wolfe, S. K. Hasan, J. R. Campbell, *J. Chem. Soc., Chem. Commun.*, 1970, 1420.

12. (a) G. Barak, Y. Sasson, *J. Chem. Soc., Soc. Commun.*, 1987, 126. (b) G. Barak, Y. Sasson, *J. Chem. Soc., Soc. Commun.*, 1987, 1266.
13. D. Yang, C. Zhang, *J. Org. Chem.*, 2001, **66**, 4814.
14. A. G. F. Shoair, R.H. Mohamed, *Synthetic Communications*, 2006, **36**, 59.
15. F. E. Kühn, R. W. Fischer, W. A. Herrmann, T. Weskamp. (2008). *Oxidative Cleavage of Olefins, in Transition Metals for Organic Synthesis: Building Blocks and Fine Chemicals*, Second Revised and Enlarged Edition (eds M. Beller and C. Bolm), Wiley-VCH Verlag GmbH, Weinheim, Germany. doi: 10.1002/9783527619405.ch51
16. J. P. Collin, J. P. Sauvage, *Inorg. Chem.*, 1985, 25, 2. (b) A. S. Kanmani, S. Vancheesan, *J. Mol. Catalysis A: Chemical*, 1999, **150**, 95. (c) A. K. Chakraborti, B. K. Banik, U. R. Ghatak, *Indian. J. Chem.*, 1984, **24B**, 291. (d) A. K. Chakraborti, U. R. Ghatak, *J. Chem. Soc., Perkin. Trans.*, 1985, **1**, 2605.
17. P. H. J. Carlesen, T. Katsuki, V. S. Martin, K. B. Sharpless, *J. Org. Chem.* 1981, **46**, 3936.
18. (a) D. G. Lee, T. Chen., In “Comprehensive Organic Synthesis”, (b) B. M. Trost, I. Fleming, S. V. Ley, Eds.; Pergamon: Oxford, 1991; Vol **17**, Chapter 3.8 (c) S. Wolfe, S.K Hassan, J.R. Campbell, *J. Chem. Soc., Chem. Commun.*, 1970, 1420.
19. P. Ferreira; W-M. Xue, E. Bencze, E. Herdtweck, F. E. Kühn. *Inorg. Chem.*, 2001, **40**, 5834.
20. (a) R. A. Sheldon and J. K. Kochi, *Metal-Catalyzed Oxidation of Organic Compounds*, Academic Press, New York, 1981; (b) G. Strukul, *Catalytic Oxidation with Hydrogen Peroxide as Oxidant*, Kluwer Academic Publishers, New York, 1992; (c) C. W. Jones, *Application of Hydrogen Peroxide and Derivatives*, Royal Society of Chemistry, Cambridge, 1999; (d) W. Adams, *Peroxide Chemistry*, Wiley-VCH,

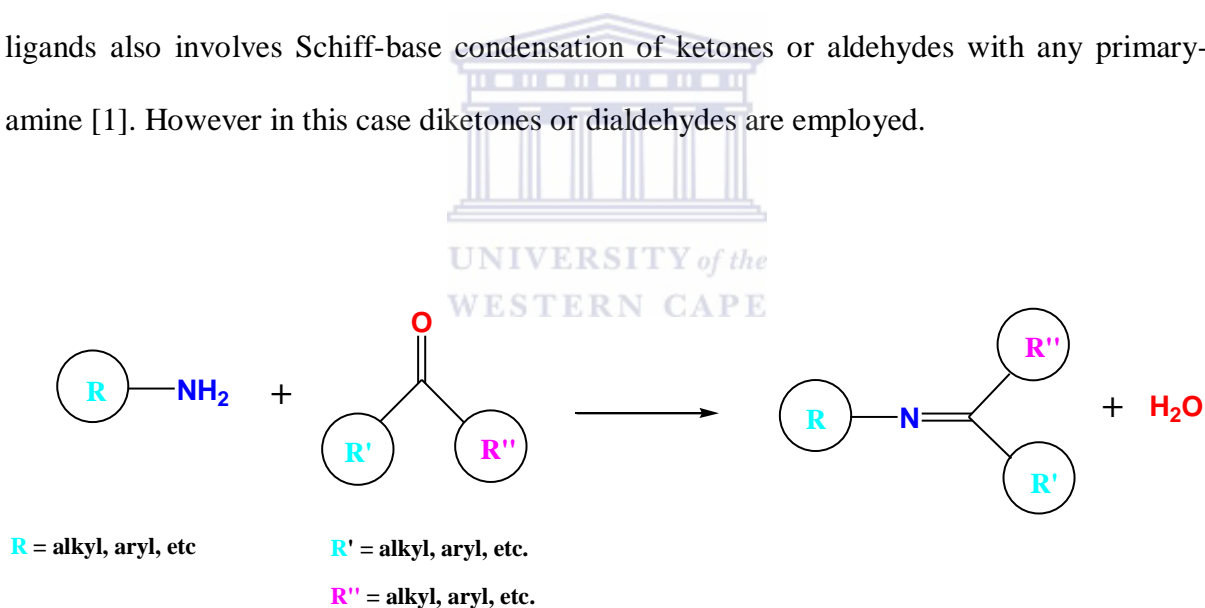
- Weinheim, 2000; (e) J. –E. Backvall, *Modern Oxidation Methods*, Wiley-VCH, Weinheim, 2004
21. A review on epoxidation using O₂ as an oxidant: T. Makaiyama and T. Yamada, *Bull. Chem. Soc. Jpn.*, 1995, **68**, 17.
22. Reviews on epoxidation using H₂O₂ as an oxidant: (a) N. Mizuno and Y. Yamaguchi, *Chem. Rec.*, 2006, **6**, 12.; (b) G. Grigoropoulou, J. H. Clark and J. A. Elings, *Green Chem.*, 2003, **5**, 1.; (c) B. S. Lane and K. Burgess, *Chem. Rev.*, 2003, **103**, 2457.
23. Recent examples of efficient metal-catalyzed epoxidation using aqueous H₂O₂ see; (a) K. Sato, M. Aoki, M. Ogawa, M. Hashimoto, D. Panyella and R. Noyori, *Bull. Chem. Soc. Jpn.*, 1997, **70**, 905. (b) M. C. White, A. G. Doyle and E. N. Jacobsen, *J. Am. Chem. Soc.*, 2001, **123**, 7194.; (c) K. Kamata, K. Yonehara, Y. Sumida, K. Yamaguchi, S. Hikichi and N. Mizuno, *Science*, 2003, **300**, 964.; (d) N. Gharah, S. Chakraborty, A. K. Mukherjee and R. Battacharyya, *Chem Comm.*, 2004, 2630.; (e) M. Klawonn, M. K. Tse, S. Bhor, C. Dobler and M. Beller, *J. Mol. Catal. A: Chem.*, 2004, **218**, 13.
24. R. Jira; R. A. Sheldon. *In Applied Homogeneous Catalysis with Organometallic Compounds*; B. Cornils, W. A. Herrmann, Eds.; Wiley-VCH: Weinheim, 1996; Vol. **1**, p 374.
25. (a) J. H. Espenson, *Chem Commun.*, 1999, 479; (b) G. S. Owens; J. Arias and M. M. Abu-Omar, *Catal. Today.*, 2000, **55**, 317; (c) F. E. Kuhn, A. Scherbaum and W. A. Herrmann, *J. Organomet. Chem.*, 2004, **689**, 4149.
26. W. A. Herrmann, R. W. Fischer, M. U. Rauch and W. Scherer, *Angew. Chem.*, Int. Ed. Engel., 1991, **30**, 1638.
27. W. A. Herrmann, R. W. Fischer, M. U. Rauch and W. Scherer, *J. Mol. Catal.*, 1994, **86**, 243.

28. (a) F. E. Kühn, W. A. Herrmann, *Chemtracts: Org. Chem.*, 2001, **14**, 59. (b) F. E. Kühn, W. A. Herrmann, In *Structural Bonding*; Meunier, B., Ed.; Springer-Verlag: Heidelberg, Berlin, 2000; Vol. 97, p 213. (c) W. Adam, C. M. Mitchell, C. R. Saha-Moller, Springer-Verlag: Heidelberg, Berlin, 2000; Vol. 97, p 237.
29. P. Gisdakis, S. Antonczak, S. Kostlmeier, W. A. Herrmann, N. Rosch, *Angew. Chem.*, Int. Ed. Engl. 1998, **37**, 2211.
30. Y. -D. Wu, J. Sun, *J. Org. Chem.*, 1998, **63**, 1752.
31. B. S. Lane, K Burgess, *Chem. Rev.*, 2003, **103**, 2461.
32. J. Rudolph, K. L. Reddy, J. P. Chiang, K. B. Sharpless, *J. Am. Chem. Soc.*, 1997, **119**, 6189.
33. W. A. Herrmann, F. E. Kühn, M. R. Mattner, G. R. J. Artus, M. R. Geisberger, J. D. G. Correia, *J. Organomet. Chem.*, 1997, **538**, 203.
34. C. Coperat, H. Adolfsson, T-A. V. Khuong, A. K. Yudin, K. B. Sharpless, *J. Org. Chem.*, 1998, **63**, 1740.
35. C. Coperat, H. Adolfsson, T-A. V. Khuong, A. K. Yudin, K. B. Sharpless, *Tetrahedr. Lett.*, 1998, **39**, 761.
36. G. S. Owens, M. M. Abu-Omar, *Chem. Commun.*, 2000, 1165
37. G. S. Owens, A. Durazo, M. M. Abu-Omar, *Chem. Eur. J.*, 2002, **8**, 3053.
38. J. Iskra, D. Bonnet-Delpon, J. -P. *Tetrahedr. Lett.*, 2002, **43**, 1001.

2.1 Introduction.

2.1.1 Diimine ligands.

Imine formation can be achieved when any primary amine reacts with an aldehyde or ketone under appropriate conditions. Diimine ligands (with two or more nitrogen atoms used as donor sites) are a family of Schiff-base compounds. Three types of diimine ligands that are well studied include α -diimine, β -diimines and γ -diimines (Figure 2.1). Different synthetic routes for the di-imine ligands have been devised. The synthesis of the di-imine ligands also involves Schiff-base condensation of ketones or aldehydes with any primary-amine [1]. However in this case diketones or dialdehydes are employed.



Scheme 2.1: General representation of a Schiff-base condensation reaction.

Schiff-base ligands due to their ease of synthesis, their inherent ability to coordinate to virtually all types of metals regardless of oxidation state and the enhanced stability imparted

to the ensuing metal complexes have been elevated to the status of the “privileged ligands” [2a]. Their design allows for the incorporation of various steric and electronic modulating functional groups as well as chiral elements thereby facilitating the synthesis of ligand-metal systems with unique physical and chemical properties [2b].

Diimines have established a niche as catalyst stabilisers in many catalytic processes such as olefin polymerisation, Heck coupling, Suzuki coupling, olefin oligomerisation and in atom transfer polymerisation [3-9]. Guo *et al.* reported an efficient synthesis, characterisation and application of β -diimines as supporting ligands in the palladium catalysed Suzuki coupling reaction of phenyl bromide and phenyl boronic acid [10]. Diimines can be tweaked as to complex to various transition metals to form stable and flexible metal complexes which act as active catalysts.

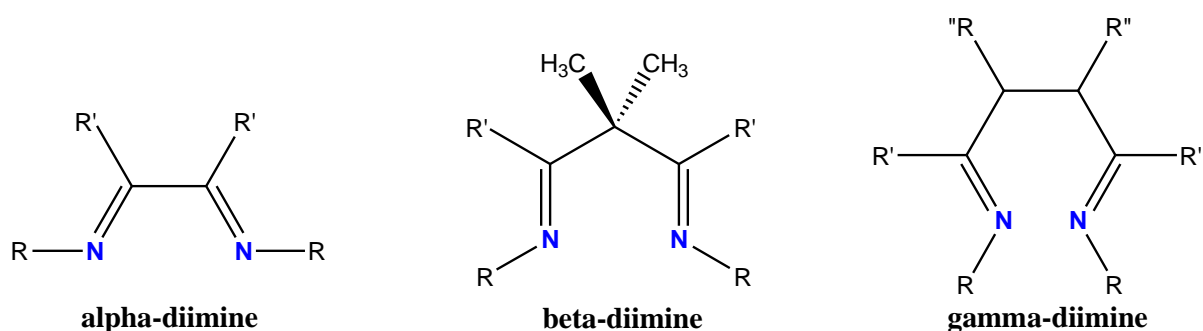


Figure 2.1: General structures of three types of diimine ligands [1].

2.1.2 Schiff-base/diimine complexes of methyltrioxorhenium (MTO).

As it is defined in chapter 1 (*vide supra*), the discovery of the methyltrioxorhenium (CH_3ReO_3 , MTO) Herrmann and co-workers opened a new avenue in the field of catalyzed epoxidation reactions. Despite the large numbers of Lewis base adducts of MTO described in the literature, only a few examples of complexes with Schiff-bases have been reported [12] (exhibited below, Figure 2.2). Considering the outstanding catalytic properties of MTO and the excellent corresponding ability of Schiff-bases, it is very interesting to synthesize some Schiff-bases especially the bidentate ones and their complexes with MTO.

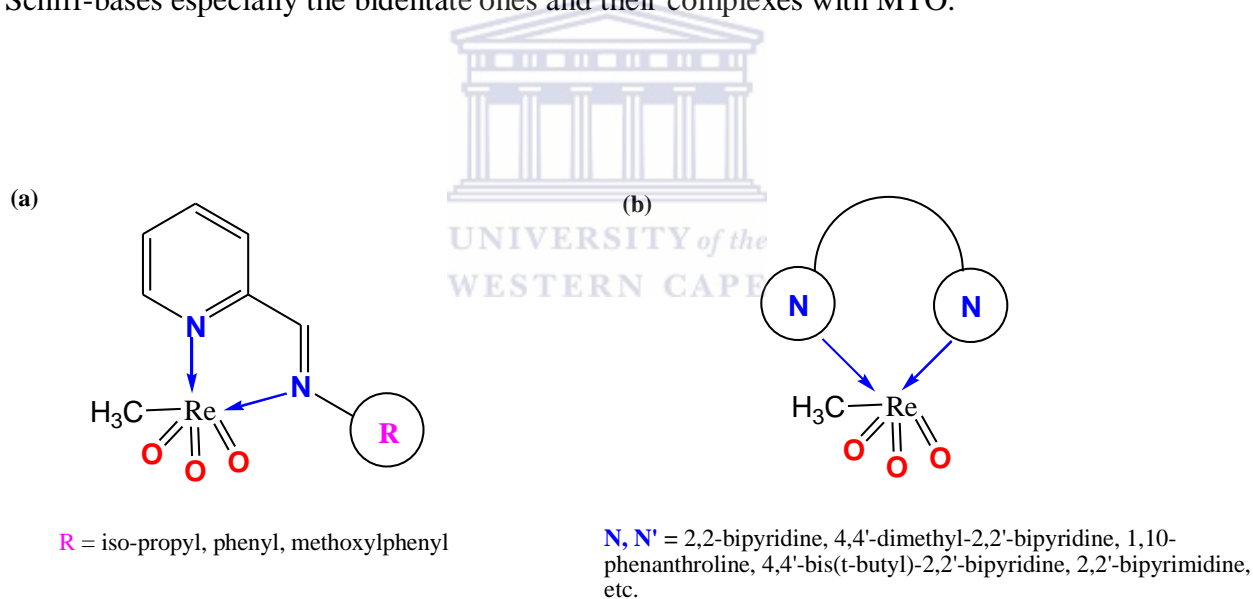


Figure 2.2: Some of Schiff-base MTO complexes documented in the literature [11,12].

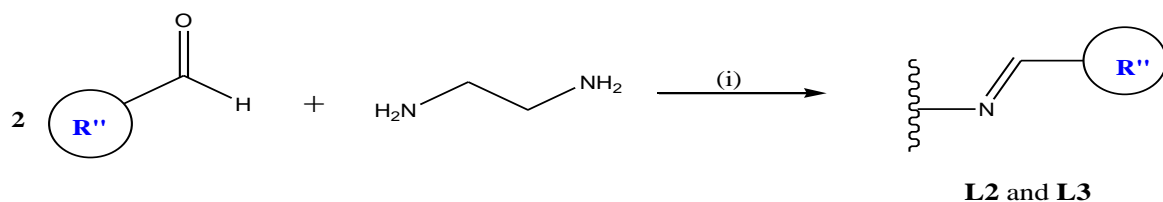
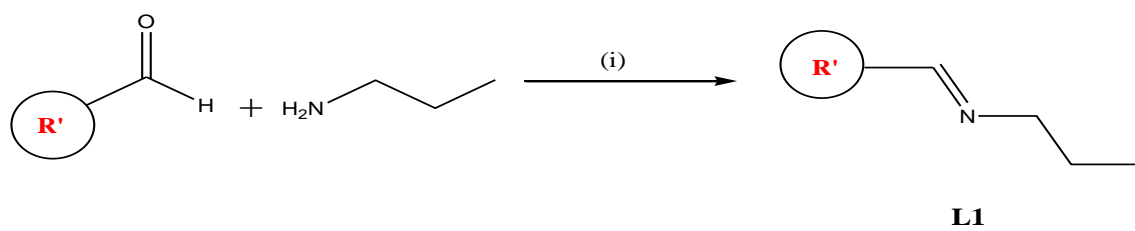
These Schiff-base complexes of MTO have been found to be highly efficient as catalysts in the epoxidation of cyclic alkenes i.e. cyclohexene and cis-cyclooctene, respectively. The afore mentioned researchers have discovered that the catalytic activity of these Schiff-base

complexes of MTO can be enhanced depending on the bidentate ligand and the type of oxidant used. They have obtained great conversions (100%) of epoxides [11, 12].

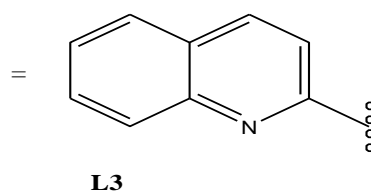
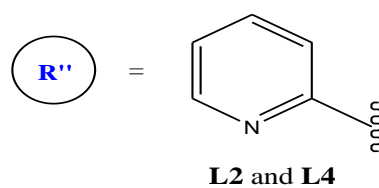
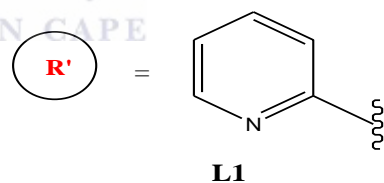
2.2 *Results and Discussion.*

2.2.1 *Mono- and bifunctional Schiff-base/diimine ligand synthesis, L1-L4.*

The synthetic methodology for these ligands was a result of the rudimentary work that has been produced by Haddleton *et al.* [2], Chen *et al.* [4] and Cloete *et al.* [5]. The synthesis of both pyridyl and quinolyl mono- and bi-functionalised ligand was carried out via Schiff base condensation of *n*-propylamine with the corresponding aldehyde in 1:1mole ratio with removal of water by using anhydrous magnesium sulphate as shown below in Scheme 2.2. After isolation by filtration and reduction of the solvent under vacuum, the pyridylimines (**L1-L3**) and quinolyimine (**L4**) were easily purified by dissolving in diethylether and cooling overnight at -5°C in order to precipitate out any unreacted aldehyde.

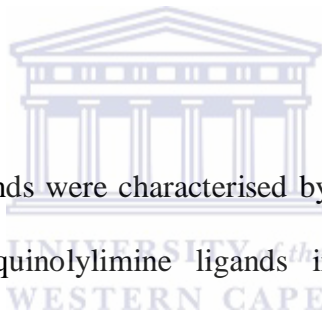


(i) dry Et₂O, 4 hrs, r.t., MgSO₄



Scheme 2.2: A Schematic representation of the synthesis of mono- and bi-functional diimine ligands, **L1- L4**.

The monofunctional ligand (**L1**) was obtained as a viscous oil in good yield (88%), which undergoes decomposition when left for prolonged periods at room temperature as reported by Hawker *et al.* [17]. However, there was no decomposition at all when the oil was stored at -4°C for extended periods. The bifunctional ligands (**L2-L4**) were obtained as a brown solid in good yields. All the ligands are soluble in common organic solvents such as CH₂Cl₂, CHCl₃, toluene, DMSO, hexane, pentane, CH₃CN etc. These ligands were fully characterised by ¹H & ¹³C-NMR spectroscopy, FT-IR spectroscopy, ESI-mass spectrometry and by elemental analysis. Results are shown in Tables 2.1 & 2.2.



The mono- and bifunctional ligands were characterised by a range of analytical techniques. FT-IR spectra of the pyridyl/quinolyimine ligands indicated three strong stretching frequencies which appeared at approximately 1647-1650, 1567-1590 and 1550-1573 cm⁻¹ and were ascribed to the azomethine fragment, $\nu(C=N)$, vibration and the pyridine-ring $\nu(C=N)$ & $\nu(C=C)$ vibrations respectively. The absence of the characteristic aldehyde band was evidence for the formation of the desired condensation product. The quinolyimine (**L3**) is distinct from the pyridylimine ligands. This ligand exhibits strong bands at 1642, 1595, 1557 and 1502 cm⁻¹, ascribed to $\nu(C=N)$ vibration and quinoline-ring $\nu(C=N)$ & $\nu(C=C)$ vibrations respectively. Table 2.1 indicates $\nu(C=N)$ vibrations of the free imine group. The obtained results confirms the condensation reaction of the aldehydes with the amino group of the propylamine, 1,2-ethylenediamine and 1,4-butanediamine chain to form the corresponding imines.

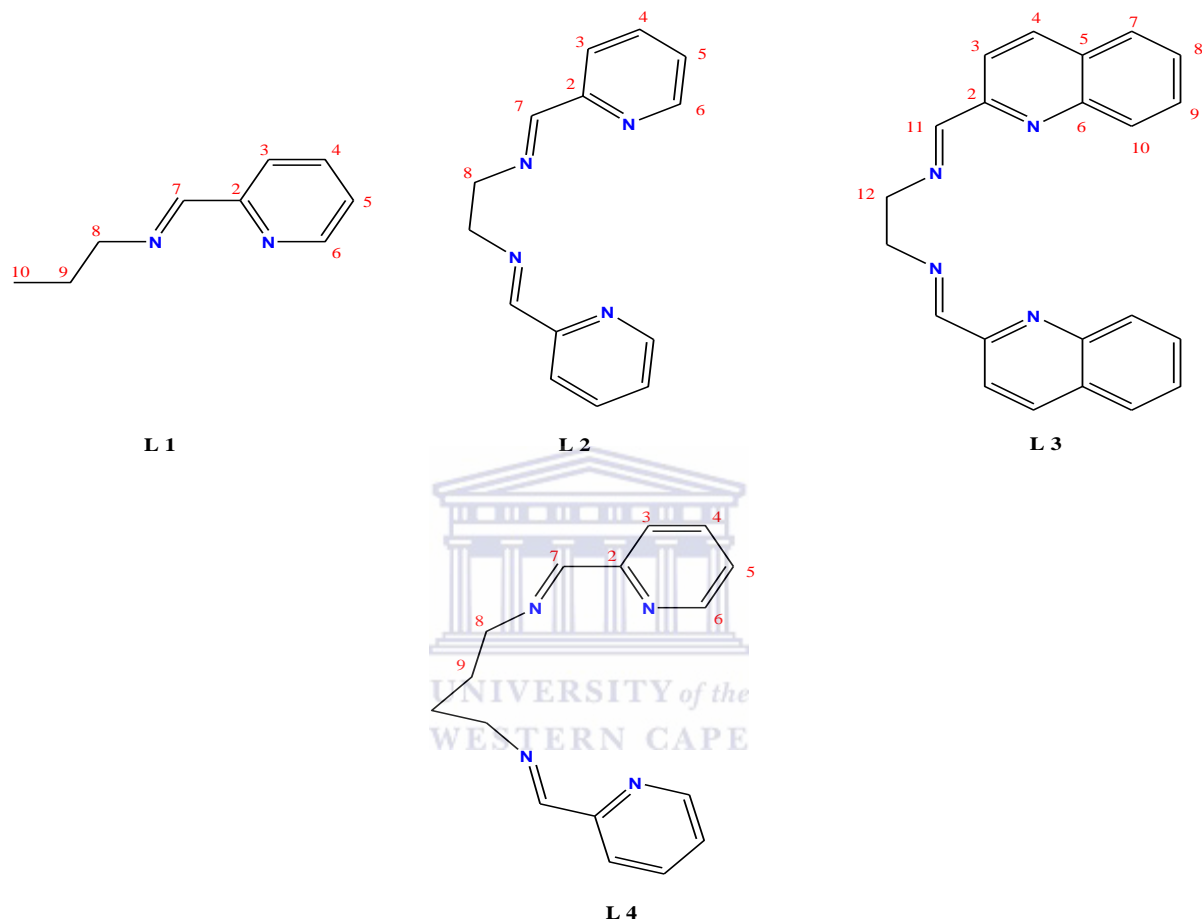


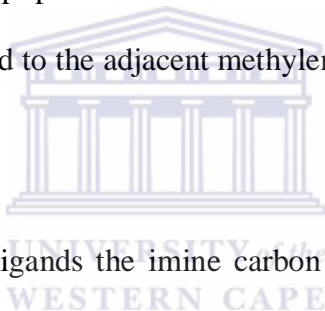
Figure 2.3: A schematic representation of the synthesized ligands, **L1-L4**, with numbering for NMR analysis.

Table 2.1: Analytical data pertaining to ligand synthesis.

Ligand	FT-IR ($\nu_{C=N}$, cm^{-1})	ESI-MS	Micro-analysis Calculated (found)		
	KBR _{pellets}	$[M+H]^+(m/z)$	C	H	N
L1	1650	149	66.14 (66.63)	7.35 (7.60)	17.15 (17.36)
L2	1650	239	70.57(69.99)	5.92(6.00)	23.51(23.66)
L3	1646	339	78.08(77.18)	5.36(5.58)	16.56(16.76)
L4	1649	268	72.15(71.81)	6.81(6.86)	21.04(20.88)

The ^1H NMR spectra of the ligands were recorded in CDCl_3 solutions to probe the solution's chemical environment and ascertain detailed information of the structures. The proton numbering scheme is shown above (Figure 2.3) in the schematic representation of the Schiff base systems (Figure 2.3). The spectral data are listed in Table 2.2. For each of the three ligands (**L1**, **L2** and **L4**), only one set of protons corresponding to the picolinylaldimine moieties of the ligand appeared in the range δ 7.1-8.6 ppm. A multiplet centred at approximately δ 7.8 ppm corresponding to two protons and another multiplet in the range δ 7.5-7.6 ppm corresponding to a single proton is observed. The former is assigned to the 3-H and 4-H and the latter is assigned to the 5-H. The 6-H proton appears as a doublet within δ 7.1-8.6 ppm.

The azomethine proton (7-H) is observed as a singlet in the range δ 7.5-8.4 ppm. A trend is observed in the spectrum of **L2** and **L3**, a singlet corresponding to two sets of two protons is observed at δ 4.82 ppm. This signal is assigned to the methylene group protons. Appearance of the protons of a solitary methylene group as a singlet suggests that not only two picolinylaldimine fragments but also two methylene groups of the ligands (**L2** and **L3**) are magnetically equivalent, at least on an NMR time-scale. Two multiplets of equal intensity are observed at δ 4.7 ppm and δ 2.4 ppm in the spectrum of **L4**. The multiplet at the lower field is assigned to the methylene group protons attached to the azomethine nitrogen and the multiplet at higher field is assigned to the adjacent methylene group protons.



In the ^{13}C NMR spectra of the ligands the imine carbon resonances were observed in the range δ 158-162 ppm. Tabulated results of ESI-MS analysis are in large agreement with the proposed formulations, indicating peaks corresponding to proton adducts of the molecular ion, $[\text{M} + \text{H}]^+$, further confirming the ligands were successfully prepared (Table 2.1). The mass spectrum of ligand **L3** is provided below (Figure 2.5).

Table 2.2: ^1H NMR spectroscopic data of Schiff-base ligands, **L1–L4**, recorded in CDCl_3 at 25°C .

Ligand	$\text{HC}=\text{N}$	Methylene	Aromatic protons
	δ (ppm)	δ (ppm)	δ (ppm)
L1	8.4	1.8(m, 2H, H^9); 3.8(t, 2H, H^8 , $^3J_{\text{H-H}}$ 7.1 Hz); 1.1 (t, 3H, H^{10} , $^3J_{\text{H-H}}$ 6.7 Hz)	7.2(t, 1H, H^5 , $^3J_{\text{H-H}}$ 6.8 Hz); 7.7(t, 1H, H^4 , $^3J_{\text{H-H}}$ 7.0 Hz); 7.9(d, 1H, H^3 , $^3J_{\text{H-H}}$ 6.9 Hz); 8.6(d, 1H, H^6 , $^3J_{\text{H-H}}$ 7.1 Hz)
L2	8.2	3.867(s, 4H, H^8)	7.1(m, 2H, H^5); 7.5(t, 2H, H^4 , $^3J_{\text{H-H}}$ 6.8 Hz); 7.7(d, 2H, H^3 , $^3J_{\text{H-H}}$ 6.9 Hz); 8.4(d, 2H, H^6 , $^3J_{\text{H-H}}$ 6.7 Hz)
L3	8.4	3.9(s, 4H, H^{11})	7.8-8.0(m, 2H, $\text{H}^{8,9}$); 7.1-7.6(d, 2H, $\text{H}^{3,4,7,10}$, $^3J_{\text{H-H}}$ 6.8 Hz)
L4	7.5	1.2(q, 4H, H^9); 1.6(m, 4H, H^8)	7.9-8.6(m, 8H, ArH)

^a- CH_3 .

The ^1H NMR spectrum of the ligand **L2** is provided below (Figure 2.4), showing a singlet peak corresponding to the methylene proton upfield (shown by 8-H).

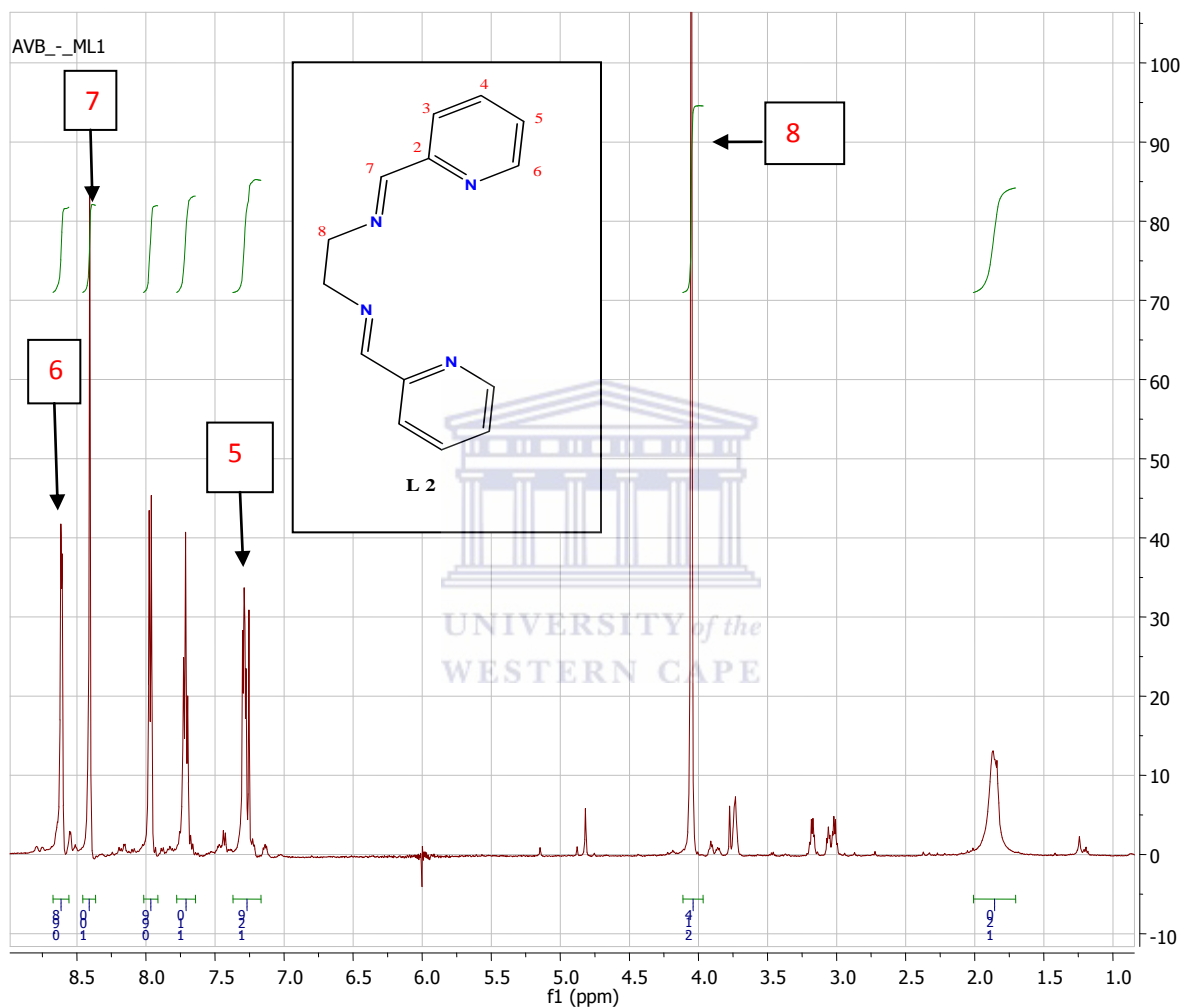


Figure 2.4: ^1H NMR spectrum of **L2**.

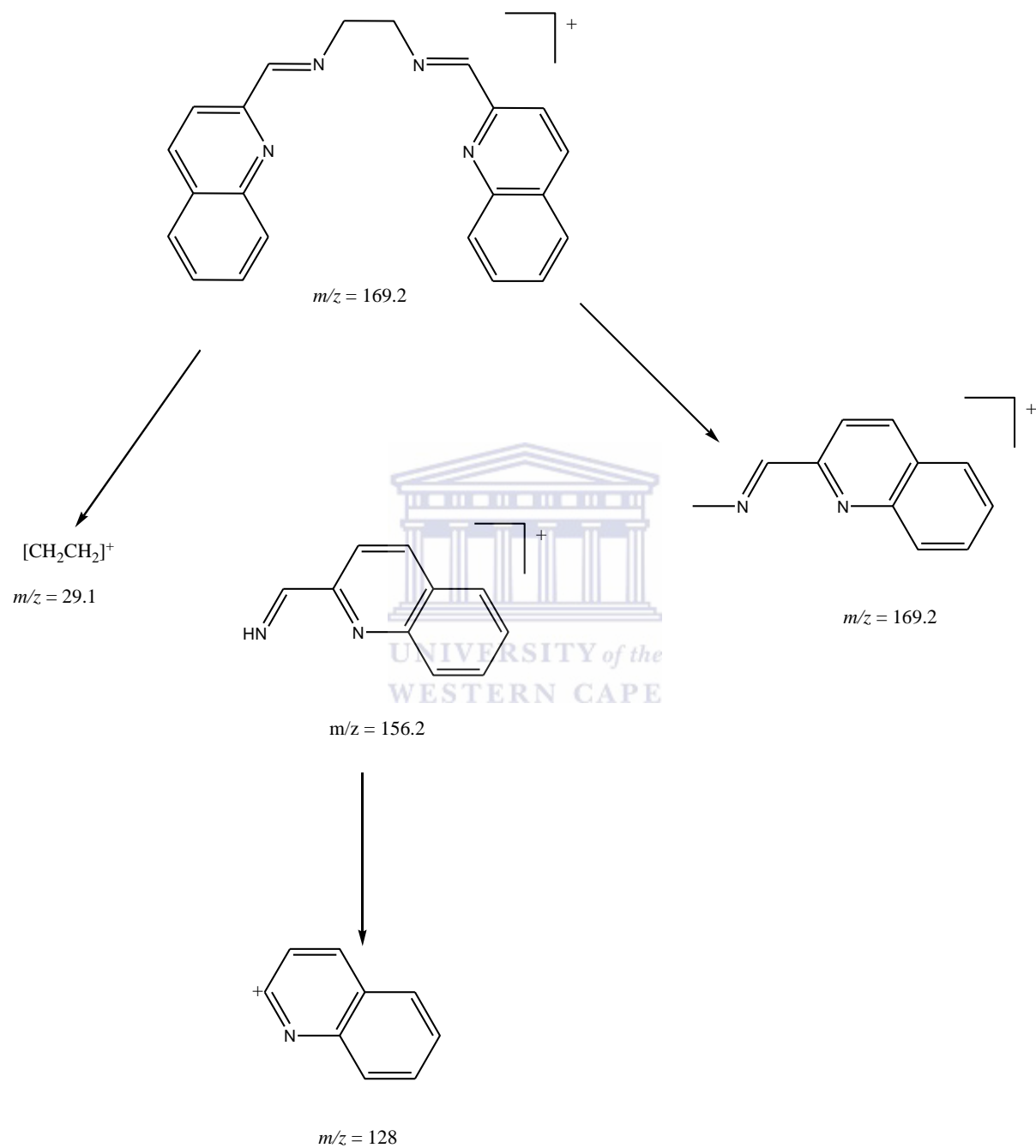
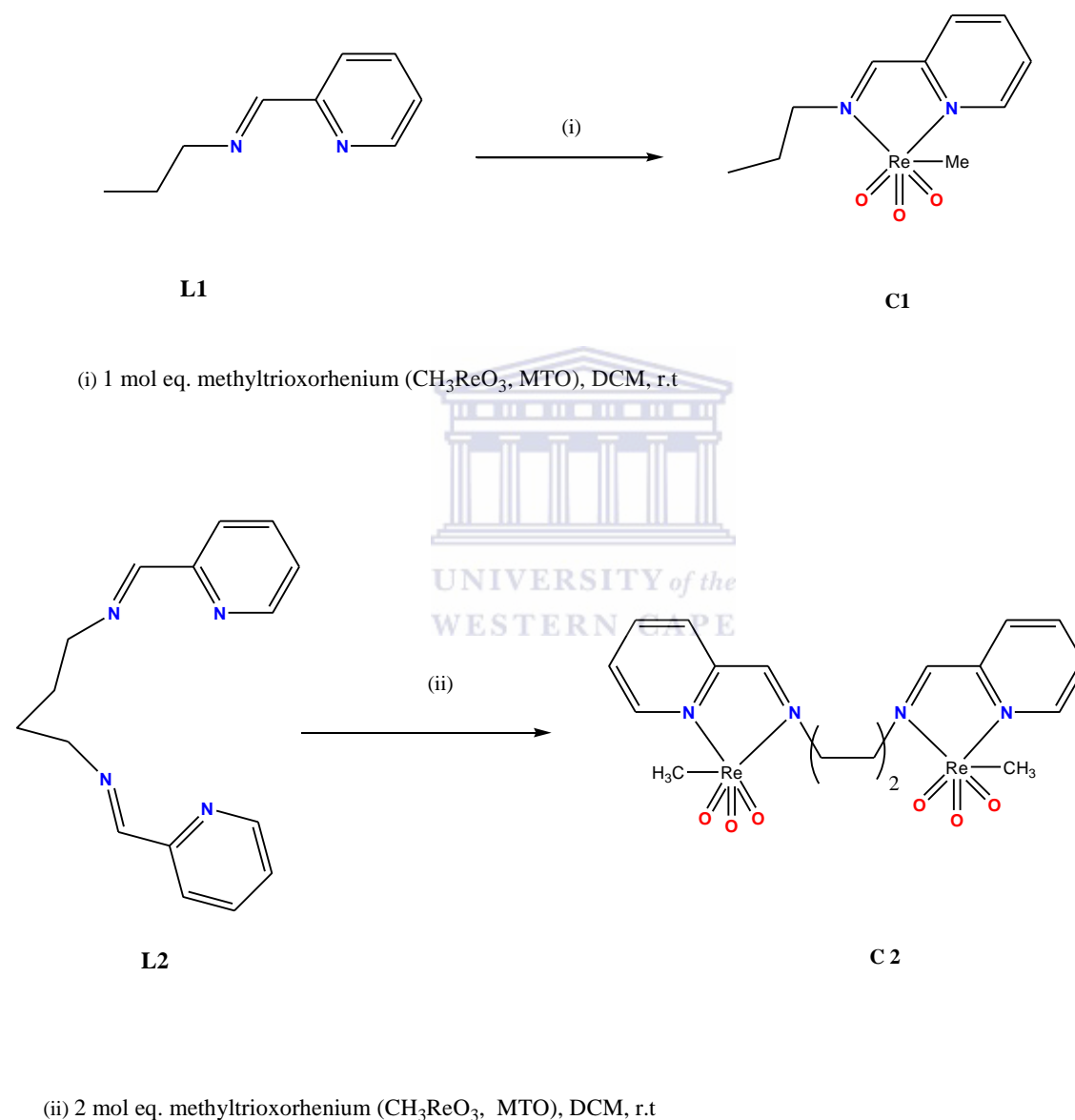


Figure 2.5: Plausible fragmentation pathway of bifunctional diimine ligand **L3**.

2.2.2 Schiff-base complexes of methyltrioxorhenium MTO, C1 and C2.



Ferreira *et al.* reported the synthesis of bidentate Lewis base adducts of MTO complexes in THF and Qui *et al.* reported on the detailed synthesis of the Schiff-base complexes of MTO in an alcoholic medium (methanol). Herein, the discrete mono- and binuclear complexes **C1** and **C2**, (see Scheme 2.3) were synthesized by treating MTO with the pyridinecarboxaldimine ligand in dichloromethane at room temperature. Both complexes were isolated as yellow crystals in yields 75–80%. In comparison with other N-coordinated Lewis base adducts, compounds **C1** and **C2** are slightly more sensitive to moisture and temperature, indicating observable trend of the previously synthesized complexes that are documented in literature [33,35]. The complexes are only soluble in dimethylsulfoxide and dimethylformamide and it was also observed that the complexes were not stable in solution as they turn from yellow to orange brown in minutes thus imposing difficulty in terms of “proper” characterization. Their colour changes from yellow to black green slowly when exposed to air, which can be avoided by storing under a water free nitrogen atmosphere.

A range of analytical techniques were thus employed in characterization of the complexes. In the IR spectra of compounds **C1** and **C2**, in comparison with that of the free ligands, the corresponding imine (C=N) bands were shifted and appeared between 1621 and 1650 cm^{-1} slightly lower than those of the Schiff-bases ligands (shown in Table 1), indicative of coordination as the double bond character of the imine functionality was reduced. The symmetric Re=O stretching vibrations appear within a narrow range of 935– 945 cm^{-1} , and the asymmetric stretching vibrations occur between 909 and 914 cm^{-1} . Compared to the vibrations of non-coordinated MTO, the Re=O bands of compounds **C1** and **C2** are strongly

red-shifted due to the pronounced donor capacity of the respective ligands in the solid state. The additional electron density donated from the ligand to the rhenium (VII) centre generally reduces the bond order of the Re=O bonds.

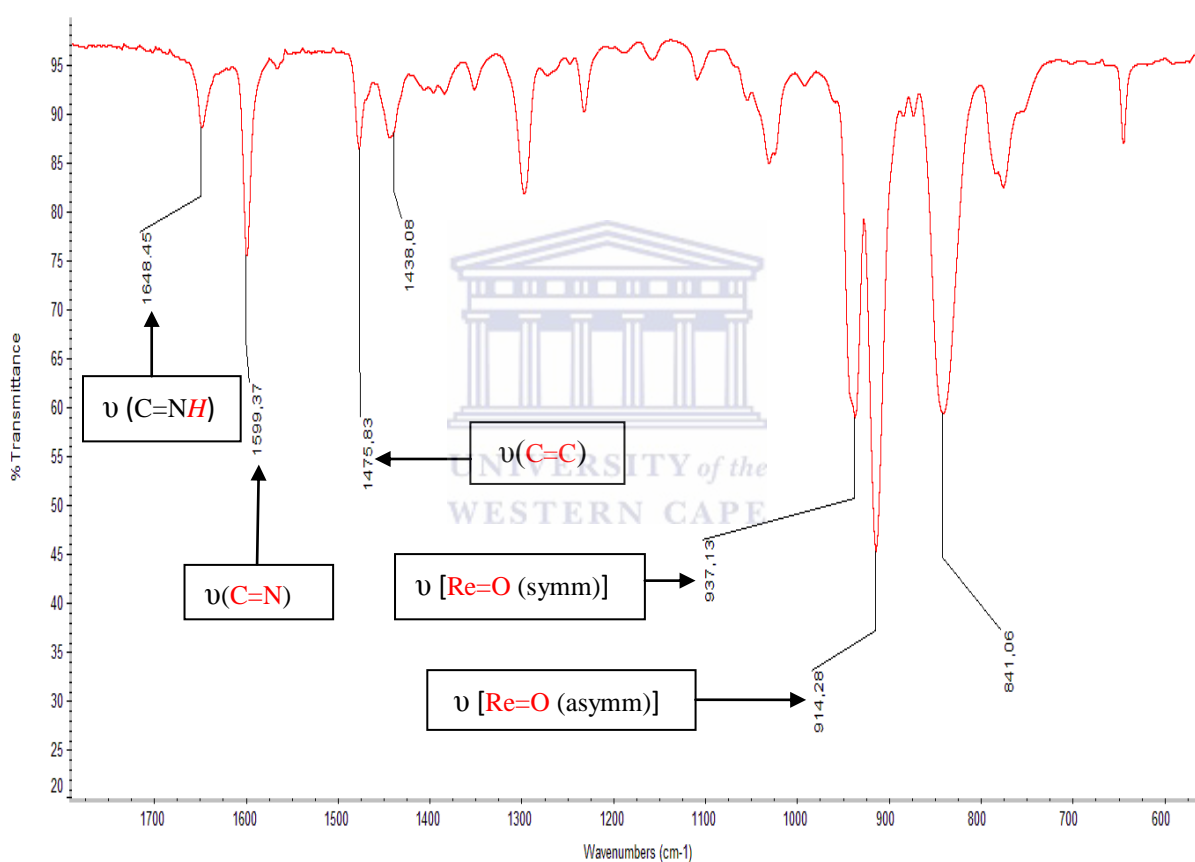


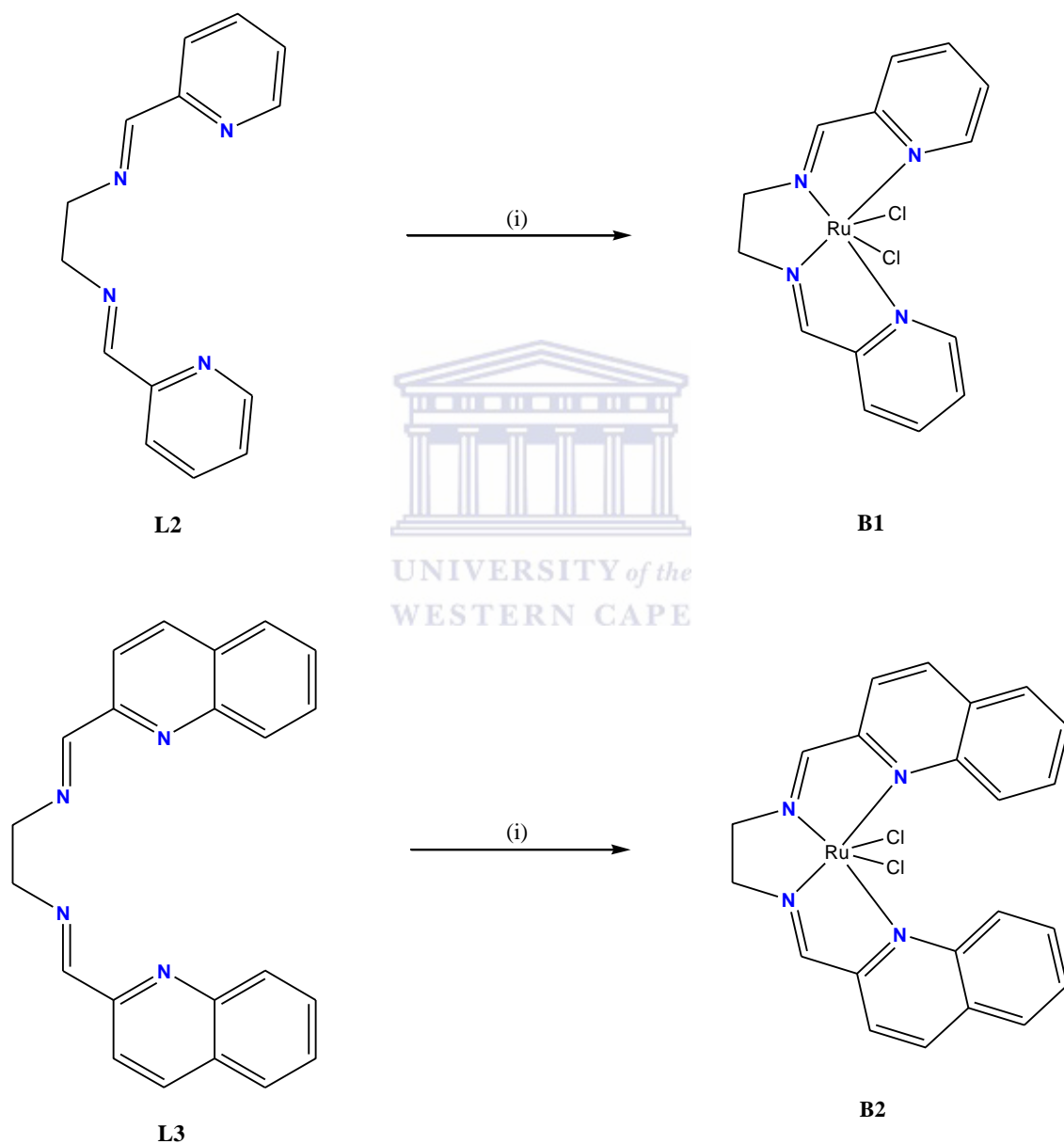
Figure 2.6: FT-IR spectrum of the complex **C2** recorded using KBr pellets.

As reported by Qui *et al.* the proton chemical shift of **C1** originating from the Re-CH₃ group of non-coordinated MTO was observed at approximately 2.67 ppm, due to pronounced electron donor character of the ligand (**L1**), the methyl signal was shifted to high-field after

complexation to the ligand, clearly indicating the electron-donor capability of the ligand. Unlike **C1**, not much information was obtained for **C2** due to the instability of **C2** in solution. Even though not stable in solution, partial information about the Re-CH₃ group shift was obtained. There was an observable high-field shift of the Re-CH₃ group signal relative to uncomplexed MTO. To further confirm our claims other spectroscopic techniques in conjunction with elemental analysis were employed in order to probe and ascertain conclusive evidence about the structure of the complex.

The complexes were further analysed by ESI mass spectra. The sensitivity of the complexes to elevated temperatures complicated the analysis and inconclusive information was obtained. For example ESI mass spectra of the complexes did not show any molecular ion but rather showed peaks of the Schiff-base ligand and the MTO separately. Qui *et al.*, reported similar problems with the analogous complexes.

2.2.3 Neutral mononuclear ruthenium(II) complexes, **B1** and **B2**.



(i) 1 mol eq. $\text{RuCl}_2(\text{dmsO})_4$, DCM, r.t., overnight

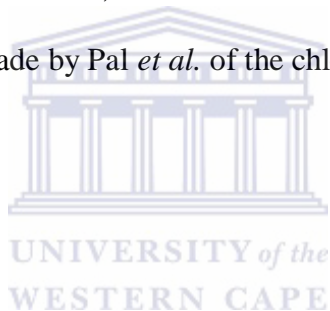
Scheme 2.4: General representation of the synthesis of neutral mononuclear ruthenium(II) complexes.

Compound **B1** is known in literature and was first synthesized by Pal *et al.* [33] but herein we describe a new synthetic methodology of **B1** with a “convenient” starting material as to increase the yield of the compound from what is reported by the aforementioned.

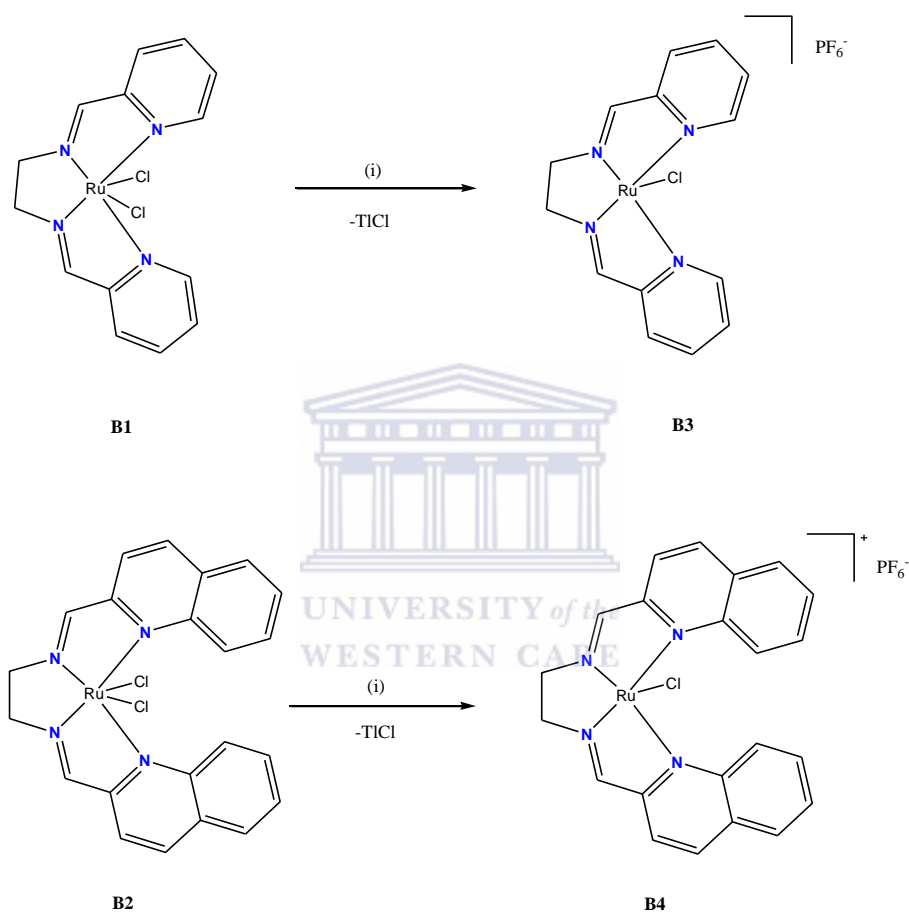
The newly devised synthetic pathway of the mononuclear compounds involved the use of Dichlorotetrakis(dimethyl sulfoxide)ruthenium (II), [RuCl₂(dms_o)₄] as the catalyst precursor. The compounds were synthesized by reaction of a 1:1 molar ration of the metal precursor with the ligands, **L2** and **L3**, in a presence of dichloromethane as a solvent at room temperature. The devised synthetic route resulted in the isolation of the compounds in moderately good yields as purplish solids. The purplish-blue compounds were isolated by chromatographic work-up using a neutral aluminium oxide column. The compounds are soluble in less polar solvents such as CHCl₃ and CH₂Cl₂ as reported by Pal *et al.*

A range of analytical techniques were employed in the characterisation of the complexes. In the FT-IR the azomethine fragment was observed to shift to lower wavenumbers in the range (1620-1595 cm⁻¹), indicative of coordination of the -HC=N fragment to the metal centre thus decreasing the double bond character of the azomethine fragment. The pyridine ring [(C=N)pyr] stretching frequencies were observed as medium to strong peaks in the range 1570–1454 cm⁻¹. The complexes were further examined with ¹H NMR. The ¹H NMR of the complexes was recorded in CDCl₃ in order to probe the solutions chemical structures. The same numbering scheme used for the Schiff base ligands is used for the proton numbering scheme of the complexes. As reported for the ligands, **L2** and **L3**, the set of protons for the picolinylaldimine moiety appear in the range δ 7.5-7.9 ppm. A multiplet corresponding to

two protons (3-H and 4-H) was observed centre at δ 7.8 ppm with another multiplet appearing in the close range (δ 7.5-7.6 ppm) ascribed to the 5-H. The doublet that appears within the range δ 9.2-9.4 ppm is assigned to 6-H. The presence of a singlet observed in the range δ 8.9-9.2 ppm was assigned to the azomethine proton (7-H). In the spectra of **C1** and **C2**, a singlet is observed at δ 4.8 ppm corresponding to two protons. This signal is assigned to the methylene group protons. Appearance of the protons of a solitary methylene group as a singlet confirmed that not only the picolinylaldimine moiety but also two methylene groups of **B1** and **B2** are magnetically equivalent, at least on an NMR time-scale. This observation is consistent with the observation made by Pal *et al.* of the chlorides being mutually *trans* in **B1**.



2.2.4 Cationic mononuclear ruthenium(II) complexes, **B3** and **B4**.

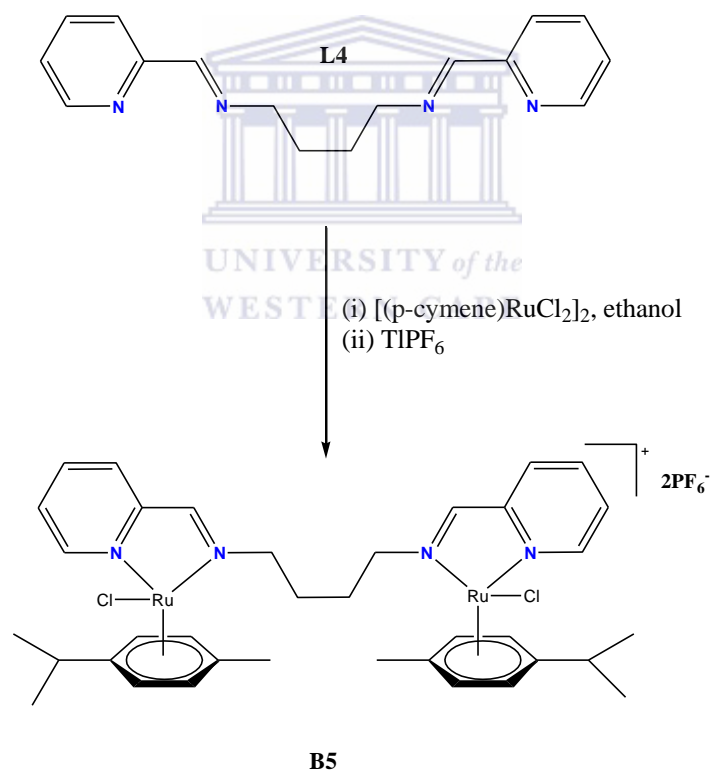


(i) Acetone, r.t, overnight, TIPF_6

Scheme 2.5: General representation of the synthesis of mononuclear cationic ruthenium(II) complexes.

The cationic ruthenium complexes are derivatives of the compounds **B1** and **B2** and were obtained by abstracting a chloride with TlPF₆ to obtain **B3** and **B4**. These derivatives were stabilized by the use of hexafluorophosphate salts via metathesis.

2.2.5 Cationic homobimetallic ruthenium complex, **B5**.



Scheme 2.6: Representation of the synthesis of cationic homobimetallic ruthenium(II) complex **B5**.

Table 2.3: ^1H NMR spectroscopic data of neutral and cationic mononuclear Ru(II) complexes, **B1–B5**, recorded in $(\text{CD}_3)_2\text{CO}$ and CDCl_3 at 25°C .

Mono- and binuclear complexes	HC=N δ (ppm)	Aromatic region δ (ppm)	Aliphatic region δ (ppm)
B1	8.8	7.8 (m, 4H ^{3,4}) 7.5-8.7 (m, 4H ^{4,6})	4.4(t, 4H, $^3J_{\text{H-H}}$ 6.5 Hz); 2.5 (qn, 4H)
B2	8.6	7.9 (m, 4H, H ^{7,8,9}) 7.8 (m, 4H ^{3,4})	4.1 (t, 4H, $^3J_{\text{H-H}}$ 6.4 Hz); 2.2(qn, 4H)
B3	8.8	7.8 (m, 4H, H ^{3,4}) 7.5-8.7 (m, 4H, H ^{4,6})	4.4 (t, 4H, $^3J_{\text{H-H}}$ 6.53 Hz); 2.5(qn, 4H)
B4	8.6	7.9 (m, 4H, H ^{7,8,9}); 7.7 (m, 4H, H ^{3,4})	4.1 (t, 4H, $^3J_{\text{H-H}}$ 6.4 Hz); 2.21(qn, 4H)
B5	8.7	5.9 (t, 2H, $^3J_{\text{H-H}}$ 6.3 Hz); 6.4 (dd, 4H, $^3J_{\text{H-H}}$ 6.3 Hz, $\text{Ar}_{\text{C}_{\text{YE}}}$); 7.8 (t, 2H, $^3J_{\text{H-H}}$ 5.7 Hz, Pyr); 8.28 (d, 2H, $^3J_{\text{H-H}}$ 7.7 Hz); 8.32 (t, 2H, $^3J_{\text{H-H}}$ 7.6 Hz); 9.58 (d, 2H, $^3J_{\text{H-H}}$ 5.8 Hz)	1.1&1.2 (d, 12H, $\text{CH}(\text{CH}_3)_2$ C_{YE} , $^3J_{\text{H-H}}$ 7.1 Hz); 4.4 (t, 4H, $^3J_{\text{H-H}}$ 6.4 Hz); 4.46 (t, 4H, $^3J_{\text{H-H}}$ 6.6 Hz); 2.8 (sep, 2H, $\text{CH}(\text{CH}_3)_2$ C_{YE})

The related cationic homobimetallic complex was prepared as a model of the multinuclear complexes. The complex was achieved by reacting the bifunctional ligand (**L4**) with the dinuclear arene ruthenium(II). This complex was isolated as an orange-yellow, air stable solid in good yield and is soluble in polar organic solvents.

2.3.1 Dendrimers as Ligands

After Vögtle *et al* in 1978, who used the term “cascade macromolecules” to elaborate on the synthesis of dendrimers [10], Tomalia *et al.* [12-14] termed this phenomena “dendrimer” as they provided detailed synthesis of poly(amidoamine) (PAMAM) dendrimers. Fréchet *et al.* [15-17] also contributed in the synthesis of “true dendrimers” in their independent study of the subject.

Dendrimers are distinguishable by the architectural components which they possess i.e. (a) an initiator core, (b) an interior layer (generations), composed of repeating units, radially attached to the initiator core and (c) exterior (terminal functionality) attached to the outermost interior generation (Fig 2.2) [12]. Generally the periphery bears functional groups, the number of which is dependent on the dendrimer generation (Fig 2.2) [18].

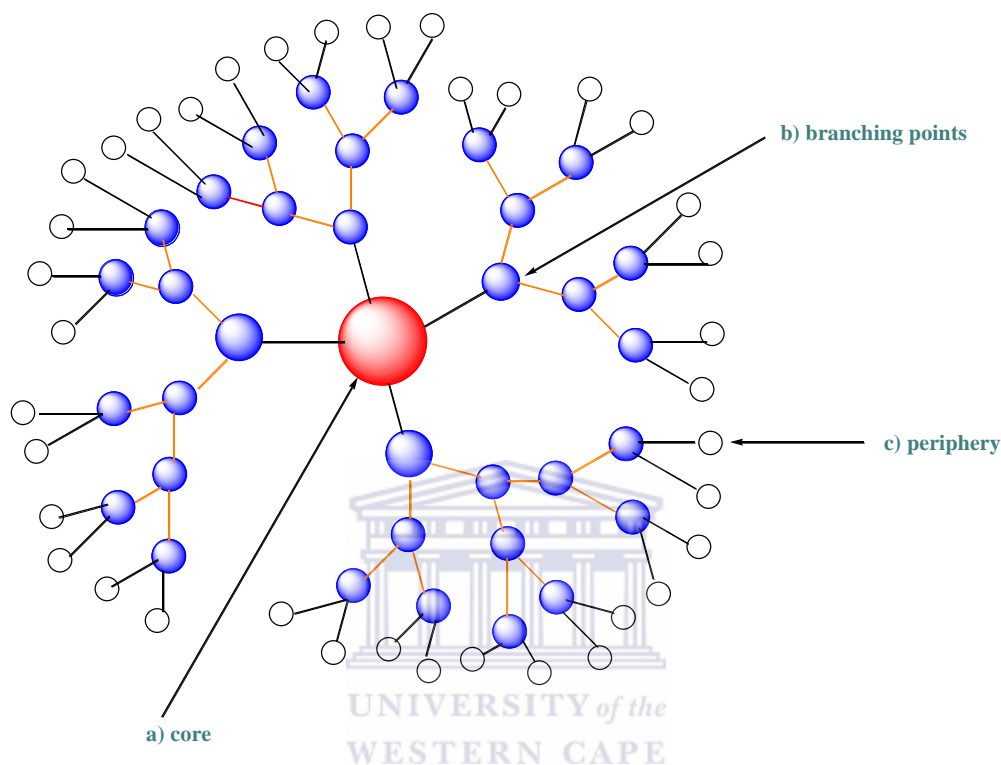


Figure 2.7: Schematic representation of a 4th Generation Dendrimer.

2.3.2 Approaches devised for the synthesis of dendrimers.

2.3.2.1 Divergent approach.

The divergent route to dendrimer synthesis, introduced by Tomalia *et al.*, details the way in which the dendrimer grows outwards from the focal point or core, diverging into space as portrayed in Figure 2.2. Starting from a reactive core, a generation is grown, and then the new periphery of the molecule is activated for reaction with more monomer. The number of active

sites on the core determines their n -directionality and limits the number of building blocks that can be added to form the next generation. The pattern is followed in a repetitive manner (iterated synthesis) exposing reactive sites on the periphery for the assembly of the next generation growth layer [19]. The divergent approach is successful for the production of large quantities of dendrimers since, in each generation-adding step, the molar mass of the dendrimer is doubled. Very large dendrimers have been prepared in this way, but incomplete growth steps and side reactions lead to the isolation and characterization of slightly imperfect samples [20].

2.3.2.2 *Convergent approach*

The convergent approach was pioneered by Fréchet *et al.* as a response to the shortcomings of the divergent synthesis. Fréchet *et al.* aimed at synthesizing dendrimers by growth that begins at what will end up being the surface of the dendrimer and works inwards by gradually linking surface units together with more monomers (Figure 2.2) to achieve the desired product. When the growing wedges are large enough, several of these are attached to a suitable core to give a complete dendrimer. This leads to the formation of a single reactive dendron, after which several of these dendrons are then reacted with a multi-functional core to obtain the dendrimer molecule (Fig 2.2) [15]. The advantages of convergent growth over divergent growth stem from the fact that only two simultaneous reactions are required for any

generation-adding step. Most importantly, this protocol makes the purification of perfect dendrimers simple [20].

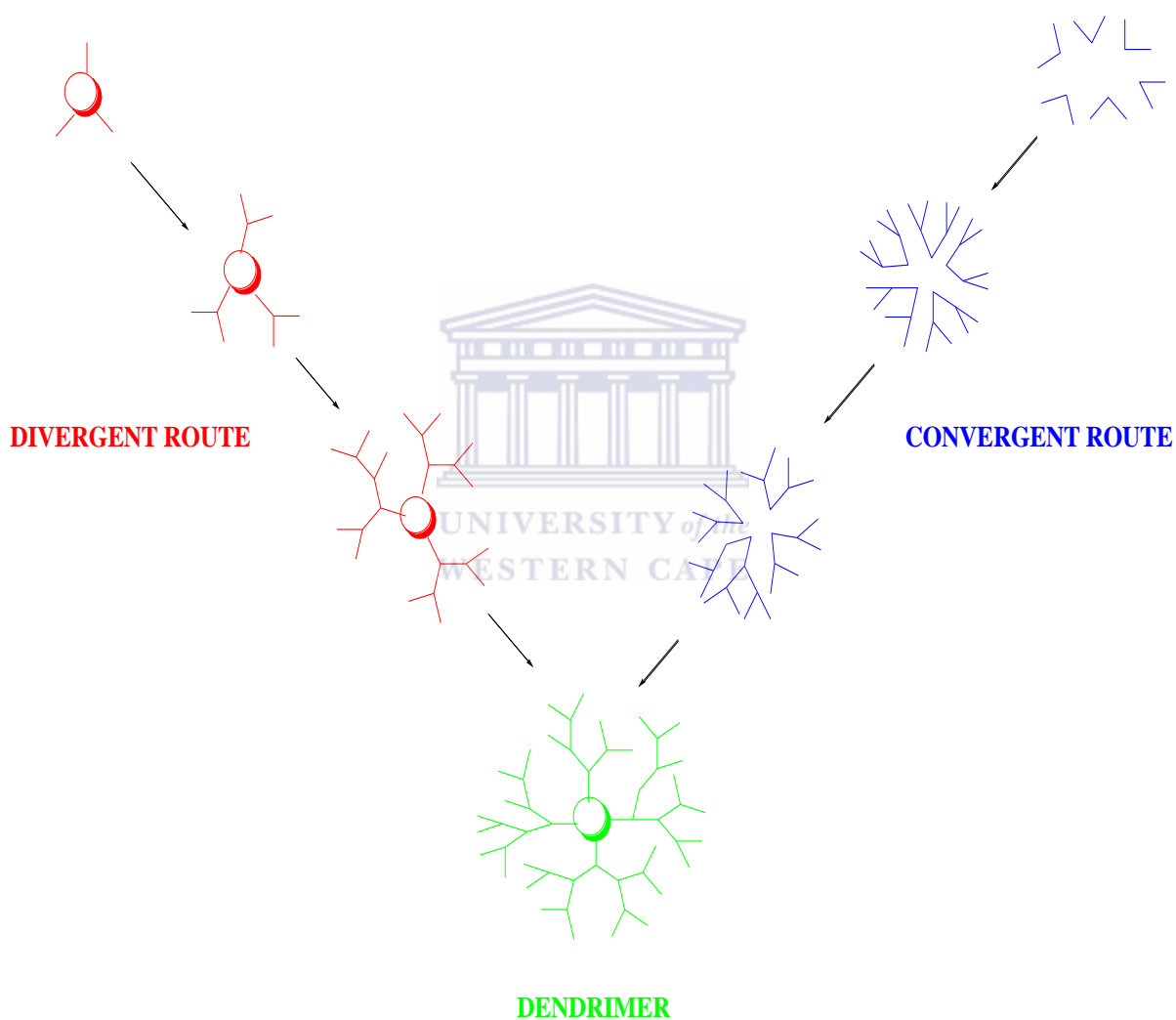
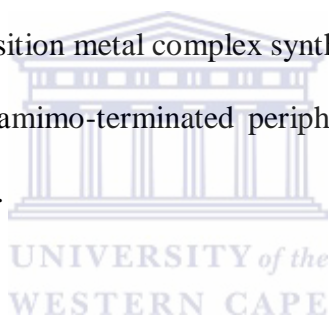


Figure 2.8: A schematic representation of divergent (left) and convergent (right) approach to dendrimer synthesis.

2.4.1 *Synthesis of peripherally modified PPI dendrimers.*

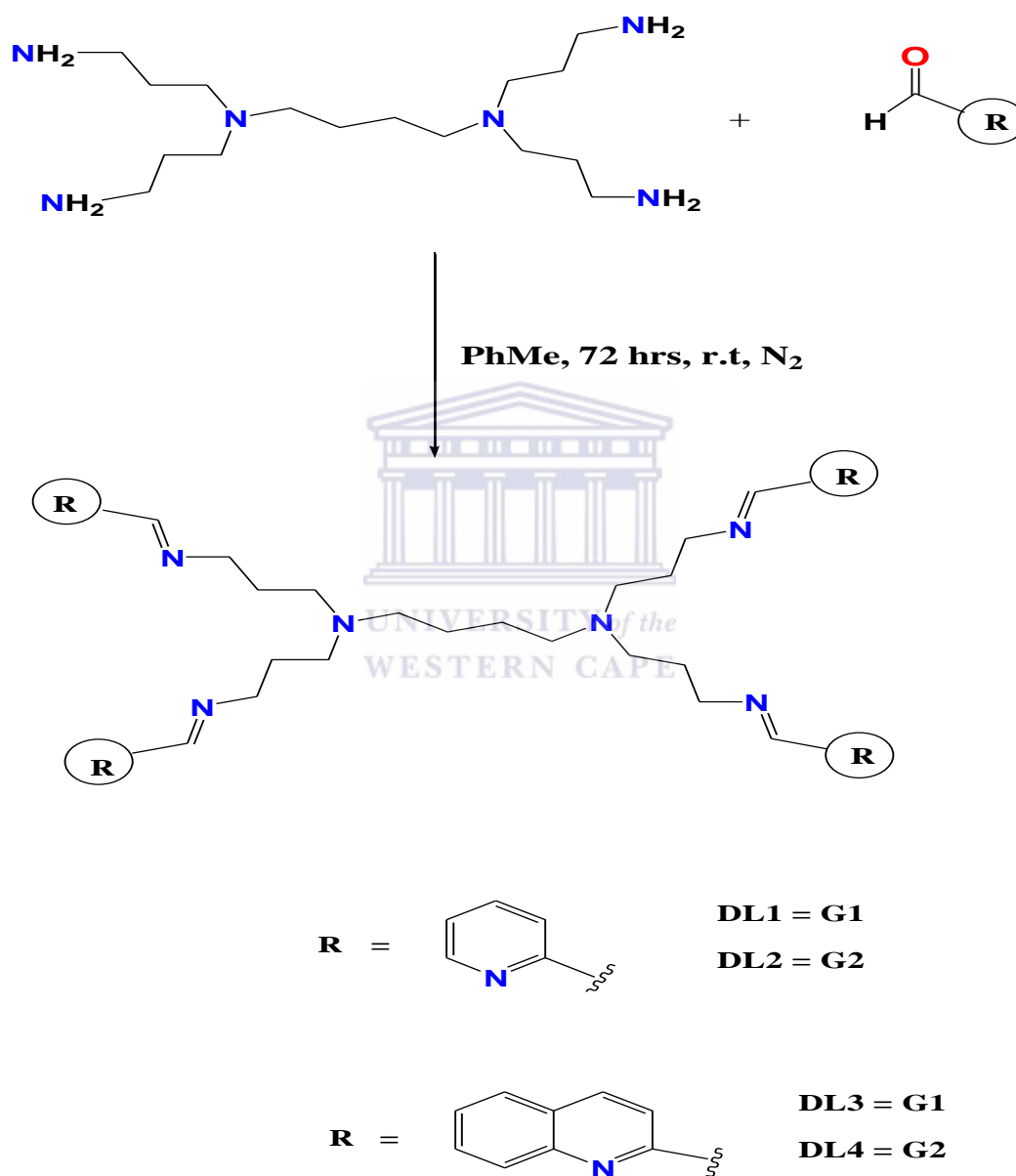
Meijer *et al.* were the first to synthesize the first poly(propyleneimine) diaminobutane (DAB) core dendrimers that are now commercially available [19]. Many different catalyst systems have made extensive use of PAMAM (polyamidoamine) and PPI poly(propyleneimine) dendrimers due to their easy accessibility [20]. Mapolie *et al.* have done extensive work in the peripheral modification of the commercially available PPI dendrimer, in attempts to produce dendritic ligands for transition metal complex synthesis [6,9,21]. They have achieved this by functionalization of the amino-terminated periphery via Schiff base condensation with various aldehyde derivatives.



2.4.1.1 *Synthesis and characterization of dendritic ligands, DL1-DL4.*

The Smith *et al.* [6,9] and Malgas *et al.* [12, 13] mode of preparation was employed for the synthesis of generation 1 (**DL1-DL2**) and generation 2 (**DL3-DL4**) dendrimeric *N, N'* donor ligands. The synthetic methodology involves the use of Schiff base condensation to achieve suitable functionalized dendritic ligand scaffolds for the synthesis of multinuclear dendritic complexes. The dendritic ligands were thus synthesised via Schiff base condensation of the 1, 4-diaminobutane poly (propylene-imine) dendrimer [DAB-(NH₂)_n] (n = 4 or 8) with an appropriate aldehyde. The ratio of [DAB-(NH₂)_n] to aldehyde was 1:4 for **DL** and **DL2** and 1:8 for **DL3** and **DL4**. The scheme below depicts the general approach to

the preparation of the dendritic ligands **DL1** and **DL2**, with the preparation of generation-1 as an example given that the preparation of generation-2 is similar.



Scheme 2.7: General representation of the synthesis dendritic scaffolds, **DL1-DL4**.

As observed by Swarts [2b], the challenge encountered with the synthesis of the peripherally modified PPI dendrimer ligands was the appearance of the unreacted aldehyde starting material regardless of all the efforts to ensure correct molar ratio. Thus preparation of the dendrimeric ligands (**DL1-DL4**) was carried out over an extended period of time to ensure complete modification of peripheral amino groups of the PPI dendrimer with the corresponding aldehyde. All these ligands were isolated as crude oily products and were further subjected to work-up with de-ionised water to remove any unreacted DAB-G1 or G2 starting material. Residual aldehyde was further removed by vacuum distillation at reduced pressure using at a Kugelrühr apparatus thus isolating pure peripherally modified dendritic ligands **DL1-DL2** as yellow oils with product yields ranging between 75-90 %. **DL3** and **DL4** was purified by refluxing in hot pentane at 36°C resulting in the isolation of a yellow solid from the original oily residue. These dendritic ligands displayed solubility in most common polar solvents, chlorinated and aromatic solvents but **DL3** and **DL4** was found to be insoluble in MeCN as reported by Mketi [2c].

To confirm successful synthesis of the dendritic ligands a range of analytical techniques were employed to establish the purity and to probe the chemical structure. As the ligands were subjected to further work-up to remove unreacted aldehyde, FT-IR was employed and the appearance of C=N, imine moiety, stretching frequency in the range 1630-1650 cm⁻¹ without the presence of the aldehyde (C=O) absorption band was indicative of the formation of the intended product. The infra-red spectroscopy investigation of the pyridylimine ligands shows three strong bands which appeared in the regions 1647-1650, 1567-1590 and 1550-1573 cm⁻¹,

assigned to imine $\nu(\text{C}=\text{N})$ vibrations and pyridine-ring $\nu(\text{C}=\text{N})$ & $\nu(\text{C}=\text{C})$ vibrations respectively. The stretching frequencies of the pyridine based dendritic ligands are consistent with the data obtained for monofunctional ligands. For quinoline based ligands these peaks are significantly lower than what was observed for monofunctional ligands because of huge amount of electron delocalisation around the quinoline ring. However, for the quinolyimine ligands (**DL3** and **DL4**) different infra-red spectra were obtained which show strong bands in the range 1642-1644, 1595-1596, 1557- 1561 and 1502-1504 cm^{-1} , ascribed to $\nu(\text{C}=\text{N})$ vibration of the imine functionality and quinoline-ring $\nu(\text{C}=\text{N})$ & $\nu(\text{C}=\text{C})$ vibrations respectively. These results confirm that the aldehydes have condensed with the amino groups on the periphery of dendrimer forming the corresponding imines. Elemental analysis results are presented in Table 2.4, which also indicate that the condensation reaction of the dendrimer (**DAB-G1** or **G2**) with various aldehydes was successful because all the results correspond well with the expected molecular formula of the ligands.

To further confirm the successful synthesis of the ligands ^1H and ^{13}C NMR spectra of the dendritic were also recorded in CDCl_3 . The spectra of these ligands revealed the symmetric nature of the dendritic structures.

In the ^1H NMR the singlet in the range δ 8.2-8.6 ppm was assigned to the imine proton as they integrated for a total of four protons that are magnetically equivalent the NMR-time scale proving the symmetry once more. The resonances for the dendrimer corresponded to the resonances of the analogous monofunctional ligands synthesized.

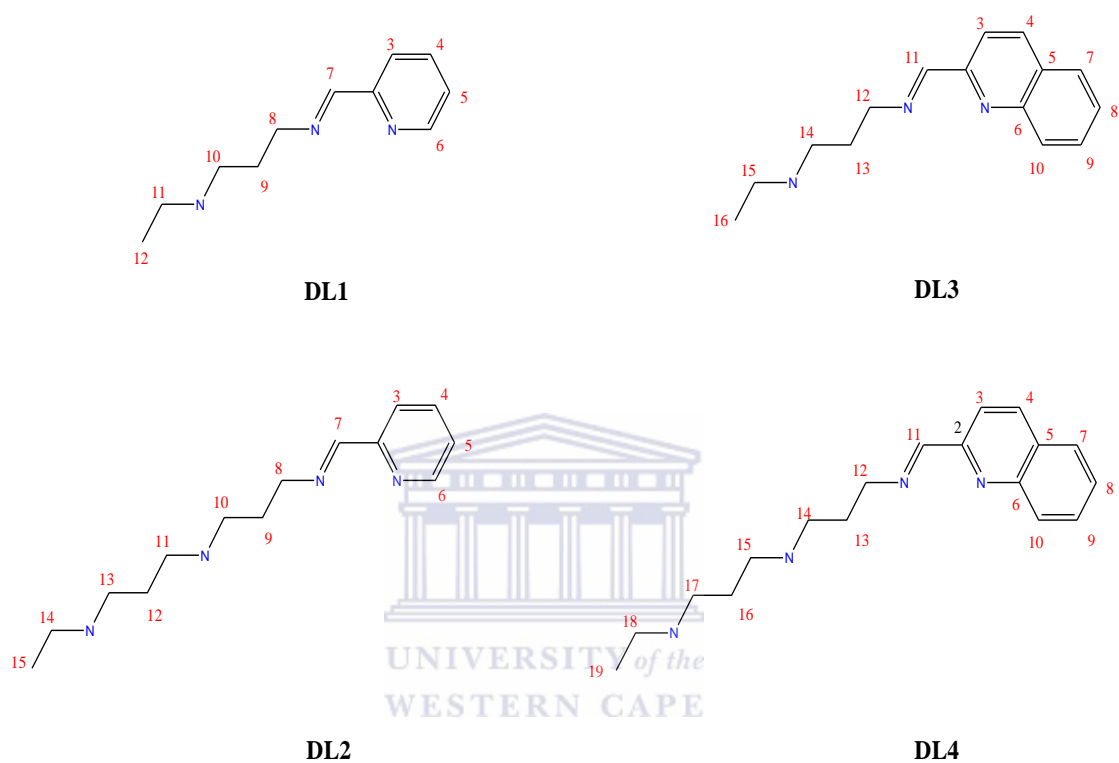


Figure 2.9: A schematic representation of the synthesized ligands with numbering for NMR analysis.

Table 2.4: ¹H NMR spectral data of dendritic ligands, **DL1-DL4**.

Ligand	HC=N	Aromatic region	Aliphatic region.
DL1	8.3 (s, 4H, H ⁷)	7.2(t, 4H, H ³ , ³ J _{H-H} 7.4 Hz); 8.7(d, 4H, ³ J _{H-H} 7.9 Hz) 7.7(t, 4H, H ⁴ , ³ J _{H-H} 7.7 Hz); 7.9(d, 4H, ³ J _{H-H} 7.9 Hz)	1.4(m, 4H, H ¹²); 2.4(t, 4H, H ^{11,9} , ³ J _{H-H} 6.7 Hz.); 2.4(t, 4H, H ⁸ , ³ J _{H-H} 6.3Hz); 3.1(qn, 8H, H ⁹)
DL2	8.3(s, 8H, H ⁷)	8.6(t, 8H, H, ³ J _{H-H} 7.52 Hz); 7.3(t, 8H, H, ³ J _{H-H} 7.4 Hz); 7.7(t, 8H, H ⁹ , ³ J _{H-H} 7.32 Hz); 7.9(d, 8H, H ⁷ , ³ J _{H-H} 7.42 Hz)	3.6(t, 16H, H ¹⁰ , ³ J _{H-H} 6.4Hz);1.6(qn, 24H, H ¹¹); 1.8(qn, 24H, H ^{12,9}); 2.5(t, 24H, H ^{10,13} , ³ J _{H-H} 7.3Hz); 2.4(t, 4H, H ¹⁴ , ³ J _{H-H} 6.9Hz); 1.4(m, 4H, H ¹⁵)
DL3	8.4(s, 4H, H ¹¹)	8.2(d, 4H, H ¹⁰ , ³ J _{H-H} 8.1 Hz); 8.1(t, 4H, H ⁴ , ³ J _{H-H} 7.6 Hz); 7.70 (t, 4H, H ⁸ , ³ J _{H-H} 7.7 Hz); 7.7 (t, 4H, H ⁹ , ³ J _{H-H} 7.8 Hz); 8.32(t, 4H, H ³ , ³ J _{H-H} 7.5 Hz);	1.41(m, 4H, H ¹⁶); 2.4(t,4H, H ¹⁵ , ³ J _{H-H} 7.75 Hz); 2.58(t, 8H, H ¹⁴);1.92(qn, 8H, H ¹³); 4.0(t, 8H, H ¹² , ³ J _{H-H} 7.0 Hz)
DL4	8.5(s, 8H, H ¹¹)	8.2(d, 8H, H ³ , ³ J _{H-H} 7.7 Hz); 8.1(d, 8H, H ⁴ , ³ J _{H-H} 7.2 Hz); 7.7(d, 8H, H ⁷ , ³ J _{H-H} 7.6 Hz); 7.7(t, 8H, H ⁸ , ³ J _{H-H} 7.2Hz); 7.6(t, 8H, H ⁹ , ³ J _{H-H} 7.0 Hz); 8.2(d, 8H, H ¹⁰ , ³ J _{H-H} 7.4 Hz)	1.3(m, 4H, H ¹⁹); 2.41(t, 4H, H ¹⁸ , ³ J _{H-H} 7.3Hz); 2.5(t, 24H, H ^{17,14} , ³ J _{H-H} 6.9 Hz); 1.92(qn, 24H, H ^{16,13}); 1.63(qn, 24H, H ¹⁵); 4.1(t, 16H, H ¹² , ³ J _{H-H} 7.2 Hz)

^a Spectra run in CDCl₃ at 25°C. Chemical shifts reported as δ ppm values, referenced to residual solvent peak. Superscript denotes proton numbering as depicted in the scheme (Figure 2.8).

The high degree of symmetry in the ligands permits us to divide the aliphatic region into two respective regions. The resonances corresponding to the propyl chains from the dendrimer branches appears in the range δ 50-60 ppm, with three carbon resonances observed. The resonances of the diaminobutane chain, that forms the core of the dendrimer, were observed in the range δ 20-30 ppm, with two carbon resonances. The same features have been observed for peripherally modified dendrimer ligands which have been previously prepared by Mapolie *et al.* [24, 26].

2.5.1 Synthesis and characterization of dendritic complexes, DC1-DC2 and V1-V6.

The following Fig 2.10(a) is a representation of the abbreviated bulky end of the entire ligands and complexes found in DC1-DC2 and V1-V6.

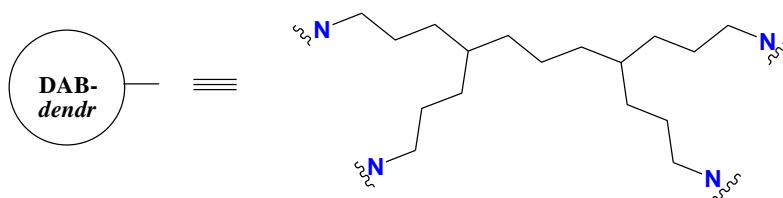
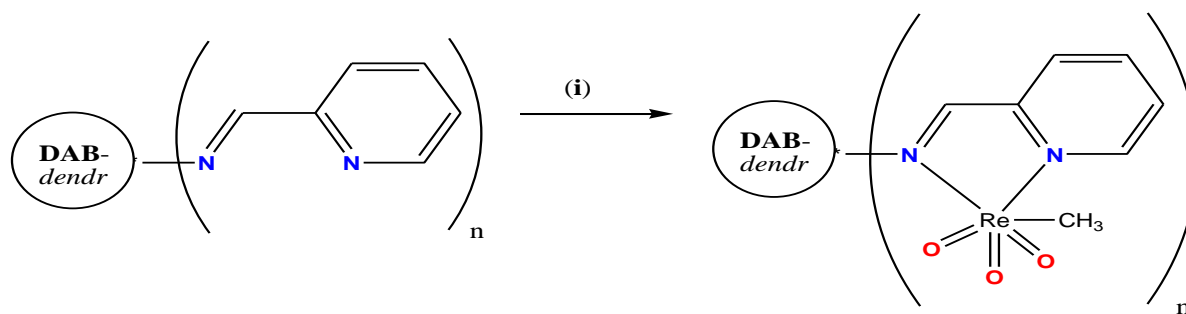


Figure 2.10 (a): General abbreviation of the diaminobutane skeleton in the dendritic complexes DC1-DC2 and V1-V6.

2.5.1.1 Dendritic Schiff-base complexes of MTO, DC1 and DC2.



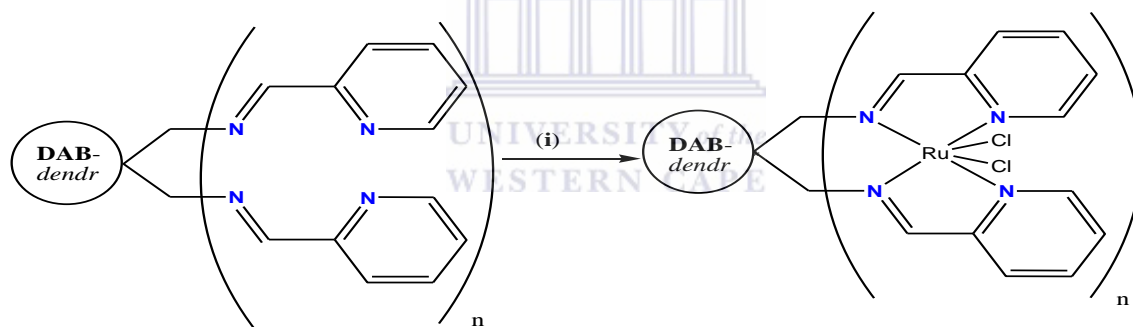
(i) 4 mol. eq. MTO, DCM, overnight, r.t, N₂

n = 4, **DC1 = G1**

n = 8, **DC2 = G2**

Figure 2.10 (b): General representation of the synthesis of MTO dendritic complexes.

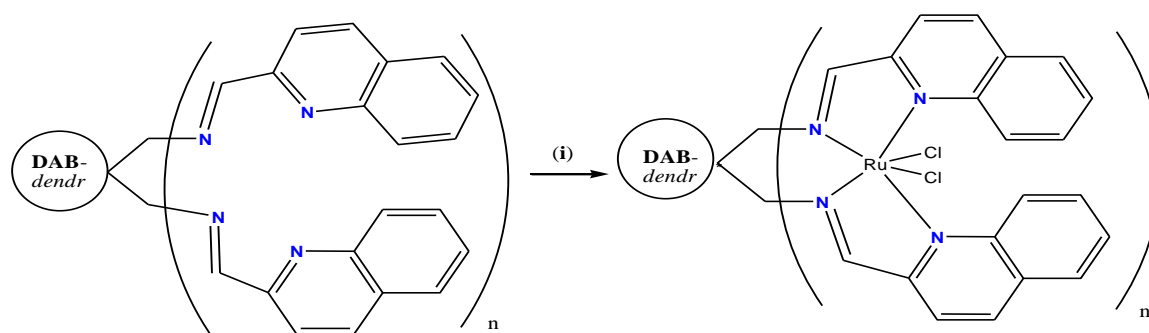
2.5.1.2 Neutral dendritic ruthenium(II) complexes, V1-V4.



(i) 2 mol. eq. RuCl₂(dmsO)₄, DCM, overnight, r.t, N₂

n = 4, **V1 = G1**

n = 8, **V2 = G2**



(i) 2 mol. eq. RuCl₂(dmsO)₄, DCM, overnight, r.t, N₂-G1

n = 4, **V3 = G1**

n = 8, **V4 = G2**

Figure 2.11: General representation of the synthesis of neutral dendritic Ru(II) complexes.

2.5.1.3 Cationic dendrimeric ruthenium complexes, **V5-V6**.

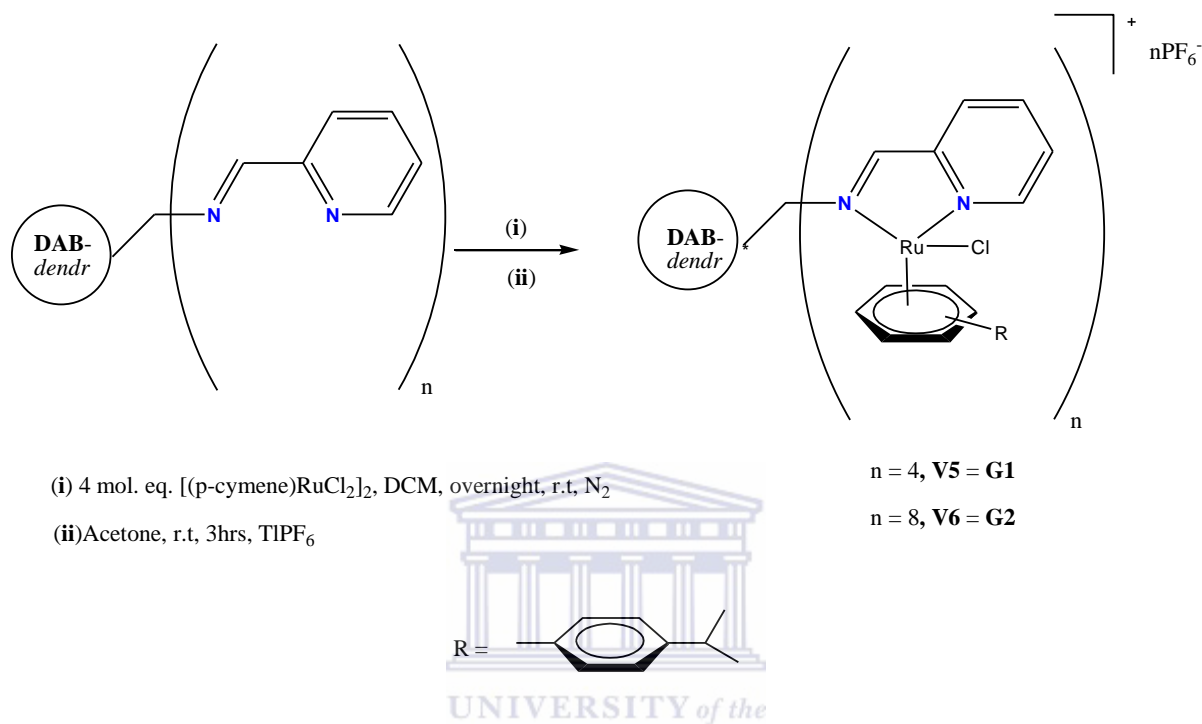


Figure 2.12: General representation of the synthesis of cationic dendritic Ru(II) complexes.

The isolation of the dendritic Re(VII) complexes, **DC1** and **DC2**, was achieved by the reaction of the dendritic ligand, **DL1** and **DL2**, with 4 mole equivalents of MTO in dichloromethane as a solvent (Scheme 2.7). The novel multinuclear Schiff-base complexes of MTO were isolated as brown amorphous solids in 60-70 % yield. As observed with the homobitelllic Schiff-base complex of MTO, the dendritic complex displayed solubility in DMSO and DMF only and were found to be sensitive to moisture and temperature as compared to MTO itself. This is noted by colour change as they change from brown to black when exposed to air. This can thus be circumvented by storing under inert, water free atmosphere. FT-IT was employed to investigate the nature of the functional groups of the

complexes. In the IR spectra of the dendritic complexes, **DC1** and **DC2**, the appearance of the symmetric Re=O stretching vibrations with a narrow range 938-945 cm⁻¹ and the asymmetric vibrations in the range 909-912 cm⁻¹ was indicative of the coordination of the MTO to the dendritic ligands, **DL1** and **DL2**, as compared to the free ligands. The additional electron density contribution from the ligand to the MTO metal centre reduces the bond order thus the Re=O bands are red-shifted due to the donor capacity of the donor capacity of the respective ligands in the solid state as observed by Qui *et al.* The ligands displayed strong bands in the interval 1626-1650 cm⁻¹ and the corresponding dendrimer bands were slightly lower than those of the ligands.



The tetranuclear and octanuclear chelating neutral (**V1-V4**) and cationic (*N,N'*) (**V5-V6**) ruthenium (II) arene metallodendrimers were achieved by reacting the known iminopyridyl poly(propyleneimine) dendritic scaffold with an appropriate molar equivalence of the metal precursor [RuCl₂(dmsO)₄] and dinuclear ruthenium complex [(*p*-cymene)RuCl₂]₂. These complexes (**V5** and **V6**) were later stabilized as hexafluorophosphates and were obtained within the reported yields [27]. As reported, these complexes were found to be soluble in dimethylsulfoxide, acetone and acetonitrile. FT-IR investigations were undertaken and it was observed that imine nitrogen (C=N)imine shifted to lower wavenumbers (~1620 cm⁻¹) confirming coordination of the ruthenium. Similar spectroscopic information was observed for the second generation metallodendrimer. The coordination of the ruthenium centre was further confirmed by MALDI-TOF mass spectrometry. The complexes showed a molecular ion peak with either the loss of a chloride ligand or one of the PF₆ counter-ions.

The ^1H NMR spectra of the ruthenium metallodendrimers (**V1-V4**) showed a significant shift in the imine protons to (**V5-V6**) indicated a loss of two-fold symmetry upon the successful coordination of the N.N'-dendritic scaffold. Four sets of doublets belonging to the p-cymene aromatic protons were observed due to this change/loss of symmetry. The protons (-CH₂-) adjacent to the imine protons appeared as two sets of signals induced by the chiral ruthenium centre. The imine protons appeared as a singlet with the range $\delta \sim 7.6\text{-}8.8$ ppm.

Since these compounds (**V5-V6**) are low-valent ruthenium complexes, the nature of the active species that would be responsible for the oxidative cleavage reactions was investigated by conducting electronic spectrum experiments, as it is precisely known for low-valent ruthenium complexes [28, 30]. The obtained electronic spectrum (Figure 2.13) indicated characteristic peaks of ruthenium tetroxide (RuO₄) with attendant vibrational fine structures at about 445 nm and 380 nm for the organic layer and at about 425 nm and 370 nm for the aqueous layer. Similar results have been reported for oxoruthenate complexes containing RuO₄ [29].

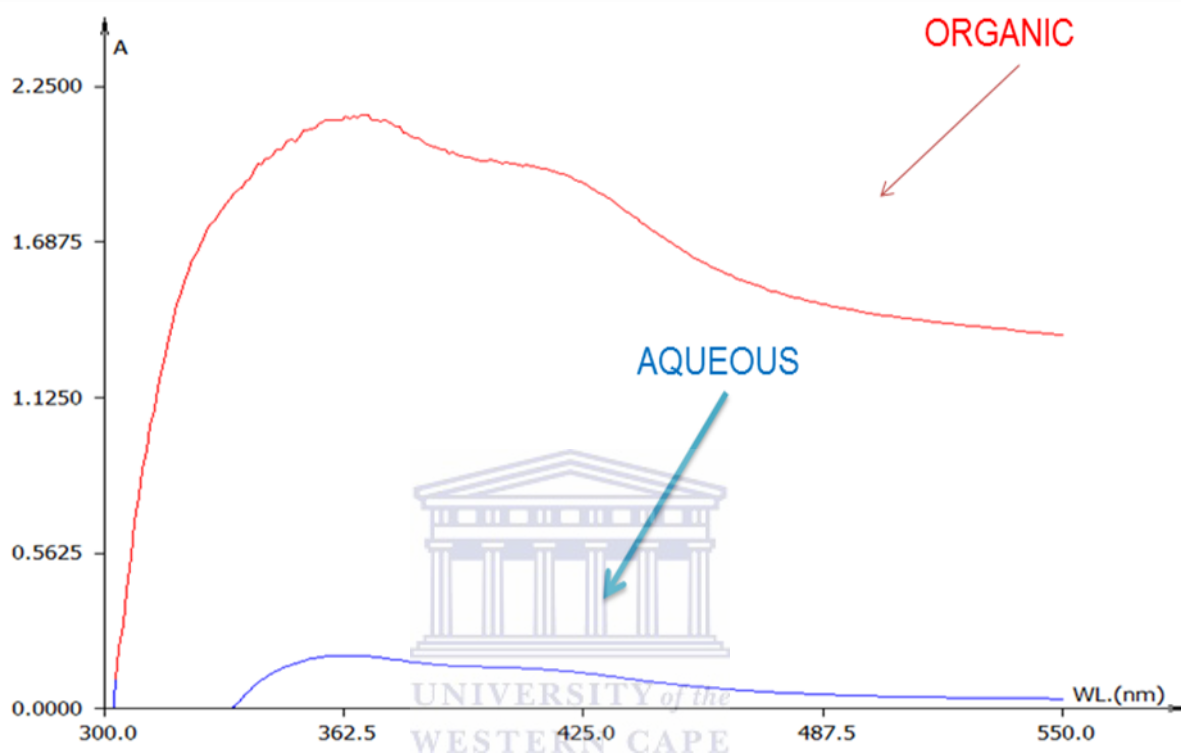


Figure 2.13: Electronic spectrum of the catalyst (**V5**) system; catalyst (0.00278 mmol, **V5**), and NaIO_4 (2.78 mmol) were added in a biphasic solvent system [CNCH_3 (cm^3), CCl_4 (5 cm^3), and H_2O (10 cm^3)] with stirring. The electronic spectrum of organic layer and electronic spectrum of aqueous layer.

AVB-DC5 proton in cdc13

Pulse Sequence: s2pu1

Solvent: CDC13
Temp: 20.0 C / 293.1 K
File: AVB-DC5-proton-cdc13
GEMINI-200 "uwcchem200"

Relax. delay 1.000 sec
Pulse 26.2 degrees
Acq. time 1.994 sec
Width 3000.3 Hz
64 repetitions
OBSERVE H1, 200.0472682 MHz
DATA PROCESSING
Line broadening 1.0 Hz
FT size 18384
Total time 3 min, 17 sec

INDEX	FREQUENCY	PPM	HEIGHT	INDEX	FREQUENCY	PPM	HEIGHT
1	2014.264	10.069	4.9	36	365.949	1.829	35.0
2	1753.464	8.765	3.8	37	275.474	1.377	13.7
3	1718.300	8.589	16.2	38	245.072	1.225	9.3
4	1697.421	8.485	9.4	39	8.447	0.042	3.9
5	1669.583	8.346	22.3				
6	1644.309	8.220	10.2				
7	1590.097	7.949	12.5				
8	1582.405	7.910	18.3				
9	1572.515	7.861	10.7				
10	1564.823	7.822	10.7				
11	1557.181	7.784	10.2				
12	1545.776	7.727	12.4				
13	1538.084	7.689	15.9				
14	1531.491	7.656	13.0				
15	1448.342	7.240	85.6				
16	1421.969	7.108	26.3				
17	1328.198	6.639	3.2				
18	1055.677	5.277	10.9				
19	1029.304	5.145	5.0				
20	836.268	4.180	3.7				
21	731.142	3.655	28.9				
22	725.281	3.626	27.6				
23	712.095	3.560	23.4				
24	701.106	3.505	51.0				
25	684.146	3.470	105.2				
26	688.286	3.441	74.1				
27	682.791	3.413	125.6				
28	676.931	3.384	120.9				
29	660.814	3.303	95.2				
30	635.540	3.177	25.3				
31	579.497	2.897	8.4				
32	541.036	2.705	61.0				
33	518.692	2.593	121.7				
34	492.686	2.463	54.3				
35	477.301	2.386	30.2				

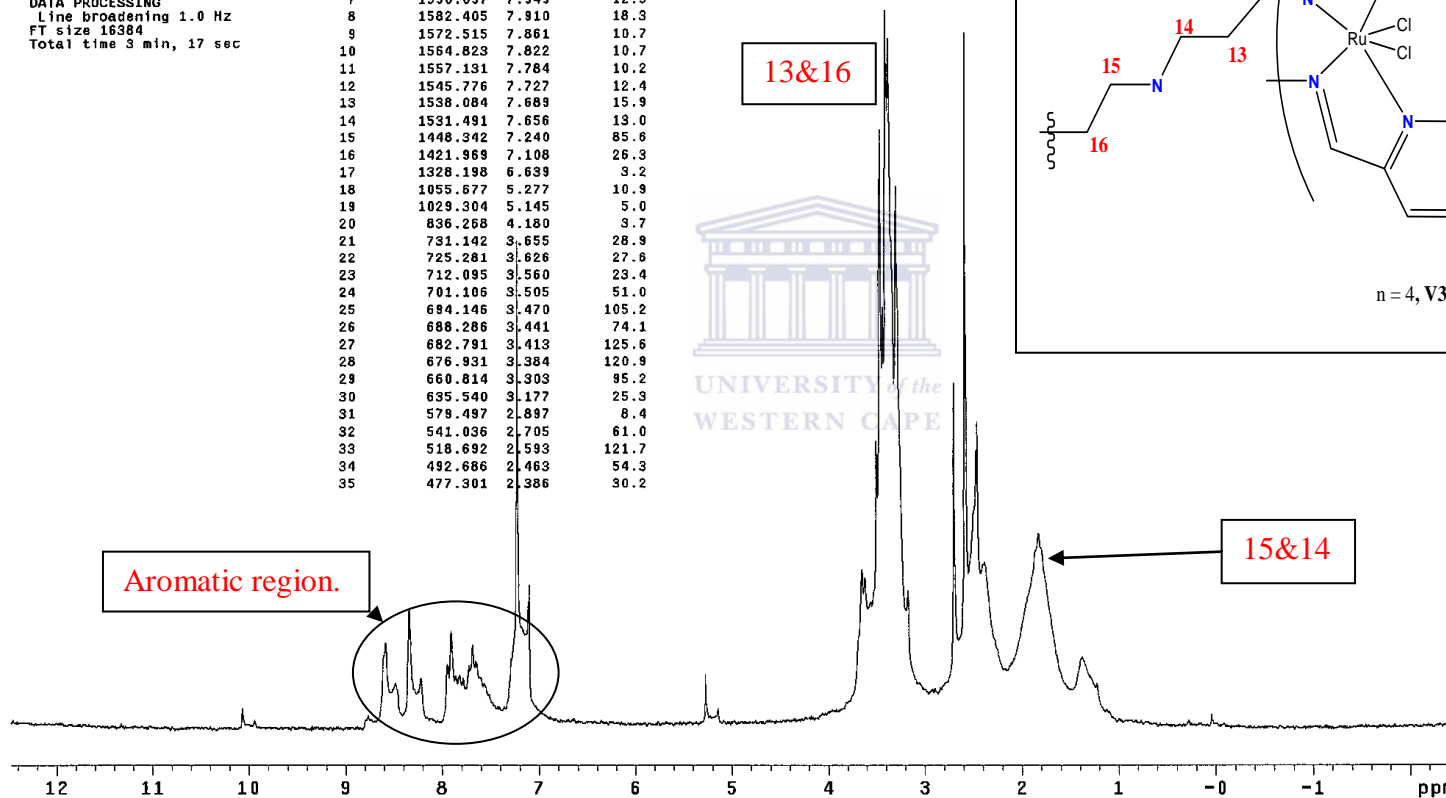
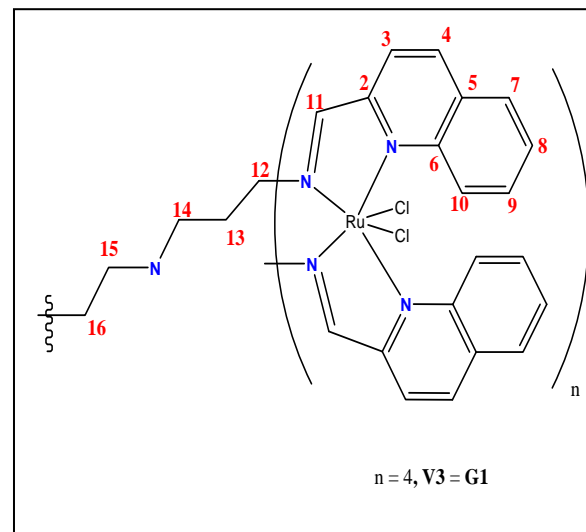


Figure 2.14: ^1H NMR spectrum of dendritic complex, V3, with inset displaying the aromatic region

Table 2.5: ^1H NMR spectral data pertaining to dendrimeric Ru(II) complexes, **V1-V6**.^a

Dendrimeric complex	HC=N	Aromatic region	Aliphatic region
V1	8.59 (s, 4H, CH_{imine})	7.55-7.89 (overlapping tt, 8H, Pyr), 8.25-8.68(overlapping, 8H, Pyr), 8.8-8.99(overlapping, 8H, Pyr)	1.08-2.07(br m, 24H), 2.12-2.78(overlapping dd, 16H), 3.10-3.76 (overlapping qn, 16H)
V2	8.63 (s, 8H, CH_{imine})	7.61-8.00 (overlapping tt, 8H, Pyr), 8.25-8.68(overlapping, 8H, Pyr), 8.67-8.77(overlapping, 8H, Pyr)	1.15-2.19(br m, 24H), 2.22-2.89(overlapping dd, 32H), 3.19-3.85(overlapping qn, 32H)
V3	8.71 (s, 4H, CH_{imine})	7.21-7.31 (overlapping tt, 8H, Pyr), 8.25-8.68(overlapping, 8H, Pyr), 8.28-8.99(overlapping, 8H, Pyr)	1.18-2.21(br m, 24H), 2.22-2.89(overlapping dd, 16H), 3.23-3.96 (overlapping qn, 16H)
V4	8.87 (s, 8H, CH_{imine})	7.81-7.39 (overlapping d, 8H, Pyr), 7.41-8.18(overlapping tt, 8H, Pyr), 8.38-9.19(overlapping dd, 8H, Pyr)	1.21-2.42(br m, 24H), 2.32-3.29(overlapping dd, 12H), (overlapping qn, 32H)
V5	8.99	7.83 (br m, 8H, Pyr), 8.26 (br m, 16H, Pyr), 9.58 (br m, 8H, Pyr)	1.06&1.12(br d, 96H, $\text{CH}(\text{CH}_3)_2$ CYE); 2.49 (br m, 4H, $\text{NCH}_2\text{CH}_2\text{CH}_2$ core), 2.99 (br m, 8H, NCH_2CH_2 branch), 1.84 (br m, 8H, $\text{NCH}_2\text{CH}_2\text{CH}_2\text{N}$ branch), 4.61&4.78($\text{NCH}_2\text{CH}_2\text{CN}$ branch), 2.31 (s, 12H, CH_3 CYE), 2.82 (br m, 8H, $\text{CH}(\text{CH}_3)_2$ CYE), 1.32 (br m, 4H, NCH_2CH_2 core), 5.99 (br m, 16H), 6.31 (br m, 16H),
V6	9.22 (br s, 8H, CH_{imine})	7.99 (br m, 8H, Pyr), 8.33 (br m, 16H, Pyr), 9.61 (br m, 8H, Pyr)	1.08&1.13(br d, 96H, $\text{CH}(\text{CH}_3)_2$ CYE); 1.39(br m, 4H, $\text{NCH}_2\text{CH}_2\text{CH}_2$ core) 1.67-3.39 (overlapping m, 60H, NCH_2CH_2 core, $\text{NCH}_2\text{CH}_2\text{CH}_2\text{N}$ 1st branch, $\text{NCH}_2\text{CH}_2\text{CH}_2\text{N}$ 1st branch, $\text{NCH}_2\text{CH}_2\text{CH}_2\text{N}$ 1st branch, $\text{NCH}_2\text{CH}_2\text{CH}_2$ 2nd branch, $\text{NCH}_2\text{CH}_2\text{CH}_2$ 2nd branch), 2.33 (s, 24H, CH_3 CYE), 2.82 (br m, 8H, $\text{CH}(\text{CH}_3)_2$ CYE), 4.82 (br m, 16H, $\text{NCH}_2\text{CH}_2\text{CH}_2\text{N}$ 2nd branch), 5.99 (br m, 16H), 6.31 (br m, 16H),

^aSpectra run in CDCl_3 and $(\text{CD}_3)_2\text{CO}$ at 25 °C. Chemical shifts given in ppm, referenced relative to residual

2.6 Conclusion

Mono-, bi- and multi-functional Schiff-base ligands were prepared by Schiff base condensation of various aldehyde starting materials. The peripherally modified Schiff-base ligands were isolated in high yields and characterised by a range of analytical techniques. The Schiff-base complexes of MTO displayed sensitivity to moist and temperature and this posed challenge when the complexes had to be analysed as they exhibited signs of decomposition. The ruthenium complexes were isolated in moderate to good yields and were also analysed by the same range of analytical techniques. The purity was confirmed by elemental analysis.

2.7. Materials and Methods

Handling of air-sensitive and/or moisture-sensitive compounds was performed in a nitrogen-filled glove box. Transformations were performed using standard Schlenk techniques under a nitrogen atmosphere. Solvents were dried by distillation prior to use, and all reagents were employed as obtained. The metal precursors ($[\text{RuCl}_2(\text{dmsO})_4]$ and $[(p\text{-cymene})\text{RuCl}_2]_2$) were prepared according to literature[31,32]. ^1H NMR (200 and 500 MHz) and ^{13}C $\{^1\text{H}\}$ (75.38 and 100 MHz) spectra were recorded on Varian VNMRS (300 MHz); Varian Unity Inova (500 MHz) spectrometers and chemical shifts was reported in ppm, referenced to the residual protons of the deuterated solvents and tetramethyl silane (TMS) as internal standard. ESI-MS (ESI+) analyses were performed on Waters API Quattro Micro and Waters API Q-TOF Ultima instruments by direct injection of sample. FT-IR analysis was performed on a Thermo Nicolet AVATAR 330 instrument, and was recorded as neat spectra (ATR) unless specified. Melting point determinations was performed on a Stuart Scientific SMP3 melting point apparatus and is reported as uncorrected.

2.7.1. Synthesis of mono- and bi-functional ligands

The work that was done on the synthesis of the diimine ligands paved a way for the synthesis and thorough characterization of the following prepared ligands.

2.7.1.2 (*E*)-*N*-((pyridin-2-yl)methylene)propan-1-amine, **L1**.

To a stirred solution of 2-pyridinecarbaldehyde (1.98 ml, 21 mmol) in Et₂O (5 ml) was added dropwise a slight excess of n-propylamine (1.87 ml, 25 mmol) that was dissolved separately in dry Et₂O (5ml). The reaction mixture was cooled in an ice-bath during the addition of the amine. The reaction mixture was stirred for 24 hrs at room temperature. After the allotted time the solvent was removed, the oily residue obtained redissolved in dichloromethane (20 ml) and washed with H₂O (10 x 20 ml portions). The organic layer was dried over MgSO₄, filtered and the solvent removed. Yield: 2.25 g, 90 %. ¹³C {¹H} NMR (75.38 MHz, CDCl₃, numbering as per Fig. 2.3): 11.65(CH₃, C¹⁰); 23.66(CH₂, C⁹); 63.08(CH₂, C⁸); 161.53(CH_{imine}, C⁷); 154.45(C_{Ar}, C²); 136.30(CH_{Ar}, C⁵); 120.98(CH_{Ar}, C⁴); 124.39(CH_{Ar}, C³); 149.18(CH_{Ar}, C⁶). *Anal.* Found: C, 66.14; H, 7.35; N, 17.15. Calc. for C₉H₁₂N₂·0.5CH₂Cl₂: C, 66.70; H, 7.714; N, 17.40. MS (ESI, *m/z*): 149.

2.7.1.3. (*7E,10E*)-*N1,N2*-bis((pyridin-2-yl)methylene)ethane-1,2-diamine, **L2**

The same synthetic procedure as outlined above for **L1** was employed for the synthesis of **L2**, using 2-pyridinealdehyde and 1,2-diamineethane as reagents. Yield: 2.46 g, 87 %. ¹³C {¹H} NMR (75.38 MHz, CDCl₃, numbering as per Fig. 2.): δppm = 68.88(CH₂, C⁸); 153.56(CH_{imine}, C⁷); 159.99(C_{Ar}, C²); 123.33(CH_{Ar}, C³); 136.55(CH_{Ar}, C⁴); 127.22(CH_{Ar}, C⁵);

149, 65(CH_{Ar}, C⁶). Anal. Found: C;67.57; H; 6.11; N, 21.55. Calc. For C₁₄H₁₄N₄·0.5CH₂Cl₂: C, 68.11; H, 5.92; N, 23.15. MS (ESI, *m/z*): 240.

2.7.1.4 (7E,10E)-N1,N2-bis((quinolin-2-yl)methylene)ethane-1,2-diamine, **L3**.

The same synthetic procedure as outlined above (**L1**) was employed for the synthesis of **L3**, using 2-quinolinealdehyde and 1,2-diamineethane as reagents. Yield: 2.16 g, 85 %. ¹³C {¹H} NMR (75.38 MHz, CDCl₃, numbering as per Fig. 2.): δppm = 68.88(CH₂, C¹²); 154.56(CH_{imine}, C¹¹); 157.99(C_{Ar}, C²); 122.33(CH_{Ar}, C³); 134.55(CH_{Ar}, C⁴); 131.82(CH_{Ar}, C⁵); 148, 65(CH_{Ar}, C⁶); 128.33(CH_{Ar}, C⁷); 128.55(CH_{Ar}, C⁸); 130.82(CH_{Ar}, C⁹); 130, 65(CH_{Ar}, C¹⁰). Anal. Found: C;77.95; H; 5.41; N, 16.50. Calc. For C₂₂H₁₈N₄: C, 78.08; H, 5.36; N, 16.56. MS (ESI, *m/z*): 339.

2.7.1.5 (7E,8E)-N1,N4-bis((pyridin-2-yl)methylene)butane-1,4-diamine, **L4**.

The same synthetic procedure as outlined above (**L1**) was employed for the synthesis of **L4**, using 2-quinolinealdehyde and 1,2-diamineethane as reagents. Yield: 2.11 g, 87 %. ¹³C {¹H} NMR (75.38 MHz, CDCl₃, numbering as per Fig. 2.): δppm = 31.12(CH₂, C⁹); 62.88(CH₂, C⁸); 152.56(CH_{imine}, C⁷); 158.99(C_{Ar}, C²); 124.33(CH_{Ar}, C³); 135.55(CH_{Ar}, C⁴); 127.82(CH_{Ar}, C⁵); 148, 65(CH_{Ar}, C⁶). Anal. Found: C; 72.11; H; 6.77; N, 21.22. Calc. For C₁₆H₁₈N₄: C, 72.15; H, 6.81; N, 21.04. MS (ESI, *m/z*): 267.

2.7.2 *Synthesis of mono- and bi-functional ruthenium and rhenium complexes, C1 and C2.*

2.7.2.1 *Schiff-base MTO complex, C1.*

To a stirring solution of MTO (124.6 mg, 0.5 mmol) in dichloromethane (3ml) was added (E)-N-((pyridin-2-yl)methylene)propan-1-amine (**L1**, 74.1 mg, 0.5 mmol). A few seconds later a yellow precipitate was formed. The yellow precipitate was collected by filtration, washed with 1x5ml of DCM, and dried under reduced pressures. Yield = 123 mg, 80%. ^{13}C { ^1H } NMR (75.38 MHz, CDCl_3 , numbering as per Fig. 2.3): 11.75(CH_3 , C^{10}); 25.66(CH_2 , C^9); 67.08(CH_2 , C^8); 163.53(CH_{imine} , C^7); 158.45(C_{Ar} , C^2); 136.30(CH_{Ar} , C^5); 120.98(CH_{Ar} , C^4); 126.39(CH_{Ar} , C^3); 150.98(CH_{Ar} , C^6). Anal. Found: C 30.12, H 3.77, N 7.00. Calc. For $\text{C}_{44}\text{H}_{64}\text{N}_{10}\text{O}_{12}\text{Re}_4$: C, 30.22; H, 3.80; N, 7.05. MS (ESI, m/z): 267 (for the ligand) and 249 (for MTO).

2.7.2.2 *Homobimetallic Schiff-base MTO complex, C2.*

The same synthetic procedure as outlined above (**C1**) was employed for the synthesis of **C2**, using **L4** as reagent. Yield: 115 mg, 85 %. Anal. Found: C 31.42, H 3.90, N 7.70. Calc. For $\text{C}_{44}\text{H}_{64}\text{N}_{10}\text{O}_{12}\text{Re}_4$: C, 31.65; H, 3.86; N, 8.39. MS (ESI, m/z): 149 (for the ligand) and 249 (for MTO).

2.7.2.3 Neutral mononuclear ruthenium complex, **B1**.

(0.4097 mmol, 198.5 mg) of the $\text{RuCl}_2(\text{dmsO})_4$ metal precursor was added to a stirred solution of the ligand (**L2**, 0.4097 mmol, 98.0 mg) in 5 ml of dry dichloromethane at room temperature. While the metal precursor was dissolved separately in 5 ml before addition. The reaction was allowed to continue stirring overnight. The volume was reduced to 1/5 th and neutral aluminium oxide was added, and the mixture transferred to a neutral aluminium oxide packed with DCM and the blue band was eluted using 10:1 mixture of dichloromethane:acetone. The blue solution was dry under reduced pressures. Yield = 135 mg, 88 %. ^{13}C { ^1H } NMR (75.38 MHz, CDCl_3 , numbering as per Fig. 2.3): $\delta\text{ppm} = 68.88(\text{CH}_2, \text{C}^8)$; $163.7(\text{CH}_{\text{imine}}, \text{C}^7)$; $158.99(\text{C}_{\text{Ar}}, \text{C}^2)$; $123.93(\text{CH}_{\text{Ar}}, \text{C}^3)$; $137.55(\text{CH}_{\text{Ar}}, \text{C}^4)$; $128.76(\text{CH}_{\text{Ar}}, \text{C}^5)$; $151, 65(\text{CH}_{\text{Ar}}, \text{C}^6)$. Anal. Found: C, 40.54; H, 3.36; N, 13.55. Calc. For $\text{C}_{14}\text{H}_{14}\text{N}_4\text{Cl}_2\text{Ru}$: C, 40.99; H, 3.44; N, 13.66.. MS (ESI, m/z): 411

2.7.2.4 Neutral mononuclear ruthenium complex, **B2**.

The same synthetic procedure as outlined above for **C2** was employed for the synthesis of **B3**, using **L3** as reagent. Yield: 85 %. ^{13}C { ^1H } NMR (75.38 MHz, CDCl_3 , numbering as per Fig. 2.3): $\delta\text{ppm} = 68.88(\text{CH}_2, \text{C}^{12})$; $163.76(\text{CH}_{\text{imine}}, \text{C}^{11})$; $159.19(\text{C}_{\text{Ar}}, \text{C}^2)$; $122.93(\text{CH}_{\text{Ar}}, \text{C}^3)$; $136.56(\text{CH}_{\text{Ar}}, \text{C}^4)$; $131.86(\text{CH}_{\text{Ar}}, \text{C}^5)$; $149.11(\text{CH}_{\text{Ar}}, \text{C}^6)$; $128.73(\text{CH}_{\text{Ar}}, \text{C}^7)$; $127.25(\text{CH}_{\text{Ar}}, \text{C}^8)$; $130.92(\text{CH}_{\text{Ar}}, \text{C}^9)$; $131.15(\text{CH}_{\text{Ar}}, \text{C}^{10})$. Anal. Found: C 50.07, H 3.48, N 11.22. Calc. For $\text{C}_{22}\text{H}_{64}\text{N}_{18}\text{Cl}_2\text{N}_4\text{Ru}$: C, 51.77; H, 3.55; N, 10.98. MS (ESI, m/z): 513 (doubly charged)

2.7.2.5 Cationic mononuclear ruthenium complex, **B3**.

The cationic complex **B3** was achieved by chloride abstraction using thallium hexafluorophosphate salt (**TIPF₆**, 51.8 mg, 0.106 mmol) from the neutral complex **B1** and subsequently stabilized via metathesis as hexafluorophosphate. Yield: 80%. ¹³C {¹H} NMR (75.38 MHz, CDCl₃, numbering as per Fig. 2.3): δppm = 68.88(CH₂, C⁸); 163.7(CH_{imine}, C⁷); 158.99(C_{Ar}, C²); 123.93(CH_{Ar}, C³); 137.55(CH_{Ar}, C⁴); 128.76(CH_{Ar}, C⁵); 151, 65(CH_{Ar}, C⁶). Anal. Found: C, 42.52; H, 2.66; N, 8.99. Calc. For C₂₂H₁₈ClF₆N₄PRu: C, 42.63; H, 2.93; N, 9.04. MS (ESI, *m/z*): 474 [M-PF₆]⁺. Melting Point: 183-185

2.7.2.6 Cationic mononuclear ruthenium complex, **B4**.

The same manipulation for isolation of complex **B3** was undertaken for the achievement of **B4** using thallium hexafluorophosphate salt (**TIPF₆**, 14.3 mg, 0.0410 mmol). Yield = 74%. ¹³C {¹H} NMR (75.38 MHz, CDCl₃, numbering as per Fig. 2.3): δppm = 68.88(CH₂, C¹²); 163.76(CH_{imine}, C¹¹); 159.19(C_{Ar}, C²); 122.93(CH_{Ar}, C³); 136.56(CH_{Ar}, C⁴); 131.86(CH_{Ar}, C⁵); 149.11(CH_{Ar}, C⁶); 128.73(CH_{Ar}, C⁷); 127.25(CH_{Ar}, C⁸); 130.92(CH_{Ar}, C⁹); 131.15(CH_{Ar}, C¹⁰). Anal. Found: C 51.07, H 3.48, N 10.22. Calc. For C₂₂H₁₈ClF₆N₄PRu: C, 51.77; H, 3.55; N, 10.98. MS (ESI, *m/z*): 457 [M-PF₆]⁺. Melting Point: 182-184

2.7.2.7 Cationic nomobimetallic ruthenium complex, **B5**.

The compound was synthesized in a similar fashion as reported in literature for a cationic mononuclear complex [27]. The ligand, (L4, 0.0830 g 0.312 mmol) was dissolved in ethanol (5 mL) and the resulting solution was added drop-wise to a stirred solution of $[\text{Ru}(\eta^6\text{-p-Pr}^i\text{C}_6\text{H}_4\text{Me})\text{Cl}_2]_2$ (0.191 g, 0.312 mmol) in ethanol (20 mL). The solution was allowed to stir overnight at r.t, filtered and the filtrate reduced to about 5 mL. TIPF_6 (0.053 g, 0.311 mmol) was added and the reaction was stirred at 0°C for 3 hrs. The r.b.f was left in the freezer for 12 hrs to precipitate the product which was filtered, washed with ethanol and diethyl ether, and dried under vacuum. Yield = 82 %. ^{13}C { ^1H } NMR (75.38 MHz, CDCl_3): δ ppm = 21.8, 22.56, 24.11(CH_3 , C_{CYE}); 167.76(CH_{imine} , C^7); 156.19(C_{Ar} , C^2); 122.93(CH_{Ar} , C^3); 136.56(CH_{Ar} , C^4); 131.86(CH_{Ar} , C^5); 155.11(CH_{Ar} , C^6); 128.73(CH_{Ar} , C^7); 127.25(CH_{Ar} , C^8); 130.92(CH_{Ar} , C^9); 131.15(CH_{Ar} , C^{10}) Anal. Found: C 50.07, H 3.48, N 11.22. Calc. For $\text{C}_{22}\text{H}_{18}\text{ClF}_6\text{N}_4\text{PRu}$: C, 51.77; H, 3.55; N, 10.98. MS (ESI, m/z): 838 (doubly charged) $[\text{M}-2\text{PF}_6]^+$. Melting Point: 185-189°C

2.7.3 Synthesis of dendritic ligands, **DL1-DL4**.

The ligand synthesis is well documented by Smith *et al.* [6, 9], Malgas *et al.* [12, 13] and the same synthetic methodology was followed. The synthesis of DL1 is described as it is the general synthetic methodology for all the dendritic ligands.

2.7.3.1 G1 DAB-[N=CH-(2-pyr)₄], **DL1**.

A moist free environment was ensured, thus a Schlenk was evacuated and purged with a stream of nitrogen gas. 2-pyridinecarboxyaldehyde (0.27 g, 2.17 mmol) was dissolved in 10 ml dry toluene and stirred for a few minutes before the addition of DAB-dendr-(NH₂)₄ generation one (0.18g, 0.56mmol) dropwise that was dissolved in 10 ml of dry toluene as well. The reaction was allowed to proceed for 72 hrs at room temperature. The solvent was removed and the yellow oil residue obtained redissolved in dichloromethane (20 ml). The organic layer was washed with water (5x20 ml portions), separated and dried over MgSO₄. The solvent was removed and the yellow oil obtained purified by vacuum distillation, using the Kugelrohr apparatus, at 90 °C and 15 mmHg for 60 min. Yield 78%. ¹³C {¹H} (75.38 MHz, CDCl₃, numbering as depicted in the schematics above Fig. 2.9): δppm = 23.2 (CH₂, C¹²); 25.4 (CH₂, C¹¹); 28.5 (CH₂, C¹⁰); 52.1 (CH₂, C⁹); 54.3 (CH₂, C⁸); 159.8 (CH_{imine}, C⁷); 162.5 (C_{Ar-pyr}, C⁶); 121.8 (CH_{Ar}, C⁵); 124.7 (CH_{Ar}, C⁴); 139.8 (CH_{Ar}, C³); 150.9 (CH_{Ar}, C²).
(a) Anal. Calc for C₄₀H₅₂N₁₀· $\frac{1}{2}$ CH₂Cl₂: C, 68.00; H, 7.47; N, 19.58. Found: C, 68.36; H, 7.51; N, 20.00%.

2.7.3.2 G1 DAB-[N=CH(2-quin)₄], **DL2**.

The ligand, **DL2**, was synthesized mimicking the synthetic procedure outlined above for the synthesis of **DL1**, using 2-quinolinecarboxaldehyde as reagent. Yield = 2.07 g, 81 %. ¹³C {¹H} (75.38 MHz, CDCl₃, numbering as depicted in the schematics above Fig. 2.9): δppm = 22.2(CH₂, C¹⁷); 24.9(CH₂, C¹⁶); 28.9(CH₂, C¹⁵); 51.4(CH₂, C¹⁴); 55.4(CH₂, C¹³);

59.7(CH₂, C¹²); 162.4(CHimine, C¹¹); 118.3(CH_{Ar}, C³); 127.3(CH_{Ar}, C⁷); 136.5(CH_{Ar}, C⁴); 147.7(CH_{Ar}, C⁶); 129.4(CH_{Ar}, C¹⁰); 129.5(CH_{Ar}, C⁷); 127.6(CH_{Ar}, C⁸); 128.7(CH_{Ar}, C⁹); 154.7(C_{Ar}, C²). Anal. Found: C, 69.30; H, 8.18; N, 20.50. Calc. For. C₈₈H₁₂₀N₂₂ · 0.5 CH₂Cl₂: C, 69.54; H, 7.99; N, 20.16. MS (ESI, *m/z*): 874

2.7.3.3 G2 DAB-[N=CH(2-pyr)₈], **DL3**.

The ligand, **DL3**, was synthesized mimicking the synthetic procedure outlined above for the synthesis of **DL1**, using 2-pyridinecarboxaldehyde as reagent. Yield = 2.07 g, 79 %. ¹³C {¹H} (75.38 MHz, CDCl₃, numbering as depicted in the schematics above Fig. 2.9): δppm = 23.4(CH₂, C¹⁶); 24.2(CH₂, C¹⁵); 28.1(CH₂, C); 51.6(CH₂, C); 53.13(CH₂, C); 59.5(CH₂, C) 161.8(CHimine, C¹¹); 121.2(CH_{Ar}, C³); 124.5(CH_{Ar}, C⁴); 136.4(CH_{Ar}, C⁵); 149.3(CH_{Ar}, C⁶); 154.5(C_{Ar}, C²); 127.3(CH_{Ar}, C⁷); 126.3(CH_{Ar}, C⁸); 128.3(CH_{Ar}, C⁹); 129.3(CH_{Ar}, C¹⁰). Anal. Found: C, 75.70; H, 7.06; N, 16.37. Calc. For. C₅₆H₆₀N₁₀ · 0.2 CH₂Cl₂: C, 75.86; H, 6.79; N, 15.75. MS (ESI, *m/z*): 874

2.7.3.4 G2 DAB-[N=CH(2-quin)₈], **DL4**.

The ligand, **DL4**, was synthesized mimicking the synthetic procedure outlined above for the synthesis of **DL1**, using 2-quinolinecarboxaldehyde as reagent. Yield = 2.07 g, 80 %. ¹³C {¹H} (75.38 MHz, CDCl₃, numbering as depicted in the schematics above Fig. 2.9): δppm = 22.0(CH₂, C¹⁹); 24.9(CH₂, C¹⁸); 27.8(CH₂, C¹⁷); 51.3(CH₂, C¹⁶); 52.8(CH₂, C¹⁵); 59.2(CH₂, C¹⁴); 161.9(CHimine, C¹¹); 117.9(CH_{Ar}, C³); 127.2(CH_{Ar}, C⁴); 135.9(CH_{Ar}, C⁵); 147.4(CH_{Ar},

C⁶); 128.9(CH_{Ar}, C⁷); 129.1(CH_{Ar}, C⁸); 127.5(CH_{Ar}, C⁹); 128.8(CH_{Ar}, C¹⁰); 154.4(CH_{Ar}, C²).

Anal. Found: C, 71.79; H, 7.15; N, 16.03. Calc. For C₁₂₀H₁₃₆N₂₂. 2 CH₂Cl₂: C, 71.28; H, 6.82; N, 14.99. MS (ESI, m/z): 874

2.7.4 Synthesis of multinuclear dendritic MTO complexes, **DC1** and **DC2**.

2.7.4.1 G1 DAB-MTO complex, **DC1**.

The synthesis of the complexes was achieved using Qui *et. al* [11] synthetic route modified as follows: dry dichloromethane was used instead of methanol to achieve the desired products. To a stirring solution of MTO (47.76 mg, 0.192 mmol) in dry dichloromethane (2.5 ml), was added a solution of dendritic ligand (G2: 35.6mg, 0.023955 mol, 2.5ml). The reaction was allowed to stir at room temperature over night under moist free atmosphere. Subsequently, the solvent was reduced to 2.5ml and the precipitated formed was filtered, washed with DCM (1x5ml) and the yellow solids dried under reduced pressures. Yield 83%. Anal. Found: C, 31.75; H 3.96; N 8.40. Calc. For C₄₄H₆₄N₁₀O₁₂Re₄: C, 31.65; H, 3.84; N, 8.41. MS (ESI, m/z): 673 (for the ligand) and 249 (for MTO).

2.7.4.2 G2 DAB-MTO complex, **DC2**.

The same synthetic procedure outlined above was followed for the synthesis of the Dendritic Complex, **DC2**. Yield 80%. Anal. Found: C, 33.50; H, 4.10; N 8.82. Calc. For

$C_{96}H_{144}N_{22}O_{24}Re_8$: C, 33.13; H, 4.17; N, 8.85. MS (ESI, m/z): 1486 (for the ligand) and 249 (for MTO).

2.7.5 Synthesis of generation I pyridyl/quinolyimine ruthenium (II) complexes, **V1-V6**.

2.7.5.1 G1 DAB pyridylimine ruthenium (II) complex, **V1**.

(0.123 mmol, 59.6 mg) of the $RuCl_2(dmsO)_4$ metal precursor was added dropwise to a stirring solution of the dendritic ligand (**DL1**, 0.0616 mmol, 41.5 mg) in 5 ml of dry dichloromethane at room temperature. While the metal precursor was dissolved separately in 5 ml before addition. The reaction was allowed to continue stirring overnight. The volume was reduced to 1/5 th and neutral aluminium oxide was added, and the mixture transferred to a neutral aluminium oxide packed with DCM and the blue band was eluted using a 10:1 mixture of dichloromethane:acetone. The blue solution was dried under reduced pressures. Yield 56%. $^{13}C \{^1H\}$ (75.38 MHz, $CDCl_3$, numbering as depicted in the schematics above Fig. 2.9): δ ppm = 25.4 (CH_2 , C^{12}); 52.4 (CH_2 , C^{11}); 47.5 (CH_2 , C^{10}); 53.41 (CH_2 , C^9); 54.3 (CH_2 , C^8); 163.8 (CH_{imine} , C^7); 162.5 (C_{Ar-pyr} , C^2); 123.8 (CH_{Ar} , C^3); 126.7 (CH_{Ar} , C^4); 139.8 (CH_{Ar} , C^5); 151.9 (CH_{Ar} , C^6). (a) Anal. Calc for $C_{40}H_{52}N_{10} \cdot \frac{1}{2}CH_2Cl_2$: C, 47.25; H, 5.15; N, 13.77. Found: C, 47.12; H, 5.20; N, 14.01. MS (ESI, m/z): 1030.14. Melting point: 157-159°C.

2.7.5.2 *G2 DAB pyridylimine ruthenium (II) complex, V2.*

The same above outlined synthetic procedure for (**V1**) was mapped for the synthesis of **V2**, using DAB-[N=CH-(2-pyr)₈] (**DL2**) as reagent. Yield = 152 mg, 68 %. ¹³C {¹H} (75.38 MHz, CDCl₃, numbering as depicted in the schematics above Fig. 2.9): δppm = 25.43(CH₂, C¹⁶); 26.48(CH₂, C¹⁵); 50.17-53.82(CH₂, C¹⁴⁻¹⁰); 58.9(CH₂, C⁹) 163.80(CHimine, C); 121.17(CH_{Ar}, C³); 124.51(CH_{Ar}, C⁴); 136.45(CH_{Ar}, C⁵); 150.50(CH_{Ar}, C⁶); 154.53(C_{Ar}, C²). Elemental Analysis (%): Calc. For C₅₆H₆₀N₁₀Cl₄Ru₂: C, 48.62; H, 5.56; N, 14.17. Anal. Found: C, 49.22; H, 5.96; N, 14.88. MS (ESI, *m/z*): 2213.42 . Melting Point: 158-162°C.

2.7.5.3 *G1 DAB quinolyimine ruthenium (II) complex, V3.*

The same above outlined synthetic procedure for (**V2**) was mapped for the synthesis of **V3**, using DAB-[N=CH-(2-quin)₄] (**DL3**) as reagent. Yield = 122 mg, 60 %. ¹³C {¹H} (75.38 MHz, CDCl₃, numbering as depicted in the schematics above Fig. 2.9): δppm = 22.17(CH₂, C¹⁷); 24.91(CH₂, C¹⁶); 28.88(CH₂, C¹⁵); 51.44(CH₂, C¹⁴); 55.38(CH₂, C¹³); 61.46(CH₂, C¹²); 163.44(CHimine, C¹¹); 118.33(CH_{Ar}, C³); 127.26(CH_{Ar}, C⁷); 136.48(CH_{Ar}, C⁴); 147.68(CH_{Ar}, C⁶); 129.36(CH_{Ar}, C¹⁰); 129.54(CH_{Ar}, C⁷); 127.63(CH_{Ar}, C⁸); 128.78(CH_{Ar}, C⁹); 159.76(C_{Ar}, C²). Elemental Analysis (%): Calc. For C₅₆H₆₀N₁₀Cl₄Ru₂: C, 55.26; H, 4.97; N, 11.51. Anal. Found: C, 55.11; H, 4.90; N, 11.71. MS (ESI, *m/z*): 1240.18 [M+Na]⁺. Melting Point: 174-177°C.

2.7.5.4 G2 DAB quinolyimine ruthenium (II) complex, **V4**.

The same above outlined synthetic procedure for (**V3**) was followed for the synthesis of **V4**, using DAB-[N=CH-(2-quin)₈] (**DL3**) as reagent. Yield = 102 mg, 62 %. ¹³C {¹H} (75.38 MHz, CDCl₃, numbering as depicted in the schematics above Fig. 2.9): δppm = 22.81(CH₂, C¹⁹); 25.92(CH₂, C¹⁸); 29.82(CH₂, C¹⁷); 52.27(CH₂, C¹⁶); 53.76(CH₂, C¹⁵); 60.75(CH₂, C¹⁴); 163.85(CH_{imine}, C¹¹); 122.93(CH_{Ar}, C³); 127.20(CH_{Ar}, C⁷); 136.99(CH_{Ar}, C⁴); 148.26(CH_{Ar}, C⁶); 128.95(CH_{Ar}, C); 129.13(C_{Ar}, C⁵); 127.46(CH_{Ar}, C⁸); 128.80(CH_{Ar}, C⁹); 159.36(C_{Ar}, C¹⁰). Elemental analysis (%): Calc. For C₁₂₀H₁₃₆N₂₂Cl₈Ru₄: C, 56.96; H, 5.41; N, 10.89. Anal. Found: C, 56.11; H, 5.21; N, 11.21. MS (ESI, *m/z*): 2595.51 [M+Na]⁺. Melting point: 179-182°C.

2.7.5.5 G1 DAB cationic pyridylimine ruthenium (II) complex, **V5**.

The same synthetic procedure reported by Govender *et. al.* was employed in the synthesis of the cationic metallodendrimers [27]. The complexes were first reported by them as well. The dendritic ligand (**DL1**, 102 mg, 0.152 mmol) or (**DL2**, 101 mg, 0.068 mmol) was dissolved in ethanol (5.0 ml) and added dropwise to a stirring solution of [Ru(η⁶-p-PrⁱC₆H₄Me)Cl₂]₂ (191 mg, 0.312 mmol for **V5** or 0.276 mmol for **V6**) in ethanol (15.0 ml). The solution was allowed to stir at room temperature overnight. The solution was then filtered and the filtrate reduced to about 5 ml. NaPF₆ (53 mg, 0.311 mmol for **V5** or 0.276 mmol for **V6**) was added and the reaction was stirred at 0°C for 3 hrs. The reaction vessel was left in the freezer for an additional 12 hrs to precipitate the product. The product was

filtered, washed with ethanol and diethyl ether, and dried under vacuum. Yield = 240 mg, 66 %. ^{13}C { ^1H } (75.38 MHz, $(\text{CD}_3)_2\text{CO}$, numbering as depicted in the schematics above Fig. 2.9): δppm = 18.59, 21.53, 22.23($\text{CH}_{3\text{CYE}}$); 24.53, 26.56, 51.33, 53.44, 64.98(CH_2 , C^{19-12}); 31.2, 84.99, 85.76, 85.98, 87.69 (CH_{CYE}); 104.29, 106.21(CH_{CYE}); 167.78(CH_{imine} , C^{11}); 128.93, 129.20, 139.19, 153.26(CH_{pyr}); 155.56(C_{pyr}). *Anal.* Found C, 41.21; H, 4.70; N, 5.71. Calc. for $\text{C}_{80}\text{H}_{108}\text{N}_{10}\text{Ru}_4\text{Cl}_4\text{P}_4\text{F}_{24}$ (2335.8): C, 41.14; H, 4.66; N, 6.00. MS (MALDI-TOF, m/z): 2192 $[\text{M}]^+$. Melting point: 169°C-172°C.

2.7.5.6 *G2 DAB cationic pyridylimine ruthenium (II) complex, V6.*

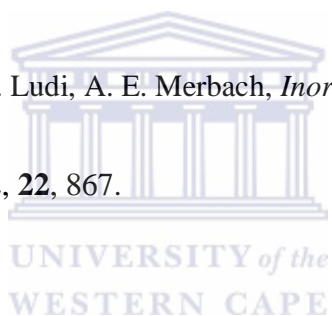
The same above outlined synthetic procedure for (**V5**) was followed for the synthesis of **V6**, using DAB-[N=CH-(2-pyr) $_4$] (**DL2**) as reagent. Yield = 132 mg, 42 %. ^{13}C { ^1H } (75.38 MHz, $(\text{CD}_3)_2\text{CO}$, numbering as depicted in the schematics above Fig. 2.9): δppm = 18.89, 21.93, 22.43($\text{CH}_{3\text{CYE}}$); 25.56-27.33, 50.44-52.23, 64.9(CH_2 , C^{19-12}); 31.2, 84.99, 85.76, 85.98, 87.99 (CH_{CYE}); 104.29, 106.21(CH_{CYE}); 168.85(CH_{imine} , C^{11}); 128.93, 129.20, 140.19, 156.26(CH_{pyr}); 155.36(C_{pyr}). *Anal.* Found C, 41.82; H, 5.02; N, 6.19. Calc. for $\text{C}_{168}\text{H}_{232}\text{N}_{22}\text{Ru}_8\text{Cl}_8\text{P}_8\text{F}_{48}$ (4811.8): C, 41.94; H, 4.86; N, 6.40. MS (MALDI-TOF, m/z): 4811 $[\text{M}]^+$. Melting point: 175°C-179°C.

References:

1. M. J. Chitanda, D.E.Prokopchuk, *Organomet.*, 2008, **27**, 2337.
2. (a) T. P. Noon and E. N. Jacobsen, *Science*, 2003, **299**, 1691; (b) A. J. Swarts, *Mononuclear and Multinuclear Palladacycles as Catalyst Precursors*, MSc Thesis, Stellenbosch University, **2011**; (c) N. Mketo, *Palladium and Copper complexes based on a dendrimeric and monofunctional N,N'-chelating ligands as potential catalysts in the oxidative carbonylation of alcohols*, MSc Thesis, **2010**.
3. D. M. Haddleton, D. J. Duncalf, *Eur. J. Inorg. Chem.*, 1998, 1799.
4. W. Massa, S. Dehgampour, *Inorg.Chem.*, 2009, **362**, 2872.
5. R. Chen, J. Bacsa, S.F. Mapolie, *Polyhedr.*, 2003, **22**, 2855.
6. J. Cloete, S.F. Mapolie, *J. Mol. Catal. A:*, 2006, **243**, 221.
7. G. Smith, R. Chen and S. Mapolie, *J. Organomet. Chem.*, **2003**, 673, 111.
8. D. Prema, A.V. Wiznycia, *Dalton Trans.*, 2007, 4788.
9. V. Amandola, C. Mangano, *Inorg.Chem.*, 2003, **42**, 6056.
10. G. S. Smith and S. F. Mapolie, *J. Mol. Catal. A: Chem.*, 2004, **213**, 187.
11. C–J. Qui, Y–C. Zhang, Y. Gao, J–Q. Zhao, *J. Organomet. Chem.*, 2009, **694**, 3418.
12. (a) A. Capape, M. D. Zhou, S. L. Zhang, F. E. Kühn, *J. Organomet. Chem.*, 2008, **693**, 3240. (b) P. Ferreira, W. M. Xue, E. Bencze, F. E. Kühn, *Inorg. Chem.*, 2001, **40**, 5834.

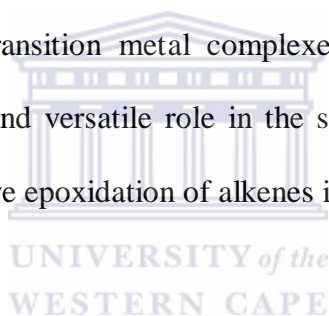
13. E. Buhleier and W. Wehner, *Synthesis*, 1978, 155.
14. D. A. Tomalia, H. Baker, J. Dewald, M. Hall, G. Kallos, S. Martin, J. Roeck, J. Ryder and P. Smith, *Polym. J.*, 1985, **17**, 117.
15. D. A. Tomalia, H. Baker, J. Dewald, M. Hall, G. Kallos, S. Martin, J. Roeck, J. Ryder and P. Smith, *Macromolecules*, 1986, **19**, 2466.
16. D. A. Tomalia, A. M. Naylor and W. A. Goddard, *Angew. Chem. Int. Ed. Engl.*, 1990, **29**, 138.
17. C. Hawker and J. M. J. Frechet, *J. Chem. Soc., Chem. Commun.*, 1990, 1010.
18. C. J. Hawker and J. M. J. Frechet, *J. Am. Chem. Soc.*, 1990, **112**, 7638.
19. C. J. Hawker and J. M. J. Frechet, *Macromolecules*, 1990, **23**, 4726.
20. J. M. J. Frechet, *J. Polym. Sci., Part A: Polym. Chem.*, 2003, **41**, 3713.
21. E.M.N. de-van Brabander Berg, E.W. Meijer, *Angew. Chem. Int. Ed. Engl.*, 1993, **32**, 1308.
22. G. R. Newkome, C. D. Shreiner, *Polymer*, 2008, **49**, 1.
23. A. Morean, *Electrochim, Acta*, 1998, **26**, 1609.
24. H. S. Li, T.A.Konovalova, *J. Phys. Chem.*, 2009, **113**, 5358.
25. R. Malgas-Enus, S. F. Mapolie and G. S. Smith, *J. Organomet. Chem.*, 2008, **693**, 2279-2286.
26. J. N. Mugo, S. F. Mapolie and J. L. van Wyk, *Inorg. Chim. Acta*, 2010, **363**, 2643.

27. P. Govender, A. K. Renfrew, C. M. Clavel, P. J. Dyson, B. Therrien, G. S. Smith, *Dalton Trans.*, 2011, **40**, 1158.
28. Murahashi, S.-I.; Komiya, N.; Hayashi, Y. H.; Kumano, T. *Pure Appl. Chem.* 2001, **73** (2), 311.
29. R. E. Connick, C. R. Hurley, *J. Am. Chem. Soc.*, 1952, **74**, 5012.
30. A. G. F. Shoir and R. H. Mohamed, *Synthetic Communications*, 2006, **36**, 59.
31. (a) M. A. Bennett, T. N. Huang, T. W. Matheson, A. K. Smith, *Inorg. Synth.*, 1985, **21**, 75;(b) M. A. Bennett, T. W. Matheson, G. B. Robertson, A. K. Smith, P. A. Tucker, *Inorg. Chem.*, 1980, **10**, 1014.
32. N. Aebischer, G. Laurency, A. Ludi, A. E. Merbach, *Inorg. Chem.*, 1993, **32**, 2810.
33. S. Pal, S. Pal, *Polyhedr.*, 2002, **22**, 867.



3.1 Introduction.

The constant endeavour, both in industry and academia, to catalytically transform C-C double bonds has developed into an active area of research. One area that is constantly developing due to “new” discoveries is the catalyzed oxidation of alkenes. Important oxidation reactions include the transformation of alcohols to either the corresponding carbonyl compounds or carboxylic acids, the oxidation of sulfides to sulfoxides and alkenes to epoxides and diols. Various studies have been devoted to oxidation of alkenes to the corresponding epoxides using transition metal complexes. The epoxide class of organic compounds plays an important and versatile role in the synthesis of intermediates for fine chemicals and as such the selective epoxidation of alkenes is a major area of research [1].



3.2 Rhenium complexes in the catalysed epoxidation reactions of olefins

The discovery of the catalytic ability of MTO by Herrmann *et al.* paved a way for exploration of MTO derivatives as inorganic rhenium compounds like Re_2O_7 or ReO_3 were long considered to have negligible catalytic oxidation activity with H_2O_2 [2]. The catalytic activity of MTO was quickly recognised and as a result further researches concerning the understanding of its active species was undertaken. The active catalyst was discovered to be the monoperoxo (**A**) and bis-peroxo (**B**) rhenium complex formed by the reaction of MTO with H_2O_2 [3]. The latter intermediate active catalyst has been fully characterised by X-ray studies [4-6].

The acidity of the rhenium centre restricted its use only to anhydrous H₂O₂ because low yield of the acid sensitive epoxide were obtained. Thus efforts made were aimed at improving the catalytic oxidation of sensitive alkenes by employing an urea-H₂O₂ adduct to circumvent the deleterious ring opening of epoxides. This process requires long reaction times. Other endeavours introduced the use of an additional tertiary base to suppress the epoxide ring opening and this resulted in the unfavourable detriment on the catalyst activity [3]. Sharpless *et al.* reported an improvement in selectivity by adding a large excess of pyridine with respect to the catalyst, without inhibition of the catalyst activity [7a]. This discovery led to the synthesis of sensitive epoxides with only 1.5 equivalents of aqueous H₂O₂ even at low catalyst loading [7a,b]. It was observed that higher catalyst loadings were necessary in the presence of bipyridine *N,N'*-dioxide as the *N,N'*-oxide suppresses the epoxide ring-opening [8]. This also ensured that unreactive terminal alkenes were converted to corresponding epoxides by making use of a less basic pyridine derivatives like 3-cyanopyridine [9].

The enhancement of the catalyst activity by an additive was further investigated by Herrmann's group. They reported the use of pyrazole as the most efficient additive and proposed a bis(peroxo)rhenium(VII)/pyrazole complex as the active oxidation species [10]. After a careful examination and comparison of the finding by Herrmann's group, Sharpless *et al.* [11] showed through mechanistic investigations [5], that incorporating the positive pyridine effect

[12], minimises the formation of the perrhenate (ReO_4^-) [12a] with the MTO decomposition thereby retaining high catalyst activity. The increased rate in the presence of pyridine was attributed to its intrinsic Brønsted basicity thus increasing the HO_2^- concentration. The HO_2^- is more nucleophilic and therefore more reactive with MTO compared to H_2O_2 . This characteristic of pyridine and related additives lowers the concentration of hydronium ions and as a result reducing the sensitivity of epoxides towards decomposition via ring-opening.

3.2.1 Mechanism of epoxidation reaction

The field of olefin epoxidation has been explored and a vast range of transitional metal catalysts have been tested and applied at both laboratory and industrial levels. Thus it has become certain to include compounds such as methyltrioxorhenium (CH_3ReO_3 , MTO) and MoO_3 as far as catalyzed oxidation reactions are concerned. These and other prominent catalysts in the field have been applied in industrial epoxidation of alkenes using the oxidants hydrogen peroxide and tertbutylhydroperoxide (TBHP) [3a,3d].

As mentioned (*vide supra*), Herrmann *et al.* have done extensive work on the subject of epoxidation with MTO [3,12c,13-15] consequently, its mechanism with H_2O_2 has been reported (Fig. 3.1) [16]. The mechanism discusses two important intermediates (*vide supra*) that have been isolated and studied as active catalysts [4], a bisperoxo complex of stoichiometry $(\text{CH}_3)\text{Re}(\text{O}_2)_2\text{O}\cdot\text{H}_2\text{O}(\mathbf{B})$ [4] obtained by reaction of MTO with excess H_2O_2 and a monoperoxo complex of composition $(\text{CH}_3)\text{Re}(\text{O})_2\text{O}_2(\mathbf{A})$ [12c, 25] obtained by reaction of MTO with 1 equiv. of H_2O_2 . Experimental data indicate that these intermediates have

similar rate constants in magnitude [12c,25,27]. Further work was pursued by density functional calculation in order to validate these findings [17,18,26]. The mechanism involves a nucleophilic attack on MTO by H_2O_2 as an activation parameter for the coordination of H_2O_2 to MTO. The protons lost in the conversion of H_2O_2 to a coordinated peroxo ligand, O_2^{2-} , are then transferred to one of the terminal oxygen atoms, which remain on the Re as an aqua ligand. The rate of this reaction is not pH dependent [19].

The concentration of the H_2O_2 used in the epoxidation reactions has been shown to be important because it directs the pathway the reaction will follow. The concentration dependent pathways can be categorised in two: high H_2O_2 and low H_2O_2 concentrations [16]. The isolable bisperoxo (**B**, path A) complex is responsible for the oxidation activity at high H_2O_2 concentration (85 wt%), while the monoperoxo (**A**) complex is responsible for epoxidation at low H_2O_2 concentration (<30 wt%) for the (path B). The studies of both catalytic pathways support a concerted mechanism in which the electron-rich double bond of the alkene electrophilically attacks a peroxidic oxygen of the complex possibly through a spiro arrangement [17-20].

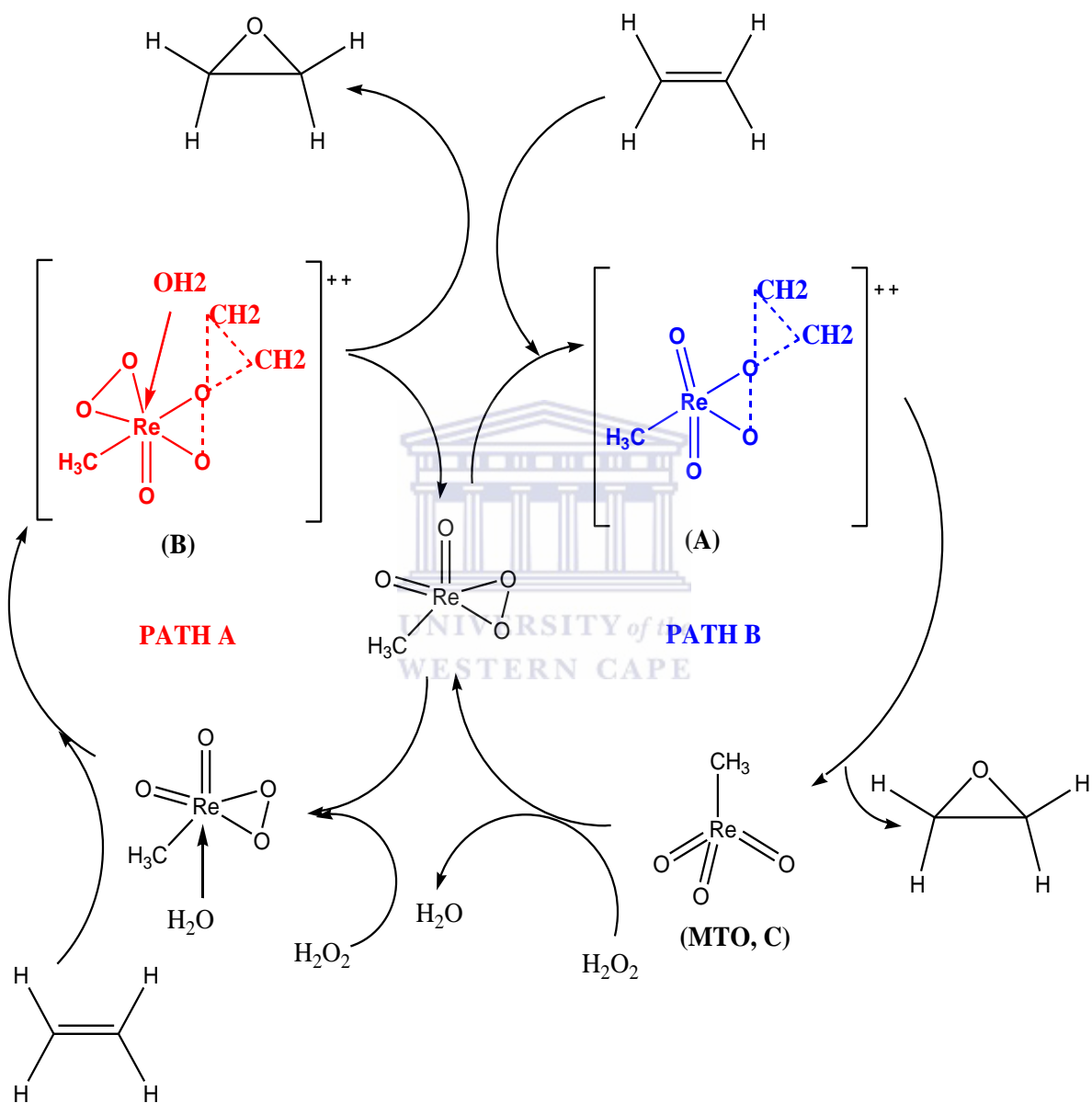
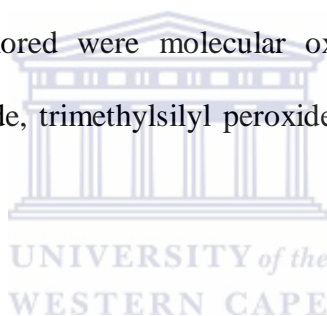


Figure 3.1: Suggested mechanism of methyltrioxorhenium (MTO, C) catalyzed epoxidation of alkenes [21,22].

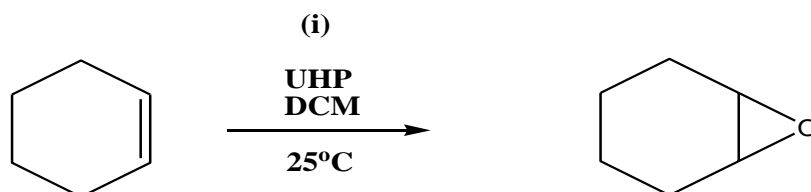
The above scheme of the suggested mechanism clearly indicates that the oxygen atom of the oxidant is activated by the catalyst in preparation to incorporate alkene/substrate to the activated oxygen atom. For both pathways, the presence of the metal is vital as it is a prerequisite for the facilitation of the transfer of the oxygen atom from the oxidant to the alkene/substrate [21,22].

Different sources of oxygen donors were used in the previous inventions for the transition metal catalyzed epoxidation reactions in order to obtain epoxides as desired products. Some of the oxidants that were explored were molecular oxygen, hydrogen peroxide, alkyl peroxides, urea-hydrogen peroxide, trimethylsilyl peroxide and sodium hypochlorite among others [23].



Deductions from the previous inventions serve as rudimentary tools for a better understanding of the epoxidation reactions of alkenes and the improvement of selectivity over the deleterious concomitant epoxide ring opening into diols. We herein report the use of MTO mono-(**C1**), bi-(**C2**), and multinuclear dendritic (**DC1** and **DC2**) catalysts (Figure. 3.3 and 3.5). To our knowledge, these MTO complexes, except **C1**, are reported herein for the first time and their catalytic activity is evaluated for the first time towards epoxidation reactions on selected cyclic substrates/alkenes.

3.3 Results and Discussion: Epoxidation of cyclohexene and cis-cyclohexene.



(i) **C1-C2** and **DC1-DC2**

Figure 3.2: A general epoxidation reaction of the alkene substrates.

This section documents the results obtained from the catalytic evaluation of the compounds **C1** and **C2** towards the epoxidation of selected cyclic alkenes (Figure 3.2) with isooctane as an internal standard. GC-FID was employed in the analysis and determination of conversion as the consumption of the substrates (cyclohexene and cis-cyclooctene, respectively) was monitored as a function of time.

3.3.1 Epoxidation reactions catalysed by mono- (**C1**) and bi-nuclear (**C2**) MTO Complexes.

Schiff-base complexes of MTO that were synthesized, **C1** and **C2**, were examined as catalysts for the epoxidation of two cyclic substrates i.e cyclohexene and cis-cyclooctene, respectively. These complexes were examined in the epoxidation reaction with urea hydrogen peroxide adduct (UHP) as the oxidant. A similar catalytic setup that was employed by Qui

et. al., a catalyst: oxidant: substrate ratio of 1:200:100, for all catalytic reactions was used. The catalysts were found to be activity as epoxidation catalysts for the transformation of the two selected olefins/substrates.

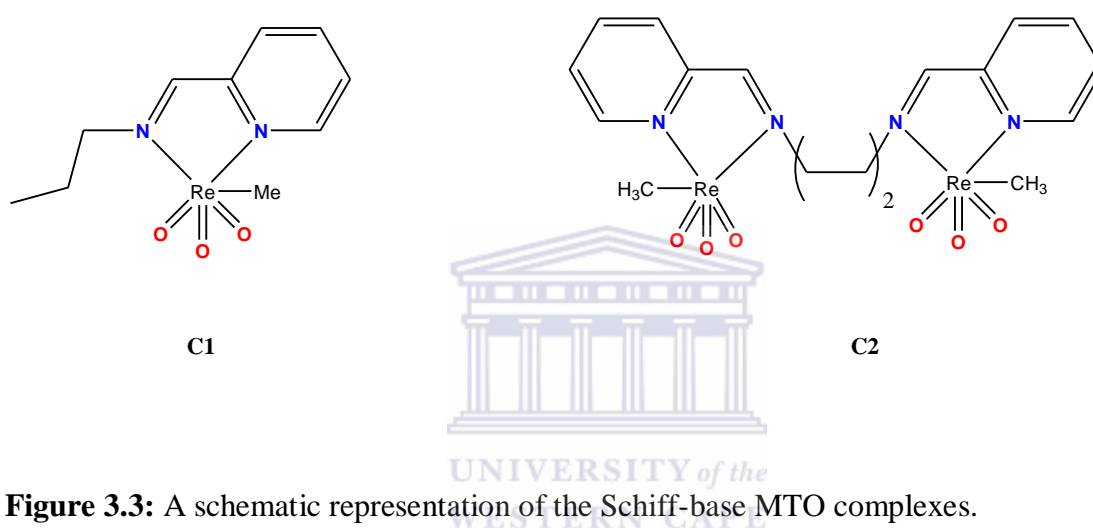


Figure 3.3: A schematic representation of the Schiff-base MTO complexes.

Complex **C1** is known and was first resolved crystallographically and tested as a catalyst for both cyclic substrates by Qui *et. al.* [24]. Herein the complex is synthesized as a benchmark for the novel synthesized homobimetallic MTO complex **C2**.

C1 was used as a catalyst for the epoxidation of the cyclic substrates i.e. cyclohexene and cis-cyclooctene, respectively. As like the previously reported protocol [24], the suitable oxidant used for the epoxidation reaction of the olefinic substrates was Urea-hydrogen peroxide adduct (UHP). The use of hydrogen peroxide (H_2O_2) as an oxidant was avoided as this is commercially available as an aqueous solution and tends to favour the further reaction of the epoxides to subsequent diols. Hydrogen peroxide needs specialized instruments or

procedures to dry and the alternative route of using urea-hydrogen peroxide as the source of hydrogen peroxide was opted. This resulted in no significant amount of diols formed for both cyclic olefinic substrates. All catalytic reactions reached completion within 4 h, exhibiting elevated reaction rates with 98 % conversion. The epoxide yield reached up to 100 % after 4h, showing the same trend reported [24].

The catalytic activity of complex **C2** followed the same trend as with **C1**, with notable completion of the catalytic reaction in a shorter time (Table 3.1). Synergy between the two rhenium centres in complex **C2**, that has been afforded by the bifunctional ligand, in the epoxidation reactions of the cyclic substrates/alkenes under the buffering effect of urea-hydrogen peroxide, afforded conversions to reaching 99 % with also no significant diols amount observed. At selected time intervals, the novel Schiff-base complex of MTO (**C2**) performed better than the benchmark complex **C1**.

Table 3.1: Catalytic data of the epoxidation of cyclohexene with MTO(C) and catalysts **C1** and **C2**.

Entry	Catalyst	Oxidant	Time (h)	Conversion (%) ^a	Selectivity (%) ^b
1	MTO	UHP	2.5	>99	>99
2	C1	UHP	2.5	72	97
3	C2	UHP	2.5	76	97
4	C1	UHP	8	>99	>99
5	C2	UHP	6.5	>99	>99

Reaction conditions: 0.955 mmol of cyclohexene; 1.9 mmol of oxidant; 0.00928 mmol of catalyst; 4 mL of DCM; 25 °C. ^aCalculated by GC. ^bCalculated by GC.

The activity of the catalysts was observed to increase as a function of time with the highest conversion being greater than 99% observed for both catalysts. Comparison of the catalytic activity of the synthesized Schiff-base complexes of MTO (C1 and C2), with that of the free MTO (in the absence of the imine ligand) showed that the free MTO performed better as the highest conversion was reached within the shortest amount of time. This is documented in the literature with other reported Schiff-base complexes of MTO [24]. A detailed trend is exhibited in the figure below (Figure 3.4).

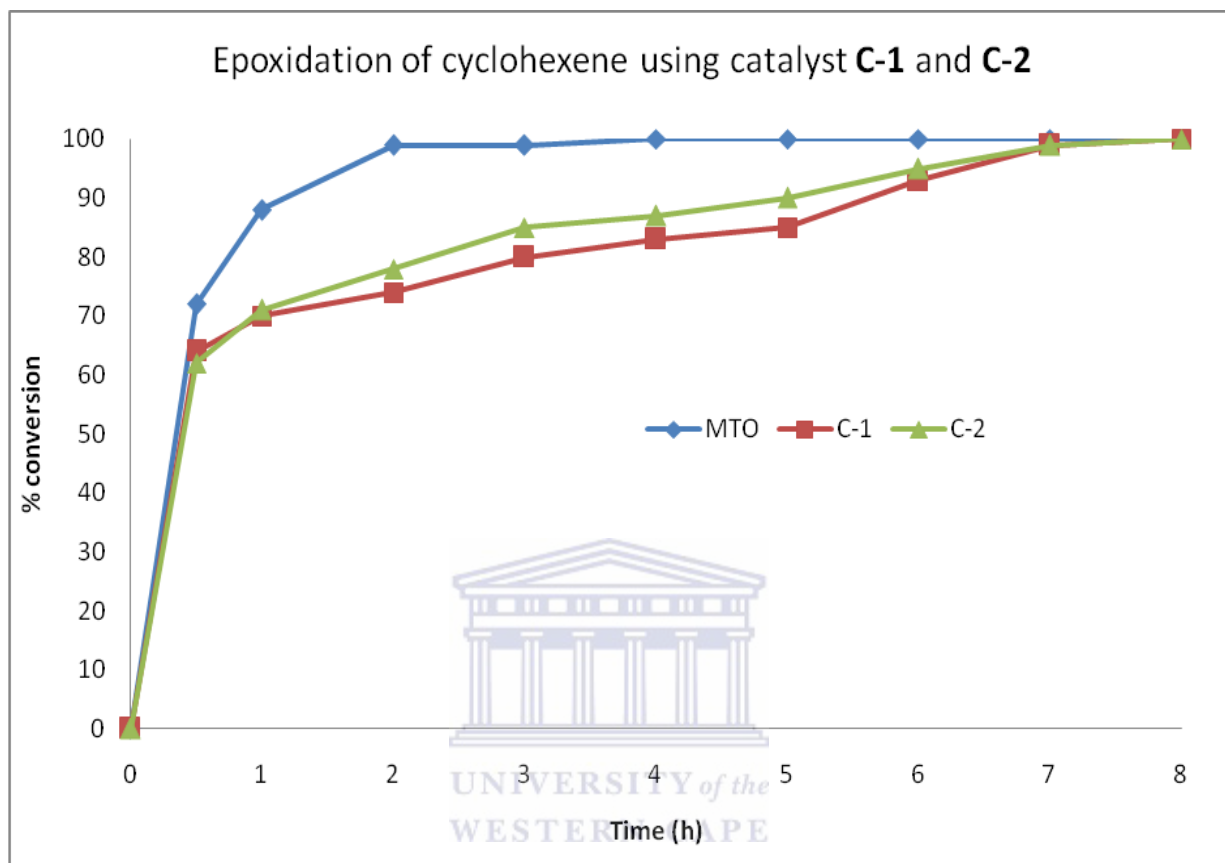


Figure 3.4: Plot of the consumption of cyclohexene as a function of time.

The reason for the lower catalytic activity of the prepared complexes is similar to what is documented in the literature [24]. Complexes derived from alkylamine (strong electron donating) tend to exhibit low catalytic activity as compared to weak electron donating ligands as the former tends to form stronger Re-N bond thus leading to a lower reactivity of the catalysts, hence the reaction times had to be prolonged in order to ensure 100% epoxide yields. This is explainable by the fact that the ligands exert their influence on the Lewis acidity of the Re atom and the immediate surroundings of terminal ligands. The formation of the catalytically

active mono and bisperoxo species is hindered as the Lewis acidity of the metal centre (Re) is reduced. Hence a decrease in the electron deficiency of the peroxy-oxygen results in the catalyst being less activated to be attacked by the nucleophilic olefin.

Complexes **C1** and **C2** showed similar trend when applied as catalyst in the epoxidation of cyclooctene. The catalytic reactions showed high reaction rate and completion within the indicated time (Table 3.2). Complexes **C1** and **C2** showed similar catalytic activity for the epoxidation of cyclooctene, and the epoxides yield reached 100% when the reaction times were prolonged.



Table 3.2: Catalytic data of the epoxidation of cis-cyclooctene with MTO(C) and catalysts C1 and C2.

Entry	Catalyst	Oxidant	Time (h)	Conversion (%) ^a	Selectivity (%) ^b
1	MTO	UHP	2.5	>99	>99
2	C1	UHP	2.5	77	97
3	C2	UHP	2.5	80	97
4	C1	UHP	8	>99	>99
5	C2	UHP	6	>99	>99

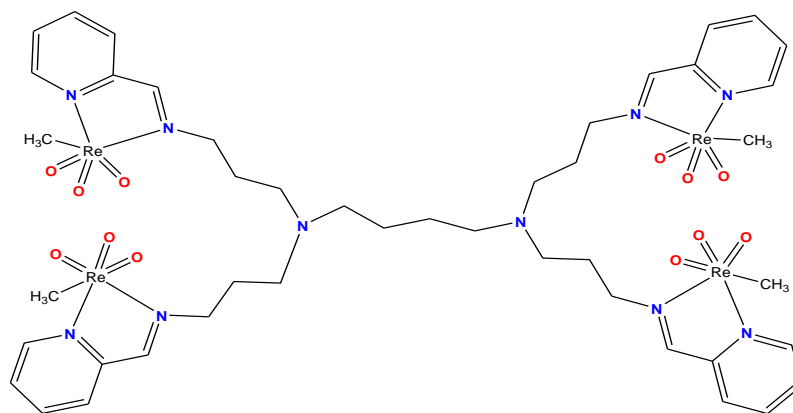
Reaction conditions: 0.955 mmol of cis-cyclooctene; 1.9 mmol of oxidant; 0.00928 mmol of catalyst; 4 mL of DCM; 25 °C. ^aCalculated by GC. ^bClaculated by GC

3.3.2 Epoxidation reactions catalysed by multinuclear Schiff-base complexes of MTO metallodendrimer, DC1 and DC2.

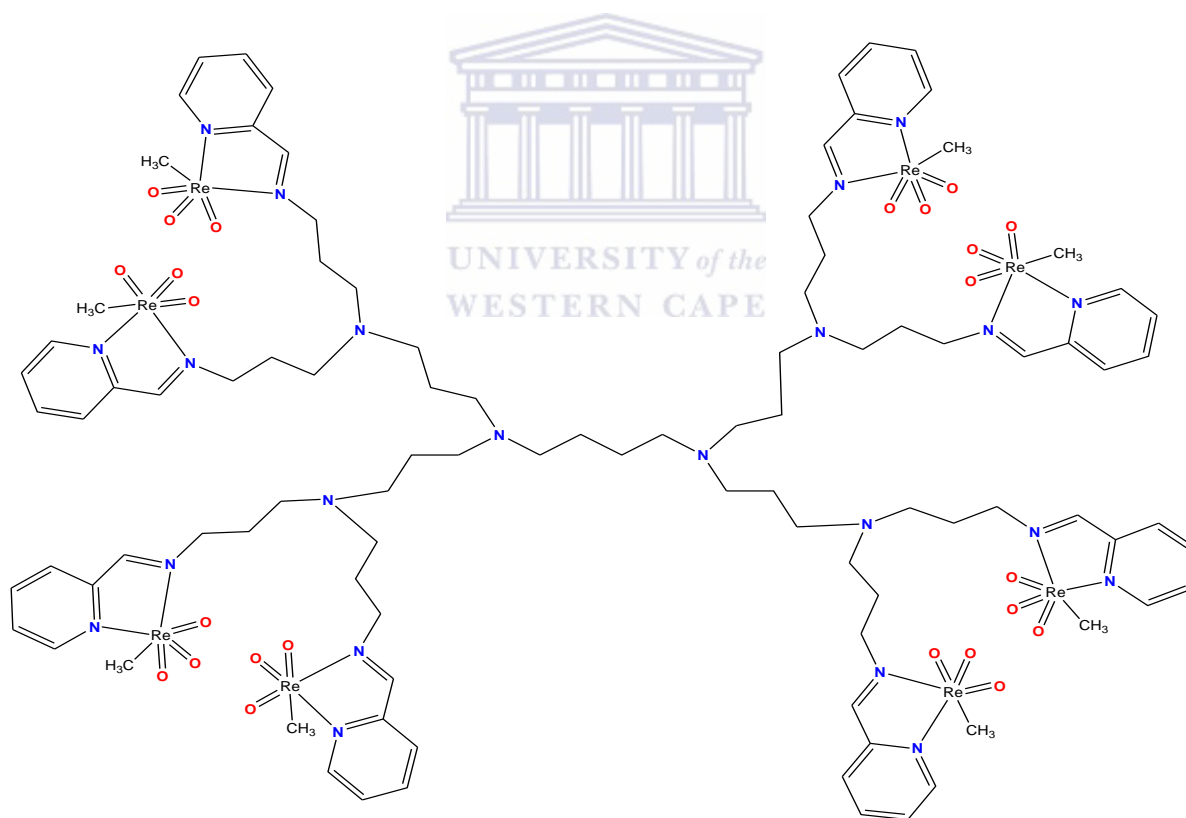
The 1st and the 2nd generation Schiff-base Re(VII) metallodendrimers were evaluated as catalysts in the epoxidation of cyclohexene and cis-cyclooctene, respectively. The dendritic catalysts were found to be highly active as catalysts in the epoxidation reactions of the two selected cyclic substrates/olefins.

The consumption and conversion of the cyclic substrates/olefins occurred within 4 hrs for all the dendritic catalyzed reactions. Drastic quantitative conversion of cyclohexene/cis-cyclooctene was observed within the first hour in comparison with the mono- and binuclear MTO complexes (Figure 3.5).





DC1



DC2

Figure 3.5: A representation of the novel 1st and 2nd generation Re(VII) metallodendrimer tested in the epoxidation of cyclohexene/cis-cyclooctene.

Table 3.3: Catalytic data of the epoxidation of cis-cyclooctene with MTO (C) and catalysts DC1 and DC2.

Entry	Catalyst	Oxidant	Time (h)	Conversion (%) ^a	Selectivity (%) ^b
1	MTO	UHP	2.5	>99	>99
2	DC1	UHP	2.5	82	98
3	DC2	UHP	2.5	85	98
4	DC1	UHP	4	>99	>99
5	DC2	UHP	3	>99	>99

Reaction conditions: 0.955 mmol of cyclohexene; 1.9 mmol of oxidant; 0.00928 mmol of catalyst; 4 mL of DCM; 25 °C. ^bCalculated by GC. ^cCalculated by GC

It was also noted that with time the pyridineimine moiety undergoes hydrolysis and this fragment was detected in the GC. This ease of hydrolysis was far more deferred in the case of the dendrimer indicating the stability impacted by the dendrimer ligand.

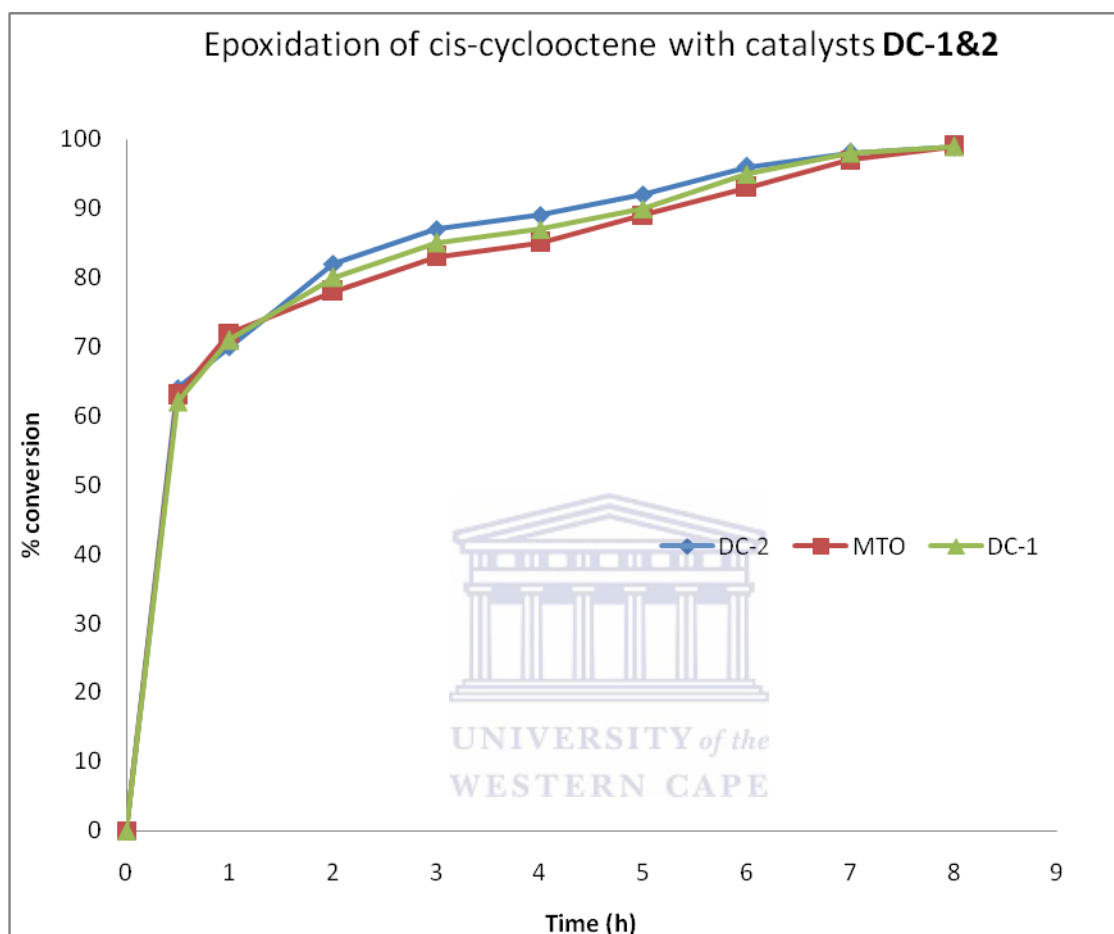


Figure3.6: Plot of the consumption of *cis*-cyclooctene as a function of time.

The activity of the dendritic catalysts yielded higher conversion as compared to the mono- and binuclear MTO complexes at any time. Although it was observed that MTO reaches the highest conversion in the least amount of time, it was also observed that the dendrimer catalysts give the highest conversion at any time but the only hindering was the prolonged reaction time in order to attain 100% epoxide yield.

Table 3.4: Catalytic data of the epoxidation of cyclohexene with MTO (**C**) and catalysts **DC1** and **DC2**.

Entry	Catalyst	Oxidant	Time (h)	Conversion (%) ^a	Selectivity (%) ^b
1	MTO	UHP	2.5	>99	>99
2	DC1	UHP	2.5	80	>99
3	DC2	UHP	2.5	82	>99
4	DC1	UHP	4	>99	>99
5	DC2	UHP	3	>99	>99

Reaction conditions: 0.955 mmol of cyclohexene; 1.9 mmol of oxidant; 0.00928 mmol of catalyst; 4 mL of DCM; 25 °C. ^bCalculated by GC. ^cCalculated by GC.

The rapid formation of the active species in the catalysis (a peroxo complex) renders these novel rhenium dendritic complexes useful in the catalyzed epoxidation of cyclohexene and cis-cyclooctene, respectively. High levels of conversion to epoxides were observed with no significant (less than 5%) diol formation.

3.4 Conclusion

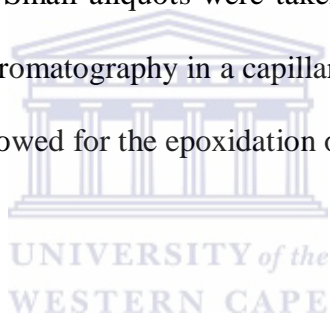
All the complexes synthesized were evaluated as catalysts in the epoxidation of cyclohexene/cis-cyclooctene reactions. The use of urea hydrogen peroxide as an oxidant resulted in all the complexes displaying high catalytic activity and selectivity when applied to the epoxidation of cyclohexene/cis-cyclooctene. No significant diols formation was observed.

3.5 Materials and Methods

Methyltrioxorhenium (MTO) was purchased from Sigma-Aldrich/Strem Chemicals. cyclohexene (99%), cyclohexene oxide (98%) cis-cyclooctene (95%), cyclooctene oxide (99%) isooctane (99.8%) were purchased from Aldrich and used without further purification. Dichloromethane was dried using standard procedures, distilled under nitrogen and kept over dried 3 Å molecule sieves. Other reagents were used as received. All preparations and manipulations were carried out under an oxygen and water free nitrogen atmosphere using the standard Schlenk techniques. The GC analysis was carried out on Agilent 7890, GC Column: Agilent 19091J-413; 325 °C: 30 m X 320 μm X 0.25 μm, 5% phenyl methyl Siloxan HP5-column.

3.5.1 *General procedure for the Epoxidation of cyclohexene/cis-cyclooctene*

The catalytic reactions were carried out under continuous stirring in a 50 ml r.b.f immersed in a water bath with temperature control. In a typical experiment, 0.025 mmol of the catalyst, 3.5 ml of methanol, and a given amount (5 mmol) of UHP were mixed in the flask under agitation until the reaction temperature was reached. At this time, 2.5 mmol of the substrate was added (time zero). Small aliquots were taken at selected reactions times. The products were analyzed by gas chromatography in a capillary column using a FID detector. A similar catalytic protocol was followed for the epoxidation of the substrates.



References:

1. (a) Gorzynski Smith, J. *Synthesis.*, 1984, 629. (b) Bonini, C.; Righi, G. *Synthesis* 1994, 225.
2. Lai, T. -S.; Zhang, R.; Cheung, K. -K.; Kwong, H. -L. Che, C. -M. *Chem. Commun.* 1998, 1583.
3. (a) W. A. Herrmann, R. W. Fischer, D. W. Marz, *Angew. Chem., Int. Ed. Engl.* 1991, **30**, 163. (b) W. A. Herrmann, R. W. Fischer, M. U. Rauch, W. Scherer, *J. Mol. Catal. A: Chem.* 1994, **86**, 243. (c) W. A. Herrmann, F. E. Kühn, *Acc. Chem. Res.* **1997**, *30*, 169. (d) G. Grivani, S. Tangestaninejad, M. H. Habibi, V. Mirkhani, M. Moghadam, *Appl. Catal A: Gen.*, 2006, **299**, 131.
4. W. A. Herrmann, R. W. Fischer, W. Scherer, M. U. Rauch, *Angew. Chem., Int. Ed. Engl.*, 1993, **32**, 1157.
5. A. M. Al-Ajlouni, J. H. Espenson, *J. Org. Chem.*, 1996, **61**, 3969.
6. (a) Z. Zhu, J. H. Espenson, *J. Org. Chem.*, 1995, **60**, 1326. (b) M. M. Abu-Omar, J. H. Espenson, *J. Am. Chem. Soc.*, 1995, **117**, 272. (c) Wang, W. -D.; Espenson, J. H. *Inorg. Chem.*, 1997, **36**, 5069. (d) Van Vliet, M. C. A.; Arends, I. W. C. E.; Sheldon, R. A. *Chem. Commun.*, 1999, 821.
7. (a) J. Rudolph, K. L. Reddy, J. P. Chiang, K. B. Sharpless, *J. Am. Chem. Soc.*, 1997, **119**, 6189. (b) A. L. Villa, D. E. Vos, C. Montes, P. A. Jacobs, *Tetrahedron Lett.*, 1998, **39**, 8521.
8. M. Nakajima, Y. Sasaki, H. Iwamoto, S. Hashimoto, *Tetrahedron Lett.*, 1998, **39**, 87.
9. C. Copéret, H. Adolfsson, K. B. Sharpless, *Chem. Commun.*, 1997, 1565.

10. W. A. Herrmann, R. M. Kratzer, H. Ding, W. Thiel, H. Glas, *J. Organomet. Chem.*, 1998, **555**, 293.
11. H. Adolfsson, A. Converso, K. B. Sharpless, *Tetrahedron Lett.*, 1999, **40**, 3991.
12. (a) W.-D. Wang, J. H. Espenson, *J. Am. Chem. Soc.*, 1998, **120**, 11335. (b) H. Tan, J. H. Espenson, *Inorg. Chem.*, 1998, **37**, 467. (c) Espenson, J. H. *Chem. Commun.* 1999, 479.
13. W.A. Herrmann, M. Dieter, W. Wagner, J.G. Kuchler, G. Weichselbaumer, R. Fischer, US Patent 5,155,247, Oct. 13, **1992**, To Hoechst Aktiengesellschaft.
14. F. E. Kuhn, A. M. Santos, W. A. Herrmann, *Dalton Trans.*, 2005, 2483.
15. J. B. Espenson, M. M. Abu-Omar, *Adv. Chem. Series*, Vol. 253, p. 99, *Am. Chem. Society*, Washington, DC, **1997**.
16. F. E. Kuhn, A. Scherbaum, W. A. Herrmann, *J. Organomet. Chem.*, 2004, **689**, 4149.
17. P. Gisdakis, N. Rosch, *Eur. J. Org. Chem.*, **2001**, 719.
18. C. di Valentin, R. Gandolfi, P. Gisdakis, N. Rosch, *J. Am. Chem. Soc.*, 2001, **123**, 2365.
19. O. Pestovski, R. V. Eldik, P. Huston, J. H. Espenson, *J. Chem. Soc. Dalton. Trans.*, 1995, 133.
20. P. Gisdakis, W. Antonczak, S. Kostlmeir, W. A. Herrmann, N. Rosch, *Angew. Chem. Int. Ed. Engl.*, 1998, **37**, 2211.
21. A. O. Bouh, A. Hassan, S. L. Scott, *Catalysis Of Organic reactions, Ed., Chemical Industries (Marcel Dekker)*, **2003**, 537.
22. R. Neumann, *A process for epoxidation of alkenes*, International patent WO,98/54165.
23. G. S. Owens, J. Arias, M. M. Abu-Omar, *Catal. Today*, 2000, **55**, 317.
24. C.-J. Qiu, Y.-C. Zhang, Y. Gao, J.-Q. Zhao, *J. Organomet. Chem.*, 2009, **694**, 3418.

25. A. Al-Ajlouni, H. Espenson, *J. Am. Chem. Soc.*, 1995, **117**, 9243.
26. P. Gisdakis, I. V. Yudonov, N. Rosch, *Inorg. Chem.*, 2001, **40**, 3755.
27. W. Adam, C. R. Saha-Moller, O. Weichold, *J. Org. Chem.*, 2000, **65**, 5001.
28. W.A. Herrmann, R.M. Kratzer, H. Ding, W. Thiel, H. Glas, , *J. Organomet. Chem.*, 1988, **555**, 293.



4.1 *Introduction.*

In Organic Synthesis, the craft of oxidative cleavage has grown tremendously elevating olefin transformation to become one of the most prevalent reactions in the field. The application of a variety of inorganic oxidizing agents to organic substrates has considerably broadened the selectivity with which such oxidations may be carried out. The extensive study documented in the literature highlights two main oxidative cleavage routes that can be summed up as conversion of olefins to vicinal diols and subsequent cleavage with NaIO_4 or other oxidants [1].

The use of ruthenium as the catalytic metal in this field of research can be attributed to its versatility, as it can catalyse a number of oxidative transformations *viz.* the oxidation of alkanes, the cleavage of double bonds, the asymmetric epoxidation of alkenes, the oxidation of alcohols and ethers and the oxidation of amines and amides [2].

4.2 *Catalytic Oxidative Cleavage of alkenes by ruthenium compounds.*

From the first example of a catalysed alkene cleavage using a form RuO_2 (aq.). $\text{Na(IO}_4\text{)}/\text{AcOH(I)}$ system, the oxidative functionalization class has broaden into a field of fundamental transformations in organic chemistry. This topic has been extensively reviewed and applied in a myriad of various settings for the synthesis and production of valuable intermediates and chemical commodities [2-8].

The earliest inventions report on the use of RuO_4 as an active species generated *in situ* from the system (I) (*vide supra*) to cleave alkenes into corresponding alkenes [3-8].

4.2.1 *In situ* generated ruthenium tetroxide promoted oxidations.

The nature of the active species, RuO_4 (II), permits transformations such as oxygenation and hydrogen abstraction of an array of organic compounds because it is a powerful oxidant in the transformation of various organic substrates. Due to its reactive nature, the reaction conditions are normally mild and performed at room temperature. The catalytic reactions are known to conveniently take place in a biphasic solvent system (*vide infra*) employing a catalytic amount of RuCl_3 or RuO_2 in conjunction with oxidants such as NaIO_4 , HIO_4 , NaOCl and NaBrO_3 , or under electrochemical conditions (see Fig. 4.1).

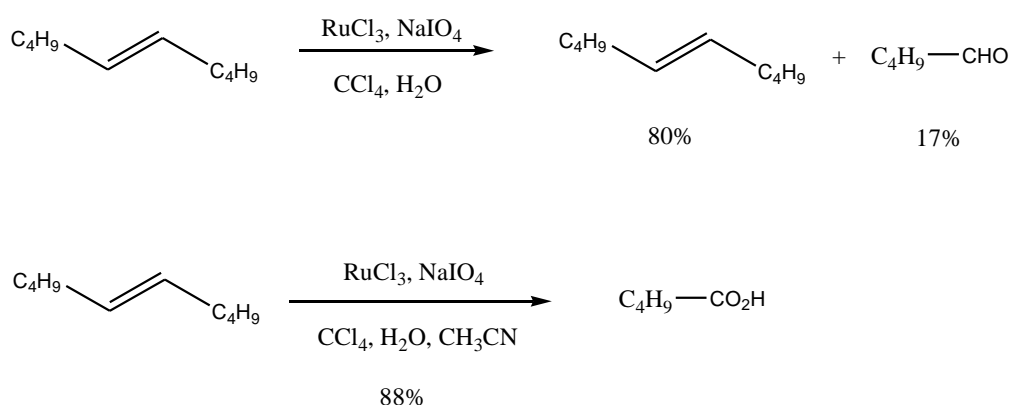


Figure 4.1: A general scheme showing the usage of catalytic amounts of RuCl_3 [10].

Addition of acetonitrile has indicated to favour the formation of carboxylic acids over aldehydes as the organic solvent, upon introduction into the reaction mixture, prevents the

inactivation of the ruthenium catalysts as this leads to sluggish, incomplete reactions by forming low-valent ruthenium carboxylate complexes [4].

4.2.1.1 Oxidative Cleavage of alkenes

The schematic depicted below (Figure 4.2) depicts olefins undergoing oxidative cleavage to afford the desired carbonyl complex in good yield. The cyclohexene reacts with a small amount of ruthenium trichloride in the presence of NaOCl dissolved in dichloromethane to give hexanedioic acid. This reaction is shown in fig. 4.2 below.

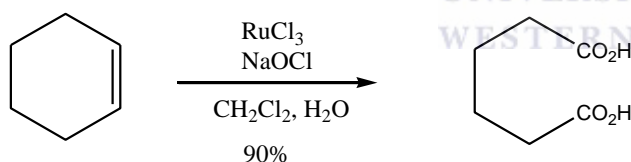


Figure 4.2: A general scheme pertaining to the synthesis of carboxylic acids [12].

The reaction conditions can be modified in order for the catalytic system to favour the formation of cis-diols/dialcohols and not acids. This occurs selectively when the reaction is carried out in short time. A typical example of such a reaction is shown below.

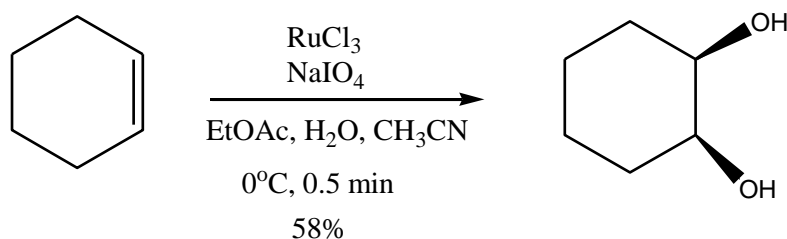


Figure 4.3: A general selective scheme for the synthesis of *cis*-dihydroxyles [11].

Epoxides can be achieved in a similar catalytic setup as for the production of carboxylic acids except that the use of a nitrogen ligand is employed in order to coordinate the active species that is generated *in situ*.

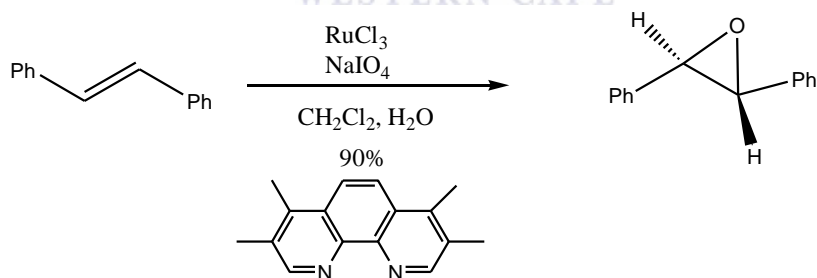


Figure 4.4: A general ruthenium scheme for the epoxidation of alkenes [13].

4.3 Mechanism of Catalyzed Oxidative Cleavage of Alkenes by ruthenium.

A stoichiometric amount of the potent oxidant, rutheniumtetroxide (**II**), has long been known to oxidatively fragment alkenes into corresponding carboxylic acids. This

transformation of olefins, catalyzed by ruthenium, has been achieved by assistances of a range of oxygen donors, e.g. NaIO₄ and NaOCl as primary oxidants [2-8]. The precise mechanistic study of reactions containing low-valent ruthenium complexes as catalysts is known, and proposes the formation of a metal-oxo (**II**) intermediate as the active species. This can be seen in the following catalytic cycle (Fig. 4.5).

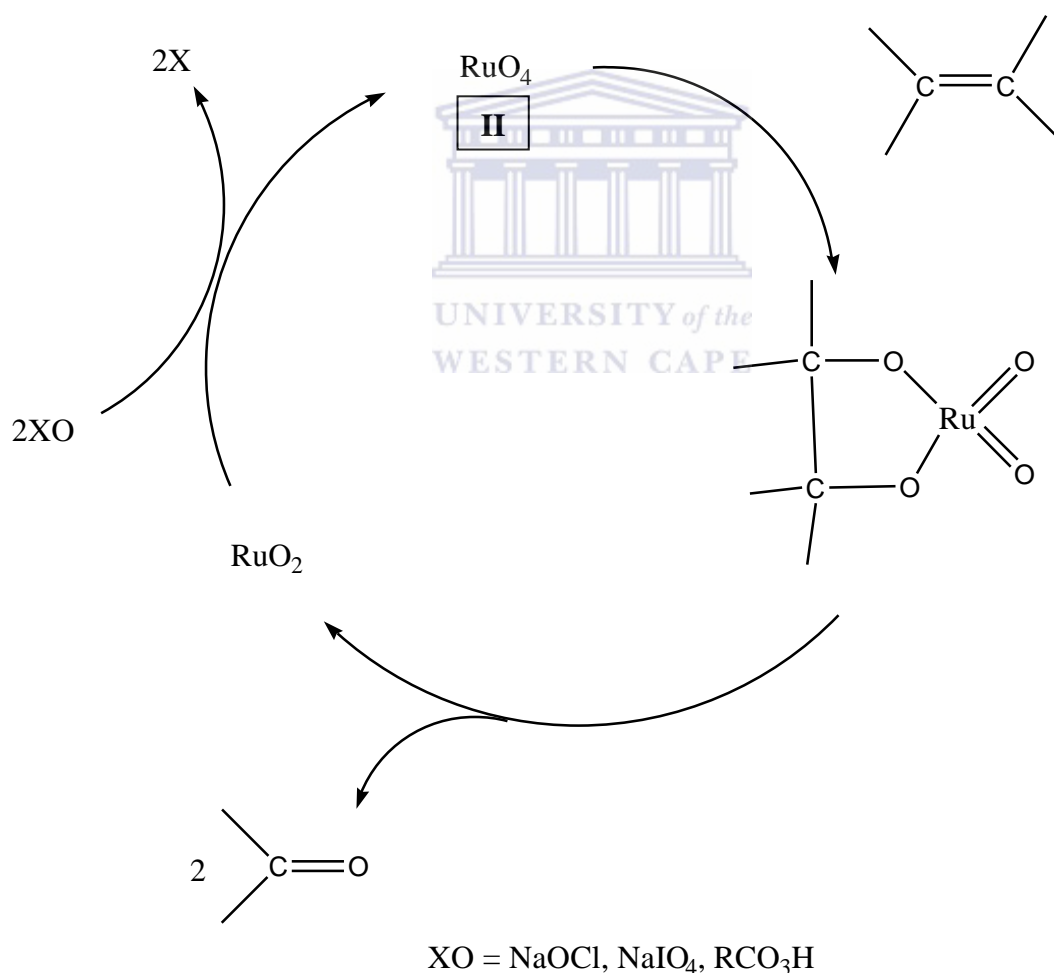


Figure 4.5: A catalytic cycle for ruthenium-catalyzed oxidative cleavage of olefins [7].

4.4 Results and Discussion: Oxidative Cleavage of 1-Octene by ruthenium catalyst

The following schematic diagram illustrates the oxidative cleavage of 1-octene to form the acid product. The reaction was carried out in a biphasic solvent system involving tetrachloromethane, acetonitrile and water.

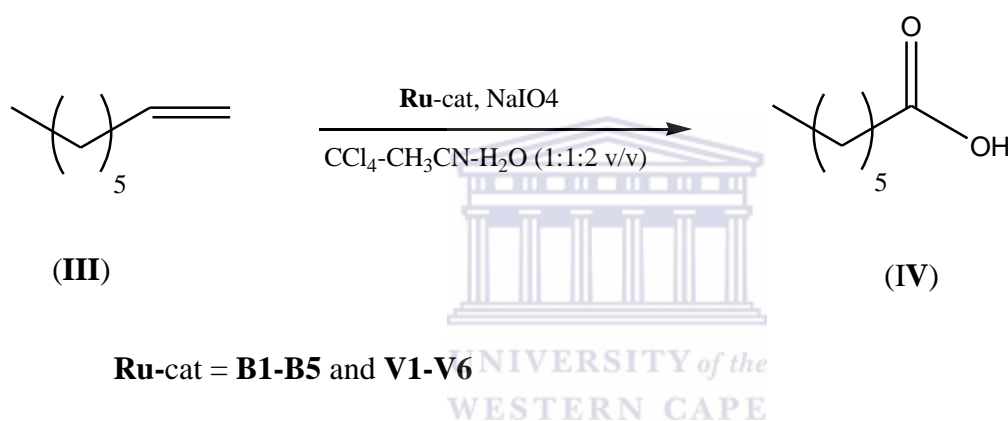


Figure 4.6: A general oxidative cleavage of 1-octene in a biphasic solvent.

The low-valent ruthenium complexes were used with sodium periodate (NaIO_4) as the cooxidant.

4.4.1 Oxidative cleavage of 1-octene by neutral and Cationic mono-, bi-, and multinuclear ruthenium catalysts.

Mononuclear chelating neutral (*N, N*) (**B1** and **B3**) and mono- and bi-nuclear cationic (*N, N*-) (**B2**, **B4** and **B5**) ruthenium (II) catalyst were evaluated as complexes for oxidative

cleavage of linear alkene (1-octene, **III**) at room temperature in a biphasic solvent (CCl₄-CH₃-H₂O). The catalytic systems were found to be highly active for oxidative cleavage of 1-octene with the chosen cooxidant (*vide supra*). The yields ranged from moderate to good, Table 4.1 summarizes the results obtained for the oxidation of the linear alkene (1-octene, **III**). The results are within the range as those previously reported and are comparable for the oxidation of the same linear olefinic substrate.



Chapter 4: Application of mono-, bi-, and multinuclear neutral and cationic Ru(II) catalysts in the oxidative cleavage of 1-octene.

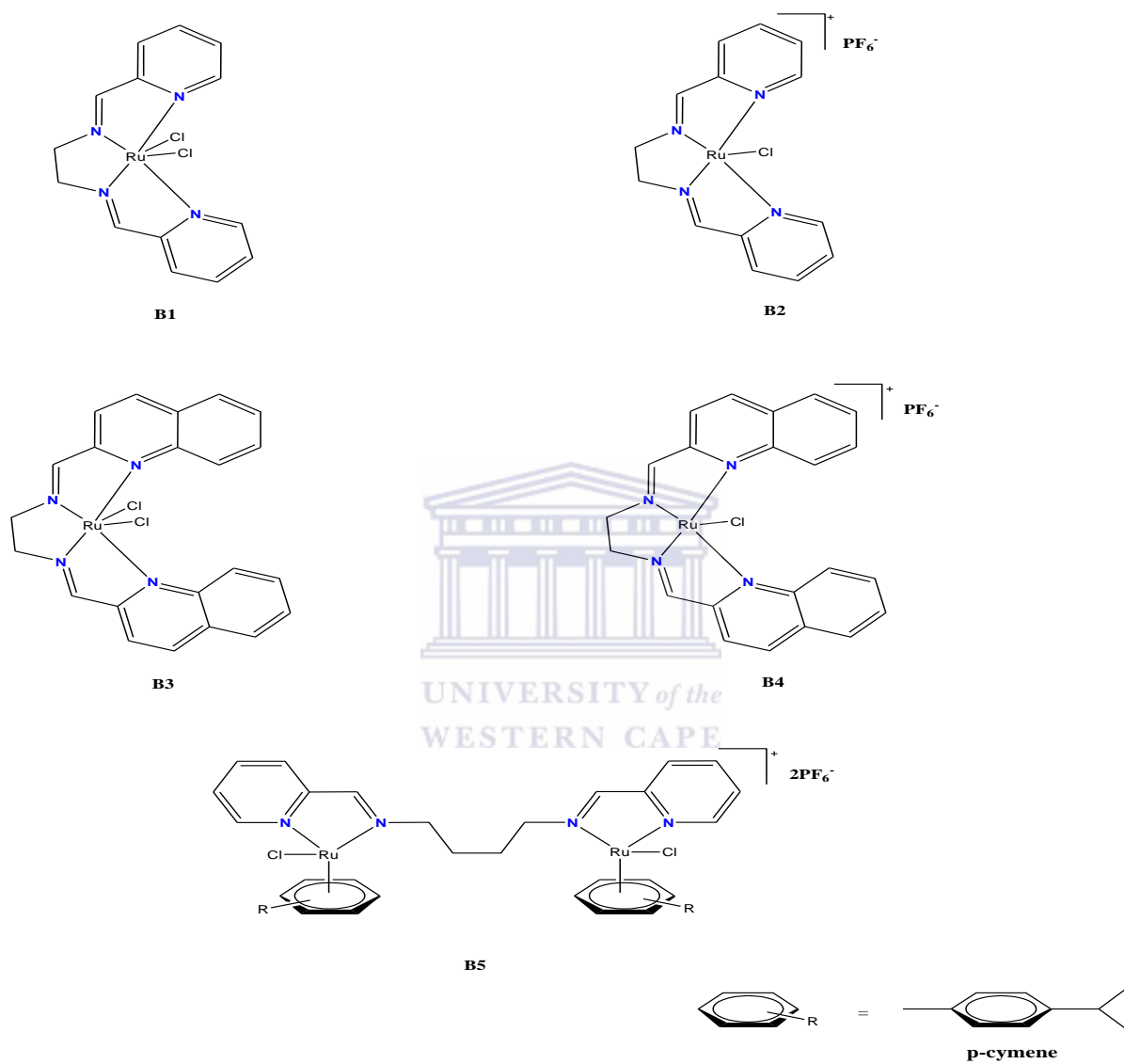


Figure 4.7(a): Scheme representing mono- and binuclear neutral and cationic (*N,N*) Ru(II) catalysts.

Chapter 4: Application of mono-, bi-, and multinuclear neutral and cationic Ru(II) catalysts in the oxidative cleavage of 1-octene.

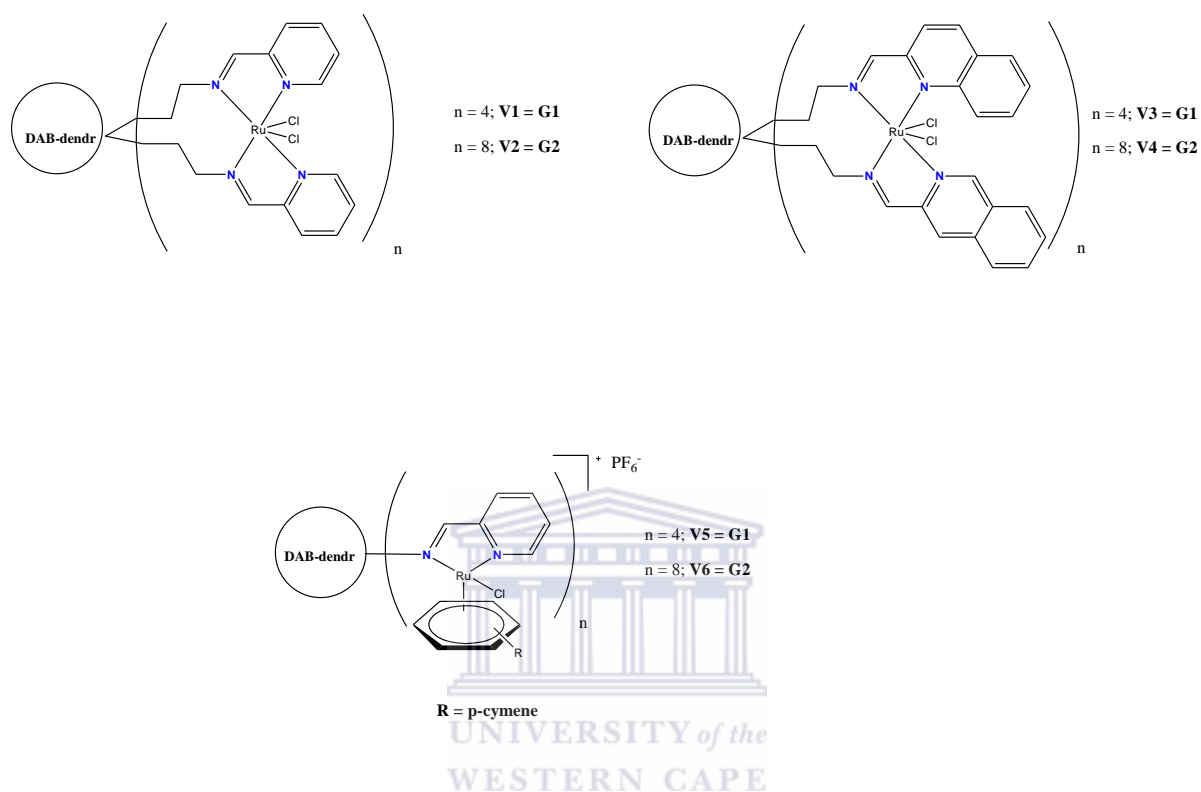


Figure 4.7(b): Scheme representing tetra- and octanuclear neutral and cationic (N,N) Ru(II) catalysts.

It was confirmed that the *in situ* generated active species, ruthenium tetroxide (**I**), under Sharpless conditions ensures the fragmentation of the C-C double bond to corresponding acids. It was also observed that there was an induction period (10-15 minutes) before the formation of the active species that was evident by the colour change to pale-yellow indicative of the presence of the active species. The colour of the catalytic reaction mixture changes from purple to yellow in the case of complex **B1-B4**. The experimental setup for the catalytic reactions is a less complex one, with the major products being the acids. The yields reported herein were higher than some of the previous reported reactions that employ a ruthenium system $[\text{RuCl}_2(\text{PPh}_3)_3]/\text{PhIO}$ [16].

Chapter 4: Application of mono-, bi-, and multinuclear neutral and cationic Ru(II) catalysts in the oxidative cleavage of 1-octene.

Competing reactions such as aldehydes formation were observed but in yields that were less than 5%. The presence of acetonitrile in the biphasic solvent system elevated the selectivity of acids over undesired products as reported for the $\text{RuCl}_3 \cdot n\text{H}_2\text{O}/\text{IO}(\text{OH})_5$ and $\text{RuCl}_3 \cdot n\text{H}_2\text{O}/\text{NaIO}_4$ systems respectively [10,12]. The completion of the catalytic reaction was confirmed by TLC.

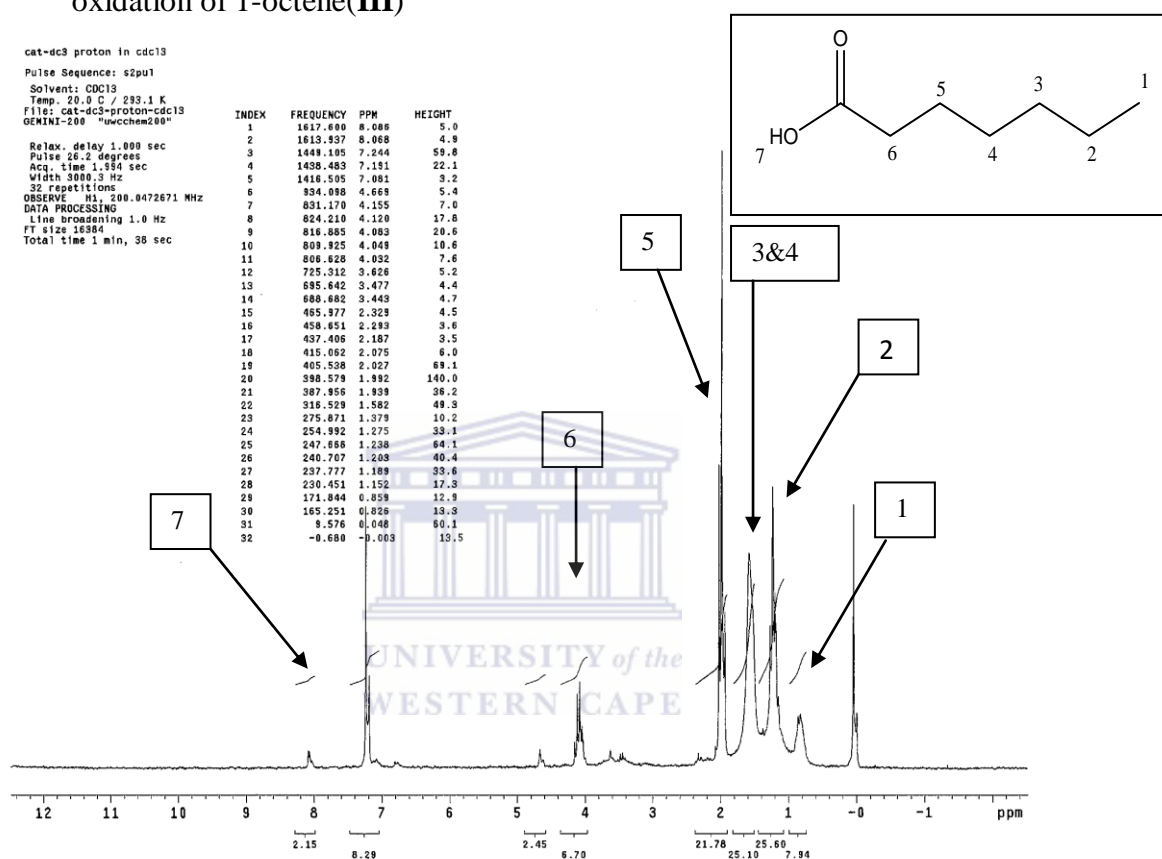


Table 4.1: Oxidative Cleavage of 1-octene to heptanoic acid by **B1-B5** and **V1-V6**/NaIO₄.

Entry	Catalysts	Yield (%)	Reaction time
		[TO]	(h)
1	B1	70(140)	2
2	B2	70(140)	2
3	B3	78(156)	2
4	B4	78(156)	2
5	B5	80(160)	2
6	V1	84(168)	2
7	V2	86(172)	2
8	V3	87(174)	2
9	V4	89(178)	2
10	V5	90(197)	2
11	V6	91(180)	2

Reaction conditions: alkene (0.556 mmol), catalyst (0.00278 mmol, **V-1**), and periodic acid (2.78 mmol) were added to a mixture of CCl₄-CH₃CN-H₂O (1:1:2 v/v), stirring at room temperature for 2 h. TO = turnover = moles of the product/moles of the catalyst.

Figure 4.8: ^1H NMR spectra of the crude product(IV) obtained after the ruthenium-catalyzed oxidation of 1-octene(III)



Reaction conditions: (a) catalyst (0.00278 mmol, **V-4**), 1-octene (0.556 mmol), and periodic acid (2.78 mmol).

The ^1H NMR was employed in order to aid with the identification of the product. The spectra of the crude product confirm cleavage of 1-octene to heptanoic acid. All the catalyst evaluated for the catalyzed oxidative cleavage of 1-octene gave heptanoic acid as the major product. Complex **B3** and **B4** gave higher yields of the acid in comparison with complex **B1** and **B2**. The higher conversion of the substrate by the former mentioned complexes was

attributed to the steric bulkiness around the active metal centre. The dendritic catalysts, **V3** and **V4**, gave higher conversion of the substrate/alkene in comparison to the dendritic catalysts, **V1** and **V2**, further confirming the results obtained for the mononuclear complexes with the same quinoline moiety. The yields of the product reached 90%, catalyzed by complex **V6**.

Thus it can be concluded that the oxidative cleavage of 1-octene with the synthesized catalyst systems required only mild reaction conditions at room temperature to achieve the results.



4.5 Conclusion

The results of the present studies convincingly demonstrate the catalytic ability of Ruthenium II-complexes towards the catalyzed oxidative cleavage of 1-octenes with NaIO₄ as a cooxidant. Under the catalytic conditions setup for the oxidation of the substrate/alkene, it can be thus concluded that the catalyst system reported herein for the first time are able to oxidize the chosen substrate/alkene.

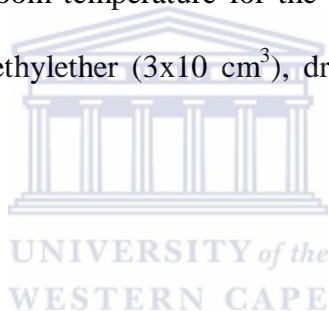
4.6 Materials and Methods

Infrared spectroscopic measurements in the range between 4000 and 450 cm⁻¹ were recorded on Perkin-Elmer spectrum-100 Series FT-IR spectrophotometer. The ¹H and ¹³C NMR measurements were recorded on a Varian XR200 MHz spectrometer. The ¹H and ¹³C

chemical shifts were referenced internally using the residual CDCl_3 (99.9%) and reported relative to the internal standard tetramethylsilane (TMS).

4.6.1 *General procedure for oxidative cleavage of 1-octene*

1-octene (0.556 mmol), catalyst (0.002782 mmol), and NaIO_4 (2.782 mmol) were added in a biphasic solvent system [CH_3CN (5 cm^3), CCl_4 (5 cm^3), and H_2O (10 cm^3)] with stirring. The reaction mixture was stirred at room temperature for the times specified in Table 4.1. The products were extracted with diethylether ($3 \times 10 \text{ cm}^3$), dried over MgSO_4 , and evaporated under reduced pressure.



References:

1. (a) R. Pappo, D. S. Allen, Jr., R. U. Lemieux and W. S. Johnson, *J. Org. Chem.*, 1956, **21**, 478; (b) T. M. K. Shing, in *Comprehensive Organic Synthesis*, B. M. Trost and I. Fleming, ed., Pergamon Press, Oxford, 1991, Vol. 7, pp 703-716.
2. J. L. Courtney, In: Mijs W. J. De Jonge CRHI (eds) *Organic Synthesis by oxidation with metal compounds*. Plenum Press, New York, pp 445-467.
3. F. E. Kuehn, R. W. Fischer, T. Weskamp, (2004) In: M. Beller, C. Bolm, (eds) *Transition metals for organic synthesis*, 2nd edn, Wiley-VHC Verlag GmbH, Weinheim, pp427-436.
4. R. W. Fischer, W. A. Herrmann, T. Weskamp, (1998) In: M. Beller, C. Bolm, (eds) *Transition metals for organic synthesis: building blocks and fine chemicals*, vol 2. Wiley, New York, pp282-289.
5. D. G. Lee, T. Chen, (1991) In: B. M. Trost, S.V. Ley, (eds) *Comprehensive organic synthesis*, vol 7. Pergamon Press, Oxford, pp 541-591.
6. H. Milmeum, (1987) In: G. Wilkison, R. D. Gillard, J. A. McCleverty, (eds) *Comprehensive coordination chemistry*, vol 6. Pergamon Press, Oxford, pp 317-410.
7. R. A. Sheldon, I. Arends, U. Hanefeld, *Green Chemistry and catalysis*,
8. E. S. Gore, *Platinum Metals Rev*, 1983, 27, 111.
9. P. N. Rylander, *Engelhard Tech Bull*, 1969, 135.
10. P. H. J. Carlsen, T. Katsuki, V. S. Martin, K. B. Sharpless, *J. Org. Chem.*, 1981, **46**, 3936.
11. L. F. Tietze, C. Schneider, A. Montenbruck, *Angew. Chem., Int. Ed. Engl.*, 1994, **33**, 980.

12. S. Wolfe, S. K. Hasan, J. R. Campbell, *J. Chem. Soc. Chem. Commun.*, 1970, 1420.
13. A. F. Diaz, K. K. Kanazawa, G. P. Gardini, *J. Chem. Soc. Chem. Commun.*, 1985, **26**, 362.
14. T. Naota, H. Takaya, S.-I. Murahashi, *Chem. Rev.*, 1998, **98**, 2599.
15. J. Halpern, *Pure and Appl. Chem.*, 1987, **59**, 173.
16. P. Muller, J. Godoy, *Helv. Chim. Acta.*, 1981, **64**, 2531.



5.1 General Conclusions

The present study detailed the synthesis and catalytic application of mono-, bi- and multinuclear ruthenium(II) and rhenium(VII) metallodendrimers. These complexes were synthesized from Schiff-bases (**L1-L4** and **DL1-DL4**) that were synthesized by condensation of primary amines and aldehydes in good yields. These Schiff-bases were subsequently reacted with the respective metal precursors ($[\text{RuCl}_2(\text{dmsO})_4]$, $[(\text{p-cymene})\text{RuCl}_2]_2$ and $\text{CH}_3\text{ReO}_3(\text{MTO})$) and formed complexes with the metals via nitrogen lone pair electrons. The Schiff-base Re(VII) complexes, **C1**, **C2**, **DC1** and **DC2**, were evaluated in the epoxidation reactions of selected cyclic alkenes while the neutral and cationic mono-, bi- and multinuclear ruthenium(II), **B1-B5** and **V1-V6**, complexes were tested as catalysts in the oxidative cleavage of a selected straight chain alkene.

The mono-, binuclear Schiff-base complexes of methyltrioxorhenium (MTO), **C1** and **C2**, and 1st and 2nd generation Re(VII) metallodendrimers, **DC1** and **DC2**, were evaluated in a comparative study as catalysts in the epoxidation of selected cyclic substrates/alkenes, i.e. cyclohexene and *cis*-cyclooctene, respectively. These Schiff-base complexes of MTO, both the discrete mono- and binuclear as well as the metallodendrimers were efficient catalysts in the epoxidation reaction of cyclic substrates/alkenes. The Schiff-base Re(VII) metallodendrimers exhibited superior catalytic efficiency than the mono- and binuclear Schiff-base Re(VII) complexes, i.e. catalytic activity. The complexes, **C1**, **C2**, **DC1** and **DC2**, displayed high selectivity towards the formation of epoxides with no significant formation of side products.

The mono-(**B1-B4**), bi-(**B5**) and multinuclear(**V1-V6**) neutral and cationic Ru(II) complexes were also subjected to a comparative study as catalysts in the oxidative cleavage of 1-octene. The chelating neutral and cationic 1st- and 2nd-generation Ru(II) arene complexes based on the poly(propyleneimine) dendrimer scaffold gave higher yields in comparison to the mono-(**B1-B4**), and binuclear(**B5**) neutral and cationic Ru(II) complexes. In the catalyzed oxidative cleavage of 1-octene, the catalytic active species was confirmed to be ruthenium tetroxide, RuO₄.

In general, the thesis has clearly described the synthesis, characterization and catalytic application of various chelating flexible Schiff-base complexes of Ru(II) and Re(VII) as catalysts for the oxidative cleavage and epoxidation reactions, respectively. The thesis explores new possibilities of development of environmental friendly and efficient catalysts based on dendritic scaffold. In brief the thesis has contributed to Inorganic synthesis and homogeneous catalysis.

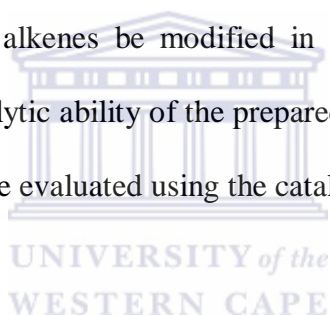
5.2 Recommendations

It is within the study of these synthesized complexes to try and better some of the shortcomings that arose from the study. It was discovered that the Schiff-base complexes of methyltrioxorhenium (MTO) were sensitive to moisture, light and temperature. The bi- and multinuclear Re(VII) complexes hindered thorough characterization as they decompose before they could be analyzed by some of the spectroscopic techniques at hand. It is recommended that a trial for stabilization of these Schiff-base MTO complexes should be

carried out to gain their better understanding. Also their crystal structures should be obtained through growing of crystals and resolving them crystallographically.

The scope of the epoxidation reactions should be widened to include more sensitive alkenes because the epoxidation catalysts behave extremely well during the study of cyclohexene and *cis*-cyclooctene, respectively. The investigation should involve the epoxidation of long chains alkenes and sterically hindered cyclic alkenes.

It is also recommended that in the future, the catalytic reaction conditions for the Ru(II) catalyzed oxidative cleavage of alkenes be modified in order to homogenize the solvent mixture so as to quantify the catalytic ability of the prepared complexes. Long chains alkenes (> C8) and cyclic alkenes are to be evaluated using the catalysts in the future.

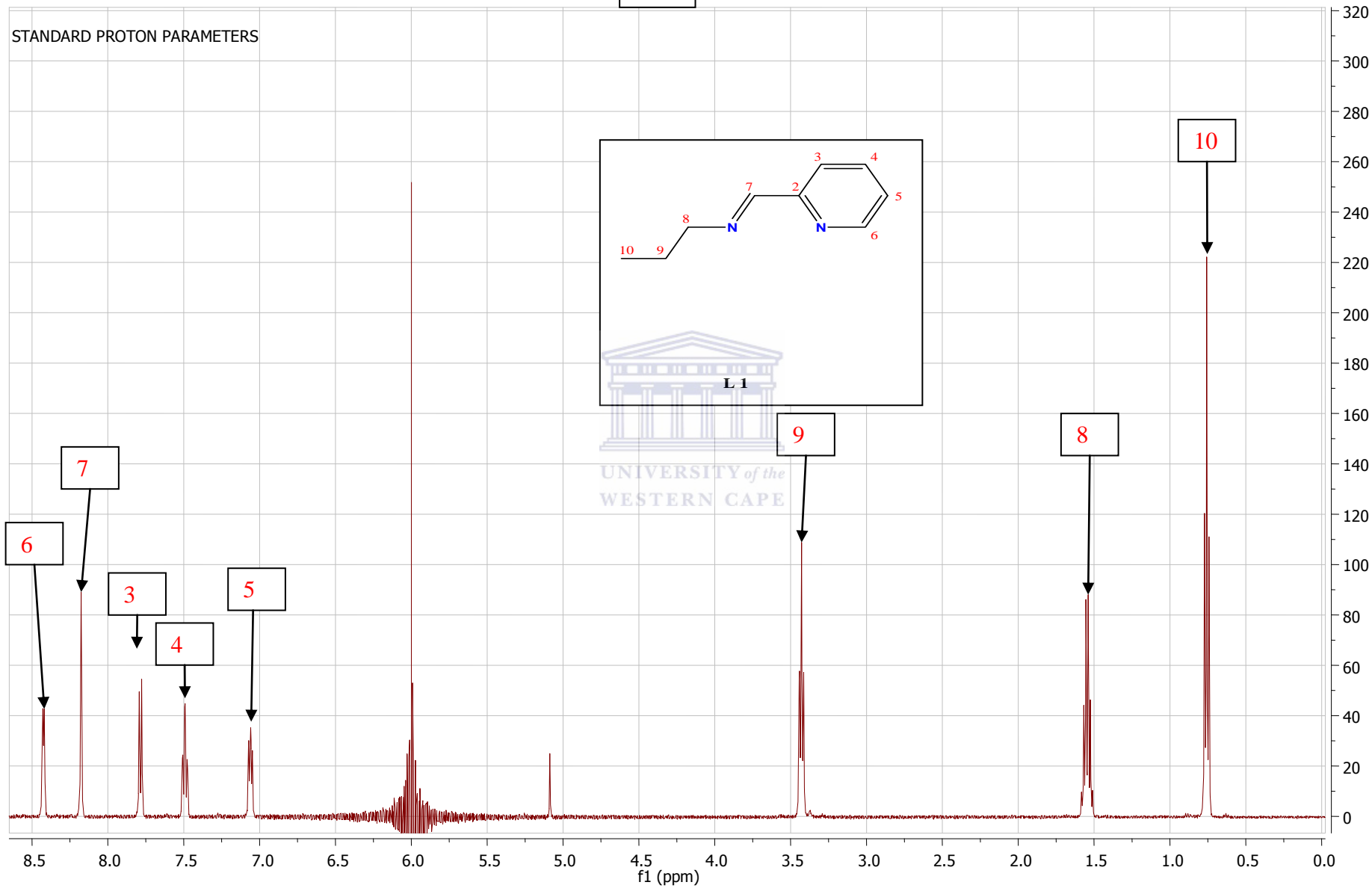


ANNEXURE: Chapter 2

- A** ^1H NMR spectrum of the ligand **L1**.
- B** ^1H NMR spectrum of the ligand **L3**.
- C** ^1H NMR spectrum of the dendrimeric quinoline based ligand **DL3**.
- D** ^1H NMR spectrum of the neutral mononuclear ruthenium complex **B2**.
- E** ESI-MS spectrum of ligand **L4** showing $[\text{M}+\text{H}]^+$ fragment (indicated by arrow).
- F** ESI-MS spectrum of dendrimeric ligand **DL4** showing $[\text{M}+\text{H}]^+$ fragment (indicated by arrow)
- G** ESI-MS spectrum of the neutral dendritic complex **V4** showing $[\text{M}+\text{H}]^+$ fragment (indicated by arrow).
- H** ESI-MS spectrum of the homobimetallic complex **B5** showing $[\text{M}+\text{H}]^+$ fragment (indicated by arrow).



A



AVB-L5 proton in cdc13 22-05-2012

Pulse Sequence: s2pu1

Solvent: CDC13

Temp: 20.0 C / 293.1 K

File: AVB-L5-proton-22-05-2012

GEMINI-200 "uwchem200"

Relax. delay 1.000 sec

Pulse 28.2 degrees

Acq. time 1.934 sec

Width 3000.3 Hz

32 repetitions

OBSERVE H1, 200.0473001 MHz

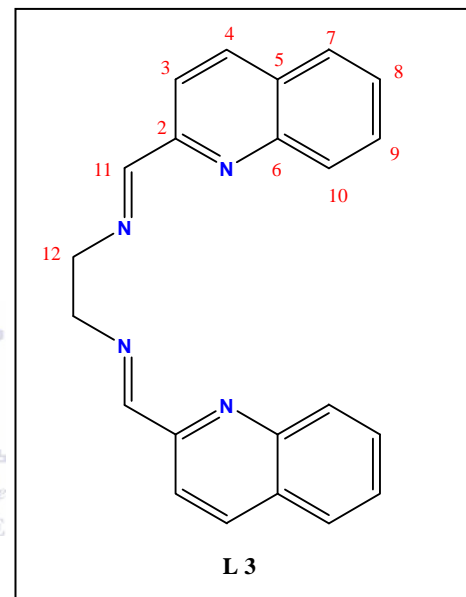
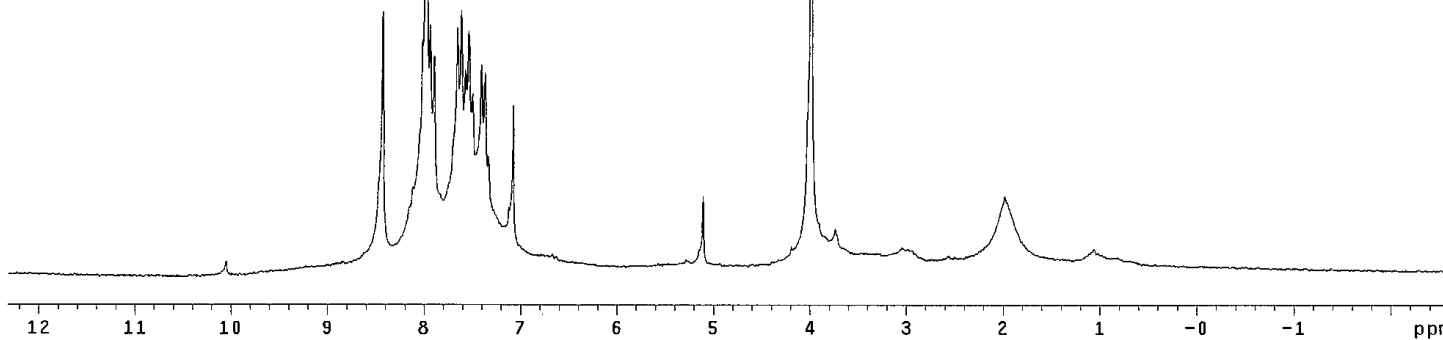
DATA PROCESSING

Line broadening 1.0 Hz

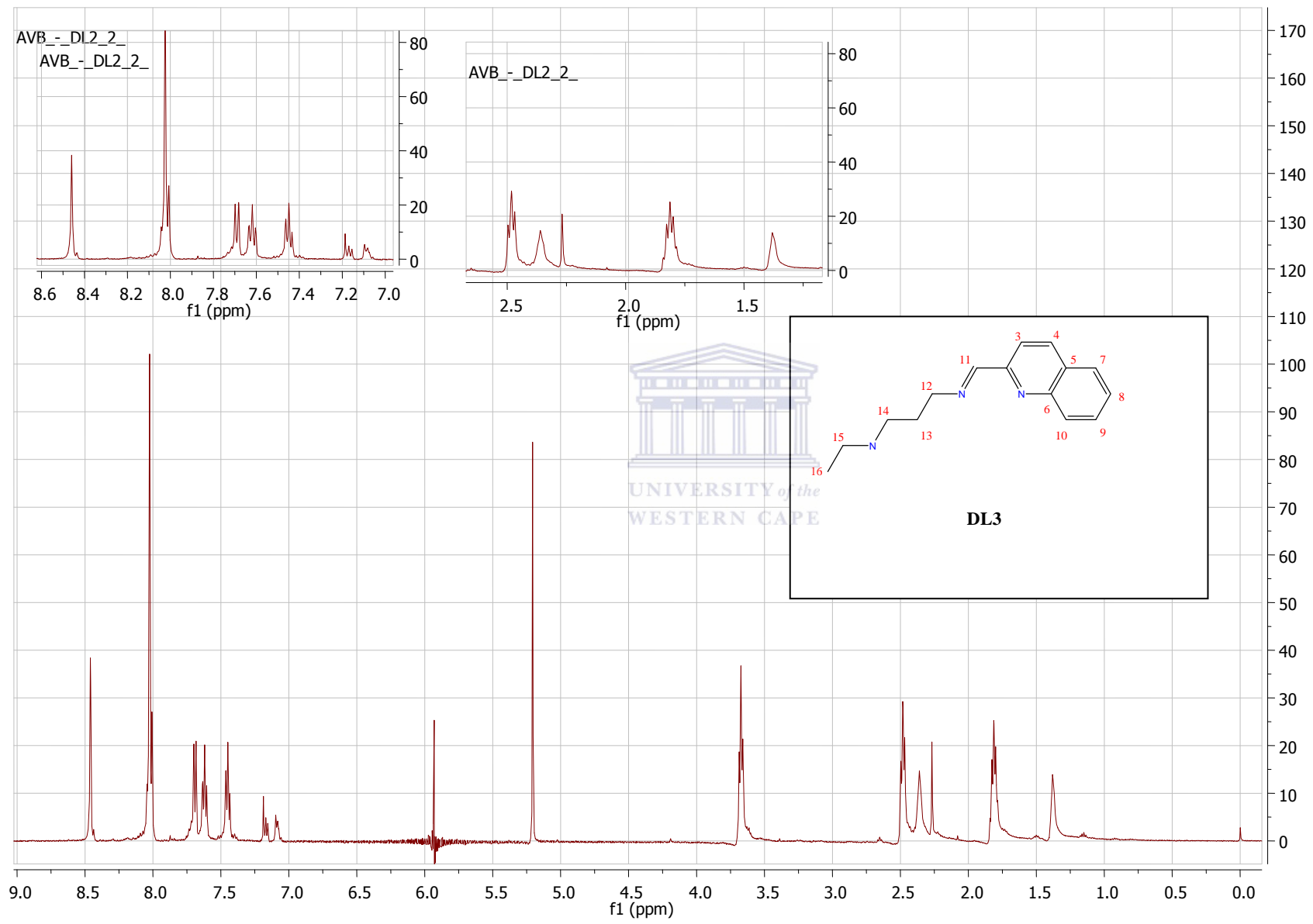
FT size 16384

Total time 1 min, 38 sec

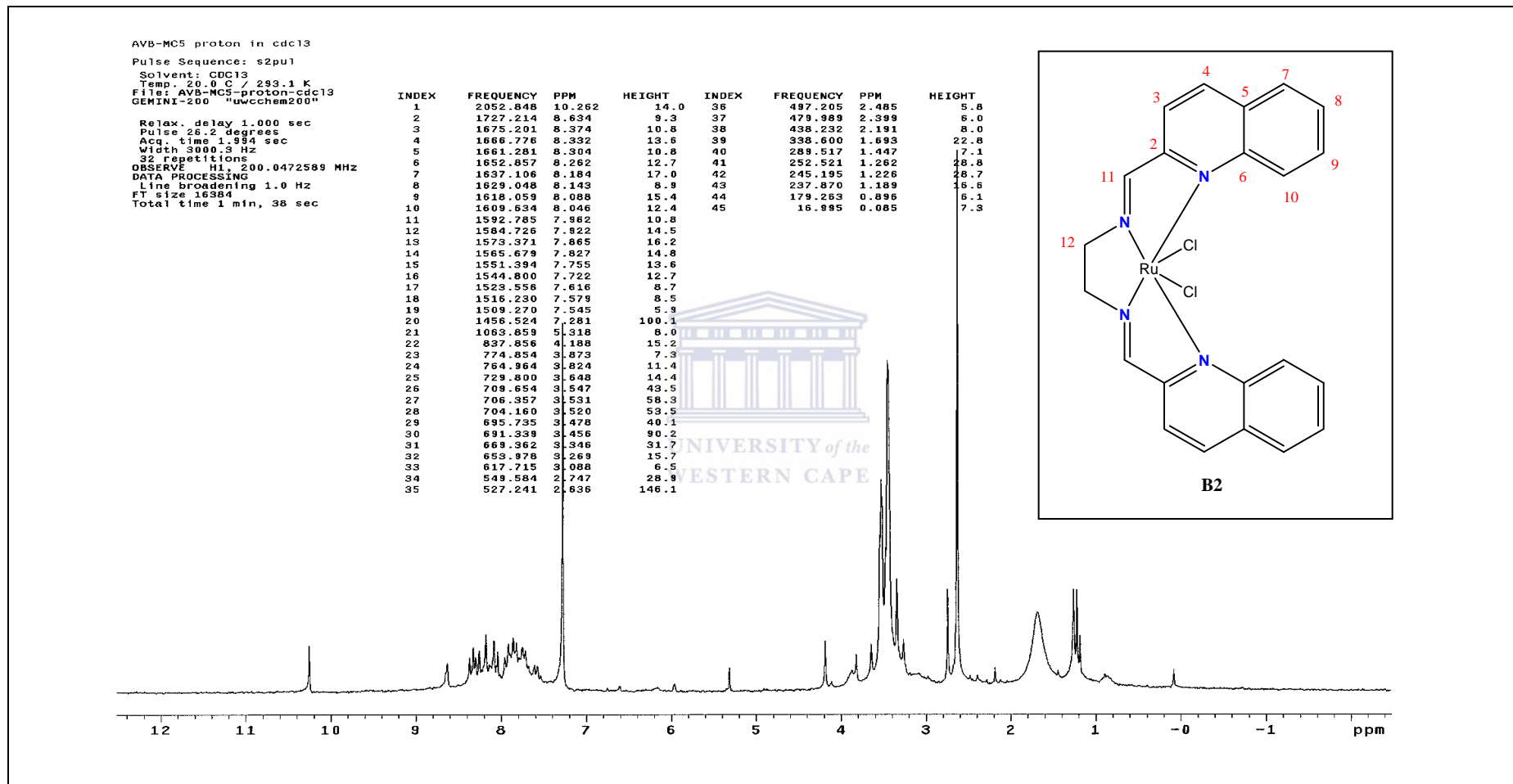
INDEX	FREQUENCY	PPM	HEIGHT
1	2010.573	10.050	2.7
2	1685.305	8.425	46.2
3	1602.889	8.013	41.2
4	1594.465	7.970	107.4
5	1587.505	7.936	43.9
6	1578.714	7.892	38.5
7	1530.730	7.652	43.2
8	1522.671	7.612	46.3
9	1514.247	7.569	36.1
10	1507.287	7.535	42.7
11	1499.229	7.494	31.9
12	1480.914	7.403	36.9
13	1473.222	7.364	35.6
14	1465.896	7.328	21.1
15	1423.406	7.115	12.2
16	1414.615	7.071	29.9
17	1333.665	6.667	4.0
18	1114.256	5.570	2.4
19	1056.381	5.281	3.0
20	1020.851	5.103	14.1
21	837.705	4.188	5.2
22	795.948	3.979	95.2
23	746.498	3.732	8.3
24	607.673	3.038	5.0
25	511.705	2.558	3.6
26	395.224	1.976	14.1
27	211.345	1.056	4.8
28	-176.923	-1.384	1.5



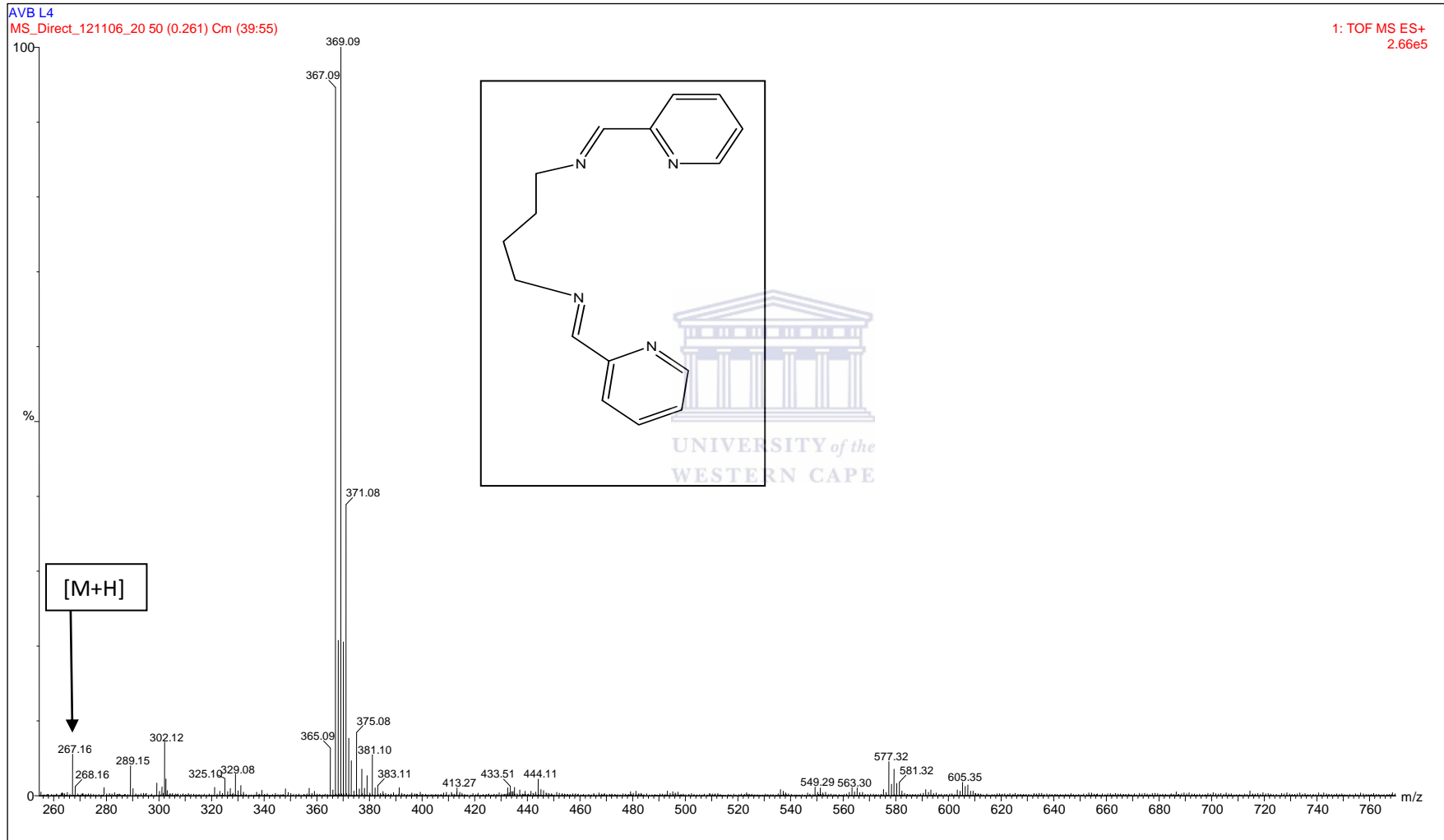
UNIVERSITY of the
WESTERN CAPE



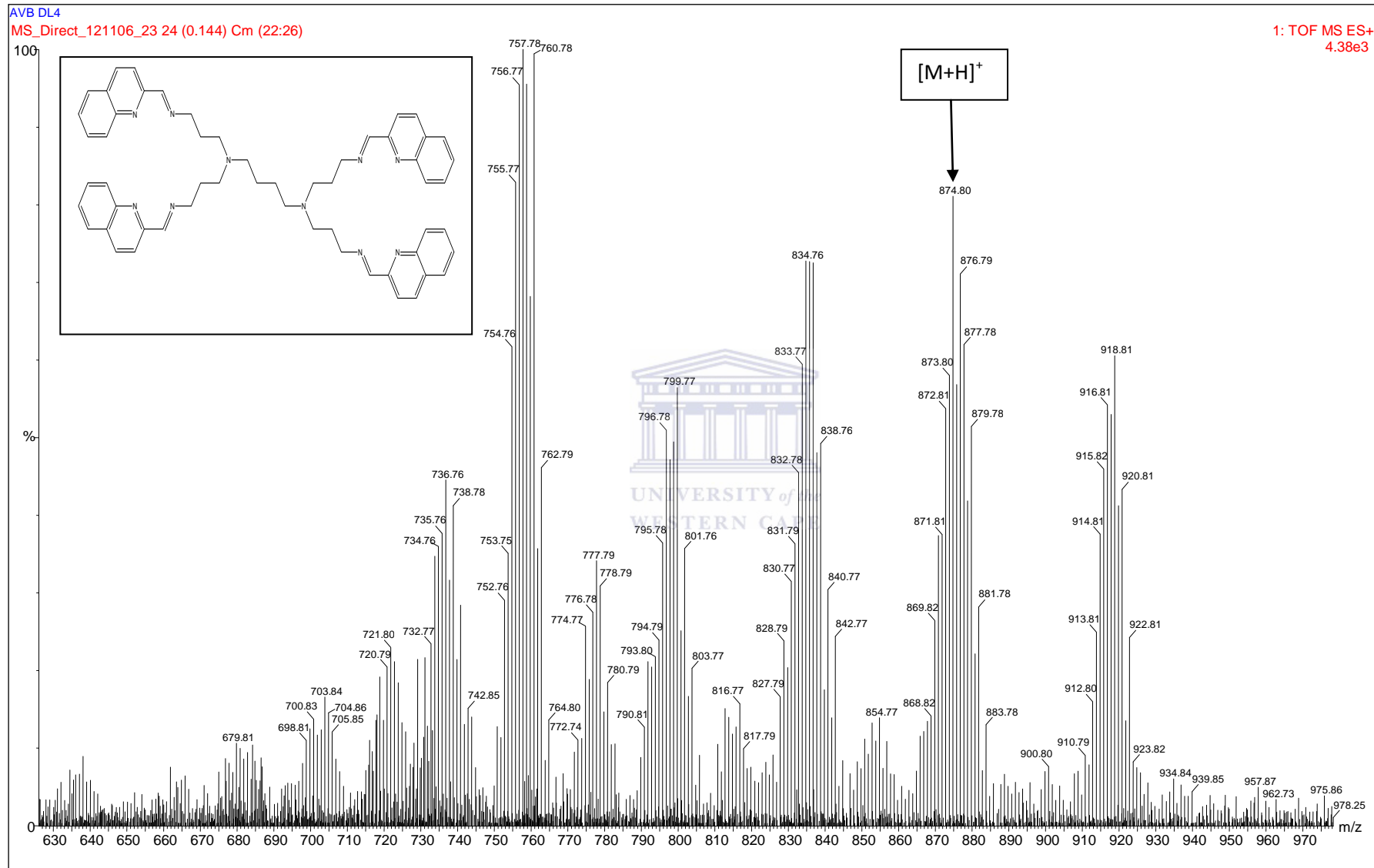
D



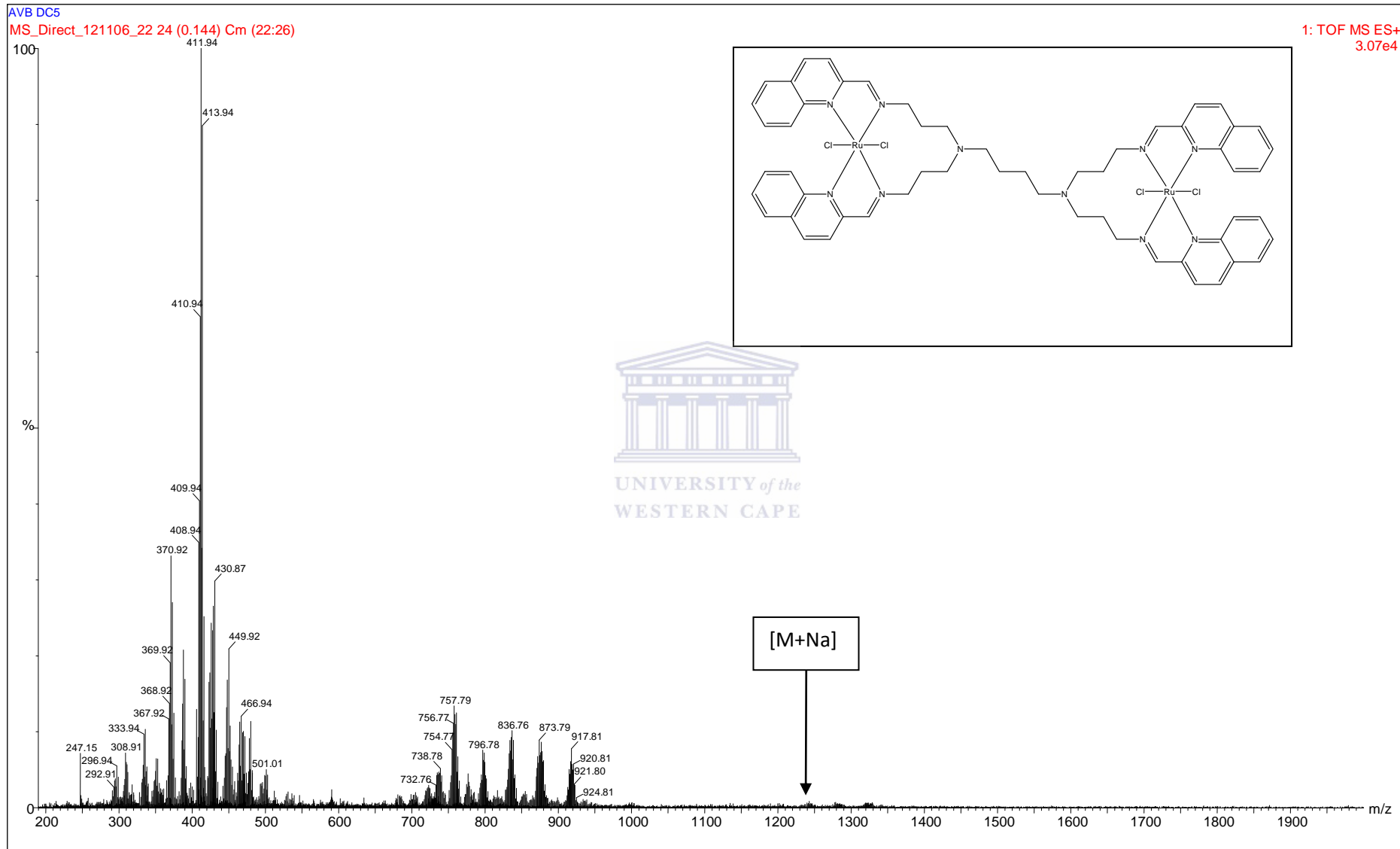
E



F

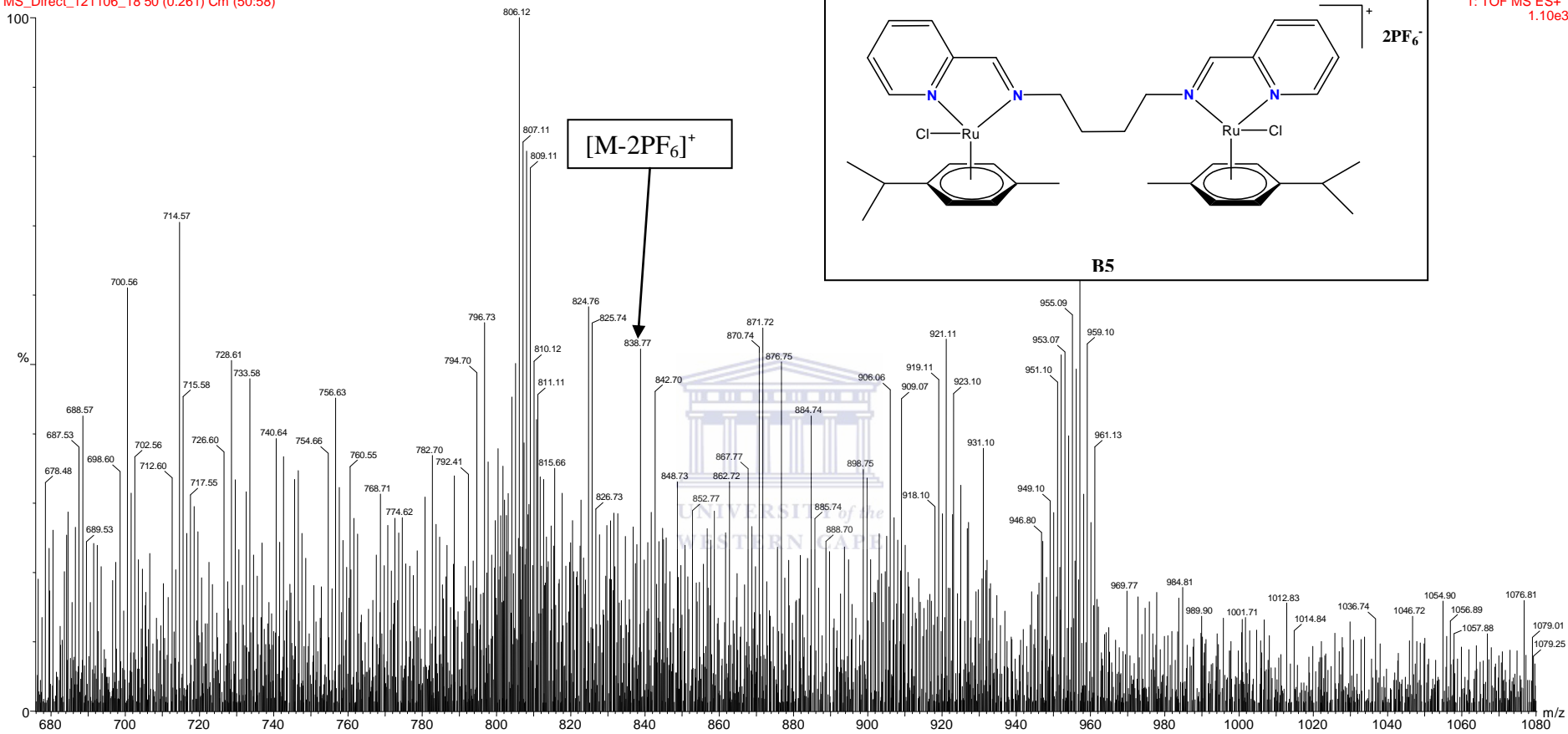


G



H

AVB BCZ
MS_Direct_121106_18 50 (0.261) Cm (50:58)



1: TOF MS ES+
1.10e3